

การแทนที่โดยโพลีเมอร์ด้วยประสิทธิภาพสูงสุดในแหล่งกักเก็บที่มีน้ำมันหนืดปานกลาง



นาย ต่อพงษ์ เยาวภา

ศูนย์วิทยทรัพยากร
จุฬาลงกรณ์มหาวิทยาลัย

วิทยานิพนธ์นี้เป็นส่วนหนึ่งของการศึกษาตามหลักสูตรปริญญาวิศวกรรมศาสตรมหาบัณฑิต

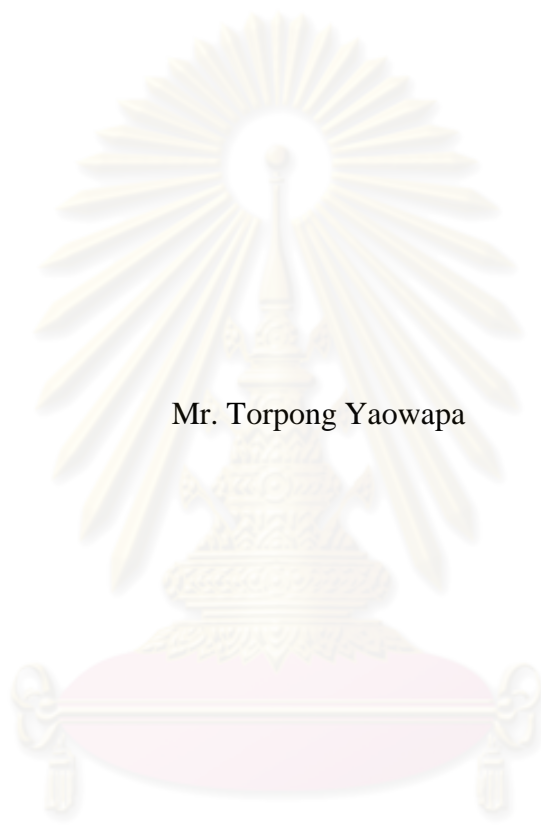
สาขาวิชาวิศวกรรมปิโตรเลียม ภาควิชาวิศวกรรมเหมืองแร่และปิโตรเลียม

คณะวิศวกรรมศาสตร์ จุฬาลงกรณ์มหาวิทยาลัย

ปีการศึกษา 2553

ลิขสิทธิ์ของจุฬาลงกรณ์มหาวิทยาลัย

OPTIMIZATION OF POLYMER FLOODING IN MEDIUM VISCOSITY OIL
RESERVOIR



Mr. Torpong Yaowapa

ศูนย์วิทยทรัพยากร
จุฬาลงกรณ์มหาวิทยาลัย
A Thesis Submitted in Partial Fulfillment of the Requirements
for the Degree of Master of Engineering Program in Petroleum Engineering

Department of Mining and Petroleum Engineering

Faculty of Engineering

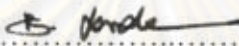
Chulalongkorn University

Academic Year 2010

Copyright of Chulalongkorn University


Thesis Title OPTIMIZATION OF POLYMER FLOODING IN
MEDIUM VISCOSITY OIL RESERVOIR
By Mr. Torpong Yaowapa
Field of Study Petroleum Engineering
Thesis Advisor Assistant Professor Suwat Athichanagorn, Ph.D.


Accepted by the Faculty of Engineering, Chulalongkorn University in
Partial Fulfillment of the Requirements for the Master's Degree


..... Dean of the Faculty of Engineering
(Associate Professor Boonsom Lerdkhirunwong, Dr.Ing.)

THESIS COMMITTEE


..... Chairman
(Associate Professor Sarithdej Pathanasetpong)


..... Thesis Advisor
(Assistant Professor Suwat Athichanagorn, Ph.D.)


..... Examiner
(Assistant Professor Jirawat Chewaroungroj, Ph.D.)


..... External Examiner
(Wisarut Thungsuntonkhun, Ph.D.)

ต่อพงษ์ เขียวภา : การแทนที่โดยโพลิเมอร์ด้วยประสิทธิภาพสูงสุดในแหล่งกักเก็บที่มี
น้ำมันหนืดปานกลาง (OPTIMIZATION OF POLYMER FLOODING IN
MEDIUM VISCOSITY OIL RESERVOIR) อ. ที่ปริกษาวิทยานิพนธ์หลัก: ผศ. ดร.
สุวัฒน์ อธิษณากร. 99 หน้า.

การแทนที่โดยโพลิเมอร์เป็นเทคนิคทางเลือกหนึ่งในการเพิ่มปริมาณการผลิตน้ำมัน
เพื่อที่จะเพิ่มประสิทธิภาพในการกวาดชิงปริมาณ ทำให้น้ำถึงหลุมผลิตช้าลง และ เพิ่มปริมาณการ
ผลิตน้ำมัน โดยการลดอัตราส่วนการเคลื่อนที่ระหว่างน้ำต่อน้ำมัน โดยทั่วไปแล้วประเภทของโพลิ
เมอร์ที่ใช้มีอยู่สองประเภท คือ โพลิอะคริลาไมด์ที่ถูกไฮโดรไลต์บางส่วน และ ซานทาน โพลิเมอร์

ในการศึกษาครั้งนี้ ได้เสนอการแทนที่โดยใช้โพลิอะคริลาไมด์ที่ถูกไฮโดรไลต์บางส่วน
และมีขายอยู่ทั่วไป ซึ่งมีความหนืดของโพลิเมอร์ที่เหมาะสมต่อสภาวะปัจจุบันของแหล่งกักเก็บ
แบบจำลองของแหล่งกักเก็บที่ถูกสมมติขึ้นมาถูกสร้างโดยยึดหนึ่งในสี่ของรูปแบบการแทนที่แบบ
ห้าจุด โดยอ้างอิงคุณสมบัติของแหล่งกักเก็บและของไหลจากแหล่งผลิตน้ำมันบนบกในประเทศ
ไทยเป็นพื้นฐาน เทคนิคที่นำเสนอนี้ถูกแบ่งออกเป็นสามแผนการหลัก แผนการแรกคือ โพลิเมอร์
สลักเดียวในความเข้มข้นต่างๆ ถูกอัดแทนที่จนกระทั่งถึงหลุมผลิต แผนการที่สองคือ โพลิเมอร์
แบบสองสลักที่ถูกลดความเข้มข้นลงตามลำดับ ถูกอัดแทนที่จนกระทั่งถึงหลุมผลิต แผนการที่สาม
คือ โพลิเมอร์แบบสองสลัก จะถูกไล่คั้นตามหลังด้วยน้ำจนถึงหลุมผลิต ผลการทดลองจากแผนการ
ทั้งหมดจะถูกนำมาเปรียบเทียบกับ การแทนที่โดยน้ำ นอกจากนี้ การวิเคราะห์ความไวต่อการ
เปลี่ยนแปลงถูกนำมาศึกษาถึงผลกระทบของตัวแปรที่ไม่แน่นอน ซึ่งมีผลต่อการแทนที่โดยโพลิ
เมอร์

การแทนที่ด้วยโพลิเมอร์แบบสองสลักและไล่คั้นน้ำตามหลังสามารถเพิ่มการใช้ประโยชน์
จากโพลิเมอร์ได้มากกว่าการแทนที่ด้วยโพลิเมอร์แบบสลักเดียว แต่ประสิทธิภาพในการผลิตน้ำมัน
จะลดลงเล็กน้อย เนื่องจากประสิทธิภาพในการกวาดลดลง อย่างไรก็ตามการลดลงของ
ประสิทธิภาพในการผลิตน้ำมันสามารถชดเชยด้วยปริมาณการใช้โพลิเมอร์ที่ต่ำลงและระยะเวลา
การผลิตที่สั้นลง

ภาควิชา วิศวกรรมเหมืองแร่และปิโตรเลียม.....ลายมือชื่อนิสิต.....

สาขาวิชา วิศวกรรมปิโตรเลียม.....ลายมือชื่อ อ.ที่ปริกษาวิทยานิพนธ์หลัก.....

ปีการศึกษา 2553.....

5271606621: MAJOR PETROLEUM ENGINEERING

KEYWORDS: POLYMER FLOODING / MEDIUM VISCOSITY OIL/
OPTIMIZATION / TWO POLYMER SLUGS

TORPONG YAOWAPA : OPTIMIZATION OF POLYMER FLOODING IN
MEDIUM VISCOSITY OIL RESERVOIR. ADVISOR: ASST. PROF.
SUWAT ATHICHANAGORN. Ph.D., 99 pp.

Polymer flooding is an alternative improved oil recovery (IOR) technique to improve volumetric sweep efficiency, slow down water breakthrough time and increase amount of oil recovery by decreasing water/oil mobility ratio. Two types of polymers commonly used for polymer flooding are partially hydrolyzed polyacrylamide (HPAM) and xanthan polymers.

In this study, we propose polymer flooding by using commercial HPAM (Flopaam 3330S) which has an appropriate in-situ polymer viscosity at reservoir conditions. A hypothetical reservoir simulation model was constructed based on a quarter five-spot flooding pattern with reservoir and fluid properties from an onshore oilfield in Thailand. The proposed technique is divided into three main scenarios. First, single polymer slug in various concentration is injected till breakthrough. Second, two slugs of polymer with progressively decreasing polymer concentration is injected till breakthrough. Third, two slugs of polymer is chased by water till breakthrough. Then, the results were compared with the ones from water flooding. Moreover, sensitivity analysis was conducted to study the impact of polymer flood's uncertain parameters.

Injection of two polymer slugs with drive water can help to increase polymer utilization than injecting only a single slug of polymer but the oil recovery factor (RF) is slightly lower due to less areal sweep efficiency. However, decrease in RF can be compensated by lower amount of polymer and shorter production time.

Department: Mining and Petroleum Engineering Student's Signature: *Torpong Yaowapa*

Field of Study: Petroleum Engineering Advisor's Signature: *Suwat Athichanagorn*

Academic Year: 2010

Acknowledgements

I would like to express my appreciation and thankfulness toward my research advisor, Assistant Professor Dr. Suwat Athichanagorn, for his guidance, support and sincere personal advice that help me mature as a researcher and will deeply influence my career and future life.

I am heartily thankful to the thesis committee members for their invaluable comments and recommendations.

I wish to give my special thanks to all faculty members in the Department of Mining and Petroleum Engineering who have offered petroleum knowledge, technical advice, and invaluable consultation. I am grateful to all classmates for discussions and true friendship.

I would like to thank Schlumberger for providing educational license of ECLIPSE 100 reservoir simulator software to the Department of Mining and Petroleum Engineering. Without the software, this study would not have been completed.

Lastly, I would like to express my sincere gratitude and deep appreciation to my family for their patient, moral encouragement and constant support.

ศูนย์วิทยทรัพยากร
จุฬาลงกรณ์มหาวิทยาลัย

Contents

	Page
Abstract (Thai)	iv
Abstract (English)	v
Acknowledgements	vi
Contents	vii
List of Tables	ix
List of Figures	x
List of Abbreviations	xiii
Nomenclature	xiv
 CHAPTER	
I. INTRODUCTION	1
1.1 Outline of Methodology.....	2
1.2 Thesis Outline	3
 II. LITERATURE REVIEW	4
2.1 Previous Works on Polymer Flooding Project.....	4
2.2 Previous Works on Polymer Properties	5
 III. THEORY AND CONCEPT	7
3.1 Polymer Flooding Process	7
3.1.1 Mobility Ratio	8
3.1.2 Polymer Flooding Fractional Flow	9
3.2 Characteristics of Polymers	10
3.2.1 Polymer Types.....	10
3.2.2 Rheological Properties of Polymer	12
3.2.3 Inaccessible Pore Volume	12
3.2.4 Polymer Retention.....	13
3.2.5 Permeability Reduction	14
3.3 Polymer Flood Simulation Model.....	15

CHAPTER	Page
3.3.1 Fluid Viscosities	17
3.3.2 Polymer Adsorption	18
3.3.3 Permeability Reductions and Dead Pore Volume	19
3.3.4 Non-Newtonian Rheology.....	20
IV. MODELING APPROACH.....	22
4.1 Field Description.....	22
4.2 Simulation Model Construction.....	22
4.2.1 Grid.....	23
4.2.2 PVT	25
4.2.3 Relative Permeability	26
4.2.4 Well Specification and Production Constraint.....	28
V. OPTIMIZATION AND SENSITIVITY STUDY.....	29
5.1 Base Case of Water Flooding	29
5.2 Single Polymer Slug	33
5.3 Two Polymer Slugs.....	42
5.4 Two Polymer Slugs with Drive Water.....	51
5.5 Sensitivity Study	61
5.5.1 Effect of Inaccessible Pore Volume.....	61
5.5.2 Effect of Polymer Adsorption	63
5.5.3 Effect of Residual Resistant Factor	65
5.5.4 Effect of Mixing Parameter.....	68
VI. CONCLUSIONS AND RECOMMENDATIONS	71
REFERENCES.....	74
APPENDICES	77
APPENDIX A.....	78
APPENDIX B	79
VITAE.....	99

List of Tables

		Page
Table 4.1	Reservoir dimensions and rock properties.....	24
Table 4.2	Input data for PVT section.....	25
Table 4.3	Input data for SCAL section.....	26
Table 4.4	Production constrain and economic limits.....	28
Table 5.1	Apparent viscosity of Flopaam 3330S.....	34
Table 5.2	Summary of results for single polymer slug.....	41
Table 5.3	Summary of apparent viscosity for Cases 2A, 2B, 2C, and 2D.....	47
Table 5.4	Summary of results for two-slug injection.....	50
Table 5.5	Summary of apparent viscosity for Cases 3B, 3C, and 3D.....	54
Table 5.6	Summary of results for two polymer slugs with drive water.....	57
Table 5.7	Summary of results for all scenarios.....	58
Table 5.8	Summary of input data for each parameter.....	61
Table 5.9	Summary of results for different inaccessible pore volumes.....	63
Table 5.10	Summary of results for different polymer adsorptions.....	65
Table 5.11	Summary of results for different residual resistant factors.....	67
Table 5.12	Summary of results for different mixing parameters.....	69
Table 5.13	Summary of percentage change in RF from base case.....	70
Table A1	Shear thinning data of Flopaam 3330S used in the simulation.....	74

List of Figures

	Page
Figure 3.1 Polymer flooding process.....	8
Figure 3.2 Schematic of macroscopic displacement efficiency improvement by polymer flooding.....	9
Figure 3.3 Graphical construction of polymer flooding fractional flow.....	10
Figure 3.4 Structure of polyacrylamide (PAM) and partially hydrolyzed polyacrylamide (HPAM).....	11
Figure 3.5 Structure of xanthan gum.....	11
Figure 3.6 Rheology of a shear-thinning fluid.....	12
Figure 3.7 Early arrival of polymer front caused by inaccessible pore volume.	13
Figure 3.8 Polymer retention mechanisms in porous medium.....	13
Figure 4.1 Top view of reservoir model.....	23
Figure 4.2 Reservoir model in 3D view.....	24
Figure 4.3 Dry gas PVT properties used in the simulations.....	25
Figure 4.4 Live oil PVT properties used in the simulations.....	26
Figure 4.5 Water-oil relative permeability curve.....	27
Figure 4.6 Gas-oil relative permeability curve.....	27
Figure 5.1 Injection rate for base case of water flooding.....	30
Figure 5.2 Bottom hole pressure for base case of water flooding.....	30
Figure 5.3 Average reservoir pressure for base case of water flooding.....	31
Figure 5.4 Water cut for base case of water flooding.....	31
Figure 5.5 Oil production rate for base case of water flooding.....	32
Figure 5.6 Oil recovery factor for base case of water flooding.....	32
Figure 5.7 Effect of polymer concentration on shear viscosity.....	33
Figure 5.8 Effect of temperature on apparent viscosity.....	34
Figure 5.9 Polymer solution viscosity function used in the simulations.....	35
Figure 5.10 Polymer shear thinning data used in the simulations.....	35

	Page
Figure 5.11 Polymer adsorption function used in the simulations.....	36
Figure 5.12 Water injection rates for Cases 1A, 1B, 1C, and 1D.....	38
Figure 5.13 Oil production rate for Cases 1A, 1B, 1C, and 1D.....	38
Figure 5.14 Water cuts for Cases 1A, 1B, 1C, and 1D.....	39
Figure 5.15 Water bank occurring when polymer loss to the formation.....	39
Figure 5.16 Polymer injection totals for Cases 1A, 1B, 1C, and 1D.....	40
Figure 5.17 Oil recovery factors for Cases 1A, 1B, 1C, and 1D.....	40
Figure 5.18 Location at which the effective polymer solution viscosity is calculated (black box).....	42
Figure 5.19 Determination of the optimal size of the first polymer slug for two- slug injection	44
Figure 5.20 Overinjection of the first polymer slug for two-slug injection	45
Figure 5.21 Underinjection of the first polymer slug for two polymer-slug injection	46
Figure 5.22 Water injection rates for Cases 2A, 2B, 2C, and 2D.....	48
Figure 5.23 Oil production rate for Cases 2A, 2B, 2C, and 2D.....	48
Figure 5.24 Water cuts for Cases 2A, 2B, 2C, and 2D.....	49
Figure 5.25 Polymer injection totals for Cases 2A, 2B, 2C, and 2D.....	49
Figure 5.26 Oil recovery factors for Cases 1A, 1B, 1C, and 1D.....	50
Figure 5.27 Two polymer slugs and drive water break through simultaneously (optimal case).....	51
Figure 5.28 Two polymer slugs break through before drive water (overinjection).....	52
Figure 5.29 Drive water is fingering through two-slug of polymer (underinjection).....	53
Figure 5.30 Water injection rates for Cases 3B, 3C, and 3D.....	55
Figure 5.31 Oil production rate for Cases 3B, 3C, and 3D.....	55
Figure 5.32 Water cuts for Cases 3B, 3C, and 3D.....	56
Figure 5.33 Polymer injection totals for Cases 3B, 3C, and 3D.....	56

	Page
Figure 5.34 Oil recovery factors for Cases 3B, 3C, and 3D.....	57
Figure 5.35 Comparative results when the first slug concentration is 500 ppm (A).....	59
Figure 5.36 Comparative results when the first slug concentration is 1000 ppm (B).....	59
Figure 5.37 Comparative results when the first slug concentration is 2000 ppm (C).....	60
Figure 5.38 Comparative results when the first slug is concentration 3000 ppm (D).....	60
Figure 5.39 Water cut for different inaccessible pore volume cases.....	62
Figure 5.40 Oil recovery factor for different inaccessible pore volume cases ...	62
Figure 5.41 Cumulative polymer adsorption for different polymer adsorption cases.....	64
Figure 5.42 Water cut for different polymer adsorption cases	64
Figure 5.43 Oil recovery factor for different polymer adsorption cases.....	65
Figure 5.44 Injection rate for different residual resistant factor cases	66
Figure 5.45 Water cut for different residual resistant factor cases	66
Figure 5.46 Oil recovery factor for different residual resistant factor cases	67
Figure 5.47 Water cut for different mixing parameter cases	68
Figure 5.48 Oil recovery factor for different mixing parameter cases	69
Figure 5.49 Tornado chart of input parameters related to polymer flooding.....	70

List of Abbreviations

API	degree (American Petroleum Institute)
BHP	bottomhole pressure
cp	centipoises
ft	feet
GOR	gas-oil ratio
HPAM	hydrolyzed polyacrylamide
IPV	inaccessible pore volume
md	millidarcies
MSTB	thousand stock tank barrels
MMSTB	million stock tank barrels
OOIP	original oil inplace
ppm	part per million
PVT	pressure-volume-temperature
RF	recovery factor
RRF	residual resistance factor
SCAL	special core analysis
STB/D	stock tank barrels per day

ศูนย์วิทยทรัพยากร
จุฬาลงกรณ์มหาวิทยาลัย

Nomenclatures

A	flow area between two cells
B_o	oil formation volume factor
B_w	water formation volume factor
B_r	rock formation volume factor
C_a	polymer adsorption concentration
C_n	salt concentration in the aqueous phase
C_p	polymer concentration in solution
d	differential
f_w	fractional flow of water
F_m	multiplier to water viscosity
F_r	shear thinning multiplier
F_{rr}	residual resistance factor
F_w	water flow rate in surface unit
g	gravity acceleration
h	formation thickness
k	permeability
k_o	oil permeability
k_r	relative permeability
k_{rg}	relative permeability to gas
k_{ro}	relative permeability to oil
k_w	initial brine permeability
k_{wp}	permeability to brine after contact with polymer solution
M	mobility ratio
n_g	gas corey exponent
n_o	oil corey exponent
n_w	water corey exponent
p	pressure
p_i	initial reservoir pressure
q_{inj}	injection rate
q_o	oil flow rate

q_{prod}	production rate
q_w	water flow rate
R_s	solution gas oil ratio
S_{dpv}	dead pore space within each grid cell
S_g	gas saturation
S_{gc}	critical gas saturation
S_o	oil saturation
S_{org}	residual oil saturation to gas
S_{orw}	residual oil saturation to water
S_w	water saturation
t	time
T	transmissibility
V	block pore volume



ศูนย์วิทยทรัพยากร
จุฬาลงกรณ์มหาวิทยาลัย

GREEK LETTERS

Σ	sum over neighboring cells
ρ	density
Φ	porosity
μ	fluid viscosity
Δ	difference operator



ศูนย์วิทยทรัพยากร
จุฬาลงกรณ์มหาวิทยาลัย

CHAPTER I

INTRODUCTION

The development of improved oil recovery (IOR) techniques in the oil industry has been ongoing. The most commonly used technique to improve oil recovery after primary depletion is water flooding. However, in the viscous oil reservoir in which the mobility ratio between injected water and oil is unfavorable, water flooding has poor displacement efficiency, resulting in an early break through and rapid increase in water/oil ratio at the producer. Consequently, the amount of remaining oil in place is quite high. Thus, it is necessary to develop other techniques to recover oil with better efficiency.

Polymer flooding is one of the techniques that can be applied in medium viscosity oil reservoir. Addition of high-molecular weight water-soluble polymers in dilute concentrations will increase the viscosity of water, resulting in a decrease in water/oil mobility ratio. This process is sometimes called “Mobility-Control Processes”. A typical polymer flooding project involves mixing and injecting polymer over an extended period of time until a slug volume equal to about 1/3 of the reservoir pore volume has been injected. This polymer slug is then followed by continued injection of water to drive the polymer slug and the oil bank in front of it towards the production wells. To achieve maximum efficiency, the polymer solution is often applied in the form of a tapered slug, i.e., the polymer concentration is reduced systematically as more pore volume is injected.

Many field-scale polymer flooding projects have been successfully implemented such as the case of the biggest oil field in China, Daqing. The project was started in 1996 and achieved oil production from polymer flooding over 10 million tons^[1]. Another example is Sanand oil field in India where polymer injection was commenced in 1995. The total oil recovery from polymer flooding is expected to be 22% higher than that from water flooding^[2]. The success of polymer flooding in many fields around the world has generated an interest to study the possibility of polymer flooding in a medium viscosity oil reservoir in Thailand.

The purpose of this study is to investigate the production performance of an oil reservoir with medium viscosity by optimizing polymer concentration and slug size. The results will be compared with performance of water flooding in order to provide comparative information.

1.1 Outline of Methodology

1. Gather and prepare data for simulation model.
2. Define the reservoir model, simulation cases and range of reservoir parameters.
3. Construct hypothetical reservoir simulation model based on a quarter five-spot flooding pattern with reservoir and fluid properties from an onshore oilfield in Thailand.
4. Perform simulation run for water flooding as base case.
5. Input polymer flood parameters such as polymer solution viscosity, polymer shear thinning data, mixing parameter, inaccessible pore volume, polymer adsorption, residual resistance factor (RRF), etc. into ECLIPSE 100 reservoir simulator with special function.
6. Perform simulation runs for polymer flooding of following scenarios:
 - *Single polymer slug*
 - *Two polymer slugs*
 - *Two polymer slugs with drive water*
7. Evaluate all scenarios to determine the optimum case of polymer flooding.
8. Conduct sensitivity analysis to study the effect of some input parameters related to polymer flooding.
9. Compare and discuss the simulation results and make the conclusion.

1.2 Thesis Outline

This thesis consists of six chapters as outlined below:

Chapter II reviews previous works related to polymer flooding and polymer properties.

Chapter III introduces the theory and concept related to this study.

Chapter IV explains the detail of model construction and polymer flood parameters used in the simulation.

Chapter V presents the results from simulations, discussion and sensitivity study.

Chapter VI concludes the results obtained from the study and recommendations for the further study.



CHAPTER II

LITERATURE REVIEW

This chapter reviews previous works that are related to polymer flooding and polymer properties.

2.1 Previous Works on Polymer Flooding Project

Polymer flooding is often applied in medium-heavy viscosity oil reservoirs instead of water flooding since it can slow down water breakthrough time, improve displacement efficiency and consequently recover more oil. Many polymer flooding projects around the world have been successfully implemented. The following literatures discuss some related works on polymer flooding.

Demin et al. ^[1] presented a technical aspect of polymer flooding in Daqing oil field. The authors also described the development of down-hole technology, design, results of the field test in Daqing. It was shown that polymer flooding can increase the recovery by more than 12% of OOIP with operational costs comparable to that of water flooding. Both volumetric sweep efficiency and displacement efficiency increased. The testing results of polymer flood in glass etched core showed that polymer fluid can pull residual oil out more than water. The reason is that polymer fluid has elastic properties. The polymer in front can pull residual oil behind and beside it. So, the authors concluded that the elasticity of the polymer fluid is the main reason of the increment in displacement efficiency.

Dass et al. ^[2] presented main practices for maintaining the quality of injection polymer/chase water and other process parameters and shows how it helped improve the efficiency and effectiveness of the polymer IOR technique in Sanand field. The authors concluded that the polymer flooding project has helped in: (1) improving oil recovery from the field; (2) slowing down the increase in water cut; (3) reducing the encroachment of aquifer water; (4) maintaining the reservoir pressure above the bubble point; (5) stopping free gas generation in the reservoir by maintaining two

phase flow; and (6) improving residual resistance factor, mobility of a brine solution before and after polymer injection, by reducing further water cut in the field.

Wassmuth et al. ^[3] demonstrated in a stepwise fashion, from laboratory test to reservoir simulations to economic analysis, the potential impact the polymer flood technology has on heavy oil recovery. For some coreflood tests, the polymer flood was able to double the oil recovery in comparison to a baseline water flood. In order to demonstrate the polymer flood technology on a field scale, simulations were conducted on a reservoir model. The result indicated that under suitable conditions the polymer flood technologies can nearly double the water flood recovery.

Hui et al. ^[4] reviewed recent development of pilot test and industrial scale application of chemical flooding in Daqing oil field. Pilot test results show that high molecular weight polymer pre-slug technology can obviously improve polymer flooding efficiency, which specifically are increase of injection pressure, decrease of water intake index, and reduction in water cut.

Azri et al. ^[5] studied IOR process in which polymer is injected into reservoir with a strong bottom aquifer drive bearing heavy-oil. The optimization was performed using a simulation model. The results showed that the optimum development concept which would help reduce impact of polymer loss to the aquifer is best to place new injectors between the existing producers slightly deeper than mid way in oil column. Since polymer loss to the aquifer is minimized, a reasonable amount of oil above the injectors is exposed to the polymer.

2.2 Previous Works on Polymer Properties

Polymer properties are important factors in polymer flooding. Several polymer products are manufactured. Nevertheless, commercial polymers fall into two types: polyacrylamides and polysaccharide. Some related studies of polymer properties are presented in this section.

Liauh and Liu. ^[6] conducted a laboratory test using capillary viscometer to measure viscosities of three types of EOR polymer solutions: xanthan biopolymer, polyacrylamide and scleroglucan polymer. The conditions involve high temperature and low shear rate. The result indicated that viscosities of different polymers respond

differently to change in temperature. The scleroglucan polymer appears to have the least effect from temperature or the least decrease in viscosity when temperature increases. The authors concluded that the relationship between viscosity and temperature is an importance consideration in selecting the most effective polymers for high temperature applications.

Demin et al. ^[7] introduced the rheology of polyacrylamide (PAM) solutions and the effect of viscous-elastic fluids of PAM solution upon production equipment. The negative effects of viscous-elastic fluids on production equipment are the increase in vibration, decrease in efficiency, shorter service life, and increase in maintenance work. After modification of the equipment and flow system, the previously mentioned negative influences of the PAM fluid can be greatly reduced.

Lee et al. ^[8] studied the rheological properties of EOR polymer solutions, mainly partially hydrolyzed polyacrylamide (HPAM). Rheological measurements were made to characterize the apparent viscosity of EOR polymers as a function of shear rate, polymer concentration, polymer molecular weight, degree of hydrolysis, salinity, hardness, and temperature. The parameters in the rheological models that correlate polymer viscosity with these variables were determined and used to develop a polymer database.

CHAPTER III

THEORY AND CONCEPT

This chapter presents the basic principles of polymer flooding process and characteristics of polymers.

3.1 Polymer Flooding Process

Polymer flooding is a mobility-controlled improved oil recovery process. It is preferable when the water-oil mobility ratio is high for water flooding or the reservoir geology is highly heterogeneous. Reservoirs with evidence of geological heterogeneity or extensive stratification and high permeability contrast between channels are potential candidates for polymer flooding by delaying water breakthrough and providing more uniform volumetric sweep of the reservoir. High viscosity solutions of large polymeric molecules dissolved in water at a small concentration are injected into the reservoir for oil displacement. The water-oil mobility ratio is lowered by the high-viscosity of the aqueous solution, resulting in lower oil saturation behind the polymer front and promoting cross-flow between swept and unswept areas. As a result, the overall oil recovery is improved with greater sweep efficiency.

Figure 3.1 shows a typical polymer flood schematic. The polymer flood process usually starts with a pre-flush of fresh water or low-salinity brine, followed by polymer solution. The final step is injecting the driving water to push the polymer slug throughout the reservoir. The polymer solution is often applied in the form of a tapered slug, lower concentration of polymer solution is usually used as a buffer to protect the polymer solution from backside dilution.

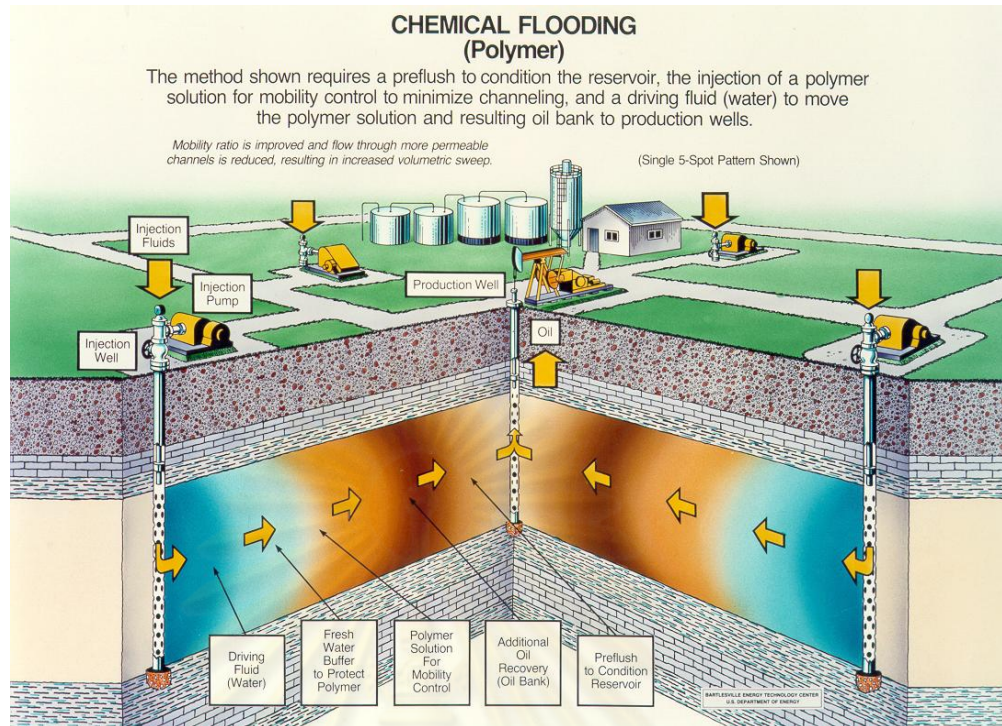


Figure 3.1: Polymer flooding process^[9].

3.1.1 Mobility Ratio

The mobility ratio is the ratio of the displacing fluid mobility to the displaced fluid mobility. It is the primary factor that affects the displacement efficiency of a given well spacing and pattern of water flood. It is defined for water flood as:

$$\text{Mobility ratio (M)} = \frac{k_{rw}/\mu_w}{k_{ro}/\mu_o} = \frac{\lambda_w}{\lambda_o} \quad (3.1)$$

Mobility ratio can be lowered by adding a polymer to the injected water in a water flood. The polymer flooding process is based primarily on maintaining a favorable mobility ratio to improve displacement efficiency. Figure 3.2 provides an example of macroscopic displacement efficiency improvement by polymer flooding over water flooding.

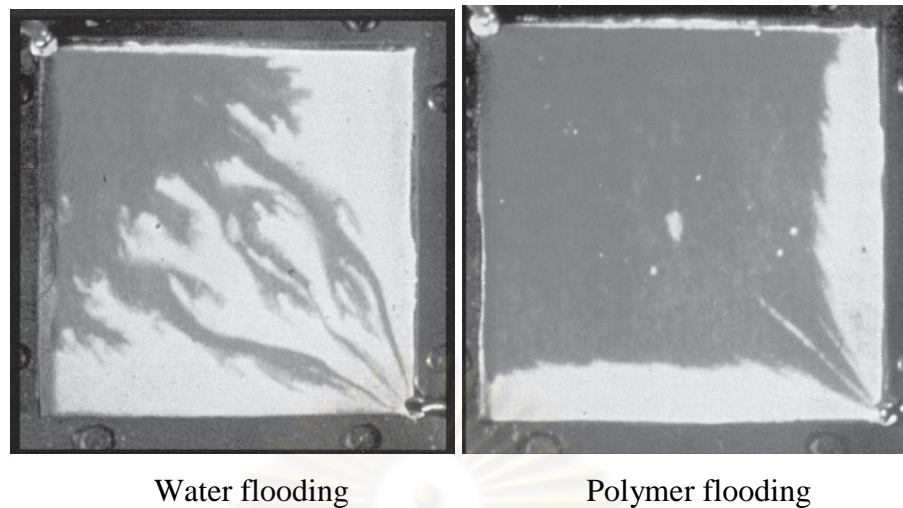


Figure 3.2: Schematic of macroscopic displacement efficiency improvement by polymer flooding^[10].

3.1.2 Polymer Flooding Fractional Flow

The effect of inaccessible pore volume, polymer adsorption, and the formation of two shock fronts are important considerations in the application of fractional flow theory to polymer flooding. Let us consider a one-dimensional pore volume with initial connate water saturation equal to the irreducible water saturation and polymer solution is injected on one end and fluids (oil and water) are produced on the other end. As the polymer solution is injected, the connate water that is contacted is pushed downstream. Higher water saturation corresponds to faster velocity, resulting in the formation of a shock water front. Behind the water front, polymer solution moves slower but also with velocity that is higher corresponding to higher saturations, thereby forming a polymer front. The velocity of the polymer front is retarded by adsorption onto the rock, but on the other hand it is speeded up due to the inaccessible pore volume. The saturation levels at the fronts can be determined graphically as shown in Figure 3.3. The water saturation at the polymer front corresponds to the point of departure of the tangent line (blue straight line) from the polymer-oil fractional flow curve (red curve) that intercepts the x-axis at $-D_p$. D_p is called the retardation factor^[11] and it accounts for the effect of adsorption and inaccessible pore volume.

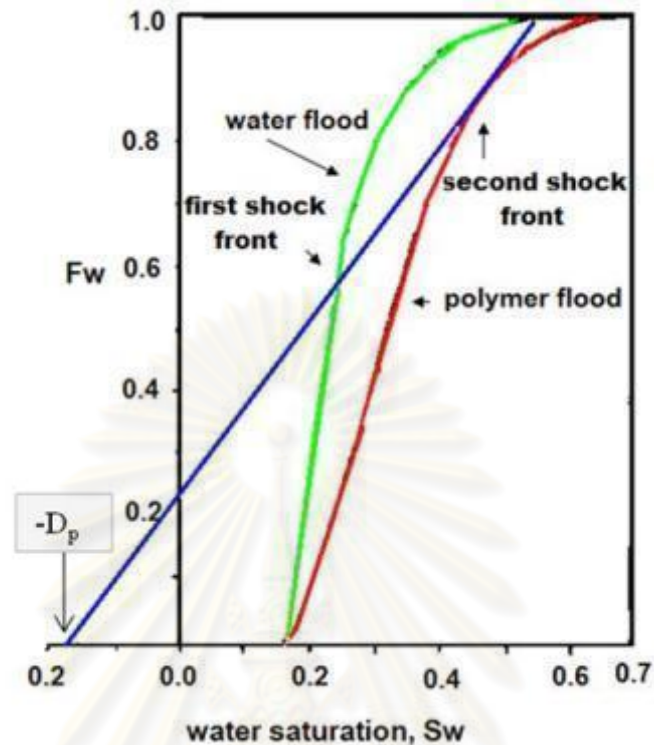


Figure 3.3: Graphical construction of polymer flooding fractional flow^[12].

3.2 Characteristics of Polymers

3.2.1 Polymer Types

Several polymers have been considered for polymer flooding, virtually all the commercially attractive polymers fall into two generic classes: polyacrylamides and polysaccharides (biopolymer).

Polyacrylamides can be manufactured by polymerization of the acrylamide monomer. Molecular weights commonly used range from 1 million to 10 million. Polyacrylamide adsorbs strongly on mineral surfaces. Thus, the polymer is partially hydrolyzed to reduce adsorption by reacting polyacrylamide with a base, such as sodium or potassium hydroxide or sodium carbonate. Hydrolysis converts some of the amide groups (NH_2) to carboxyl groups (COO^-). Figure 3.4 shows the structure of partially hydrolyzed polyacrylamide (HPAM) and polyacrylamide (PAM).

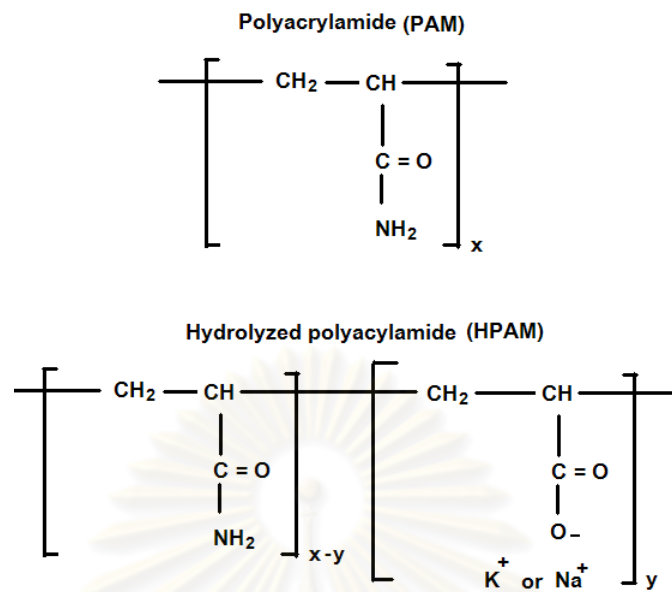


Figure 3.4: Structure of polyacrylamide (PAM) and partially hydrolyzed polyacrylamide (HPAM) ^[13].

Polysaccharides are biopolymers produced commercially by microbial action. The most widely used is xanthan gum. Typical structure of the xanthan gum is shown in Figure 3.5. The xanthan molecule shows practically no decrease of viscosity yield as a function of rising salinity. The reason for this is that the molecule is, because of the side chain structure, essentially stiffer than the polyacrylamide molecule. This may also be the reason for its good shear stability.

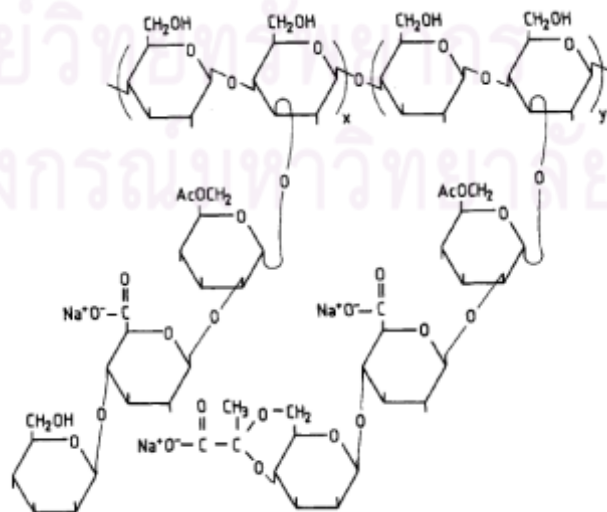


Figure 3.5: Structure of xanthan gum ^[14].

3.2.2 Rheological Properties of Polymer

Polymer solution often exhibits non-Newtonian rheological behavior. Normally, the apparent viscosity of polymer solutions used in IOR processes decreases as shear rate increases. Fluids with this rheological characteristic are said to be shear thinning^[15]. The apparent viscosity decreases because the polymer molecules are able to align themselves with the shear field to reduce internal friction. Often it is possible to represent the rheological properties of a shear thinning fluid by the power-law model. However, shear thinning is often just one part of the rheological behavior. Figure 3.6 shows a typical rheogram of a shear-thinning fluid. At low and high shear rates, the fluid behaves as Newtonian fluid in that the apparent viscosity is constant.

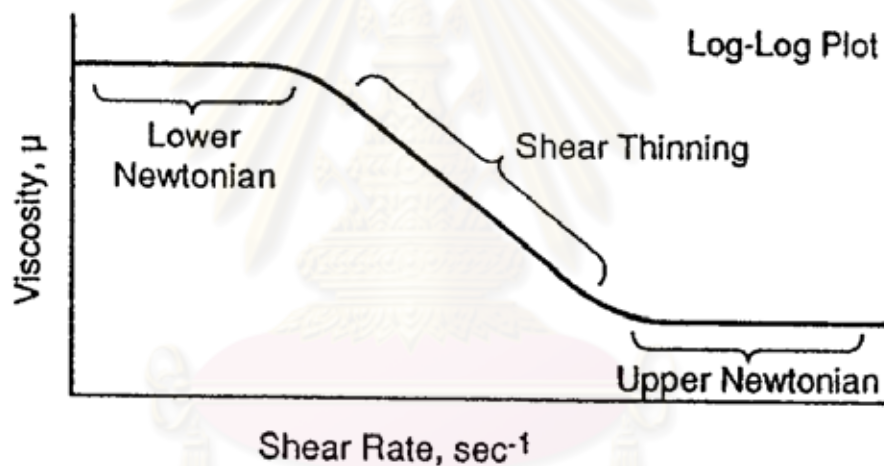


Figure 3.6: Rheology of a shear-thinning fluid ^[16].

3.2.3 Inaccessible Pore Volume

Since polymer molecular sizes are larger than some pores in a porous medium, the polymer molecules cannot flow through those pores. The volume of those pores that cannot be accessed by polymer molecules is called inaccessible pore volume (IPV). In an aqueous polymer solution with tracer, the polymer molecules will run faster than the tracer because they flow only through the pores that are larger than their sizes. This results in earlier polymer breakthrough in the effluent end as shown in Figure 3.7.

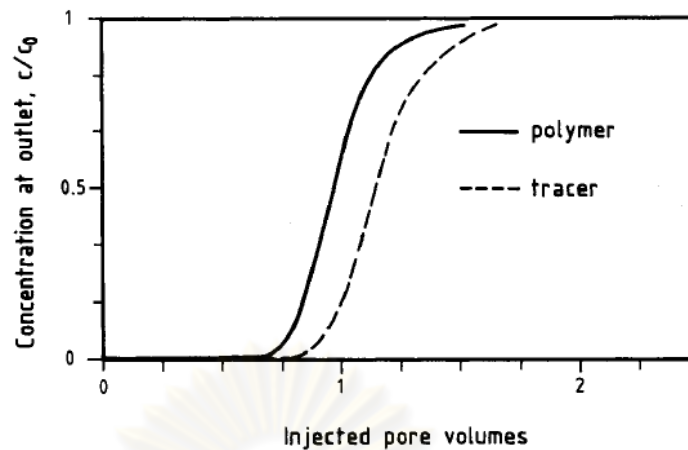


Figure 3.7: Early arrival of polymer front caused by inaccessible pore volume ^[14].

3.2.4 Polymer Retention

All polymers experience retention in permeable media because of adsorption onto solid surfaces or trapping within small pores. Polymer retention varies with polymer type, molecular weight, rock composition, brine salinity, brine hardness, flow rate, and temperature. Different mechanisms of polymer retention are adsorption, mechanical trapping, and hydrodynamic retention as shown in Figure 3.8. Adsorption refers to the interaction between polymer molecules and the solid surface. Mechanical entrapment and hydrodynamic retention mechanisms are related and occur only in flow-through porous media.

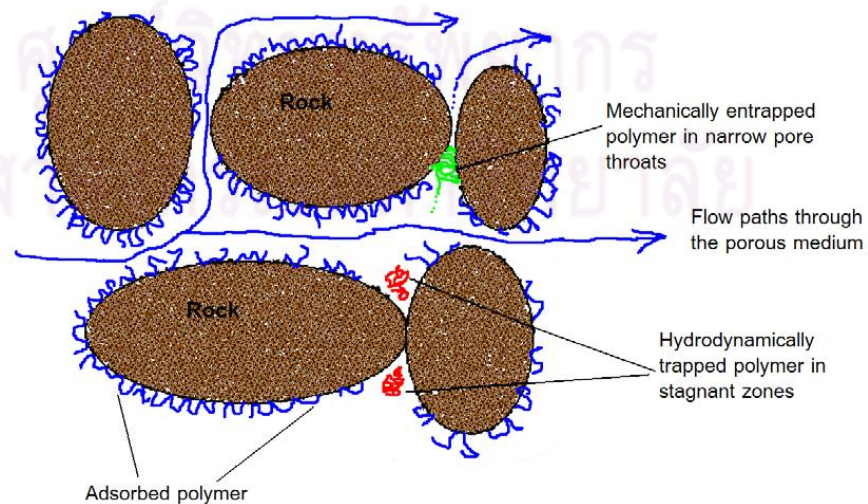


Figure 3.8: Polymer retention mechanisms in porous medium ^[17].

3.2.5 Permeability Reduction

Permeability reduction or pore blocking is caused by polymer adsorption. Therefore, rock permeability is reduced when a polymer solution is flowing through it, compared with the permeability when water is flowing. This permeability reduction is defined by the residual resistance factor (F_{rr}) as expressed in Equation 3.2.

$$F_{rr} = \frac{k_w}{k_{wp}} \quad (3.2)$$

where

F_{rr}	=	residual resistance factor
k_w	=	initial brine permeability
k_{wp}	=	permeability to brine after contact with polymer solution

ศูนย์วิทยทรัพยากร
จุฬาลงกรณ์มหาวิทยาลัย

3.3 Polymer Flood Simulation Model ^[18]

The reservoir simulator used throughout this study is ECLIPSE 100 with special option for polymer flood model, which takes into consideration non-Newtonian rheology, polymer adsorption, permeability reduction and inaccessible pore volume.

The Polymer Flood option uses a fully implicit five-component model (oil/water/gas/polymer/brine) to allow detailed mechanisms involved in polymer displacement process to be studied. The flow of the polymer solution through the porous medium is assumed to have no influence on the flow of the hydrocarbon phases. The standard black-oil equations are therefore used to describe the hydrocarbon phases in the model. The equations are as follows:

For oil,

$$\frac{d}{dt} \left(\frac{VS_o}{B_r B_o} \right) = \sum \left[\frac{TK_{ro}}{B_o \mu_o} (\delta P_o - \rho_w g D_z) \right] + Q_o \quad (3.3)$$

For water,

$$\frac{d}{dt} \left(\frac{VS_w}{B_r B_w} \right) = \sum \left[\frac{TK_{rw}}{B_w \mu_w \text{ eff } R_k} (\delta P_w - \rho_w g D_z) \right] + Q_w \quad (3.4)$$

For polymer,

$$\frac{d}{dt} \left(\frac{V^* S_w C_p}{B_r B_w} \right) + \frac{d}{dt} \left(V \rho_r C_p \frac{1-\phi}{\phi} \right) = \sum \left[\frac{TK_{rw}}{B_w \mu_p \text{ eff } R_k} (\delta P_w - \rho_w g D_z) \right] C_p + Q_w C_p \quad (3.5)$$

For brine,

$$\frac{d}{dt} \left(\frac{VS_w C_n}{B_r B_w} \right) = \sum \left[\frac{TK_{rw} C_n}{B_w \mu_s \text{ eff } R_k} (\delta P_w - \rho_w g D_z) \right] + Q_w C_n \quad (3.6)$$

$$S_w^* = S_w - S_{dpv} \quad (3.7)$$

where S_{dpv} = dead pore space within each grid cell
 C_a = polymer adsorption concentration

ρ_r	=	mass density of the rock formation
ϕ	=	porosity
ρ_w	=	water density
Σ	=	sum over neighboring cells
R_k	=	relative permeability reduction factor for the aqueous phase due to polymer retention
C_p, C_n	=	polymer and salt concentrations respectively in the aqueous phase
$\mu_{a,eff}$	=	effective viscosity of the water, polymer and salt components
D_z	=	cell center depth
B_r, B_w	=	rock and water formation volume factors
T	=	transmissibility
k_{rw}	=	water relative permeability
S_w	=	water saturation
V	=	block pore volume
Q_w	=	water production rate
P_w	=	water pressure
g	=	gravity acceleration

The model makes the assumption that the density and formation volume factor of the aqueous phase are independent of the local polymer and sodium chloride concentrations. The polymer solution, reservoir brine and the injected water are represented in the model as miscible components of the aqueous phase, where the degree of mixing is specified through the viscosity terms in the conservation equations.

The principal effects of polymer and brine on the flow of the aqueous phase are represented by Equations (3.3) to (3.7) above. The fluid viscosities ($\mu_{w,eff}$, $\mu_{p,eff}$, $\mu_{s,eff}$) are dependent on the local concentrations of salt and polymer in the solution. Polymer adsorption is represented by the additional mass accumulation term on the left hand side of the Equation (3.5). The adsorption term requires the user to specify the adsorption isotherm C_a as a function of the local polymer concentration for each

rock species. The effect of pore blocking and adsorption on the aqueous phase relative permeability is treated through the term, R_k , which requires the input of a residual resistance factor for each rock type.

The equations solved by the ECLIPSE polymer model are a discretized form of the differential Equations (3.3) - (3.7). In order to avoid numerical stability problems which could be triggered by strong changes in the aqueous phase properties over a time step (resulting from large changes in the local polymer/sodium chloride concentrations), a fully implicit time discretization is used. The ECLIPSE polymer flood model is therefore free from this type of instability.

3.3.1 Fluid Viscosities

The viscosity terms used in the fluid flow equations contain the effects of a change in the viscosity of the aqueous phase due to the presence of polymer and salt in the solution. However, to incorporate the effects of physical dispersion at the leading edge of the slug and also the fingering effects at the rear edge of the slug, the fluid components are allocated effective viscosity values which are calculated by using the Todd-Longstaff technique^[18].

To get the effective polymer viscosity, it is required to enter the viscosity of a fully mixed polymer solution as an increasing function of the polymer concentration in solution ($\mu_m(C_p)$). The viscosity of the solution at the maximum polymer concentration also needs to be specified and denotes the injected polymer concentration in solution (μ_p). The effective polymer viscosity is calculated as follows:

$$\mu_{p,\text{eff}} = \mu_m (C_p)^\omega \mu_p^{1-\omega} \quad (3.8)$$

where ω = Todd-Longstaff mixing parameter

The mixing parameter is useful in modeling the degree of segregation between the water and the injected polymer solution. If $\omega = 1$, then the polymer solution and water are fully mixed in each block. If $\omega = 0$, the polymer solution is completely segregated from the water.

The partially mixed water viscosity is calculated in an analogous manner by using the fully mixed polymer viscosity and the pure water viscosity (μ_w),

$$\mu_{w,\text{eff}} = \mu_m (C_p)^\omega \mu_w^{1-\omega} \quad (3.9)$$

In order to calculate the effective water viscosity to be inserted into Equation (3.9), the total water equation is written as the sum of contributions from the polymer solution and the pure water. The following expression then gives the effective water viscosity to be inserted into Equation (3.9):

$$\frac{1}{\mu_{w,\text{eff}}} = \frac{1-\bar{C}}{\mu_{w,\text{eff}}} + \frac{\bar{C}}{\mu_{p,\text{eff}}} \quad (3.10)$$

$$\bar{C} = \frac{C_p}{C_{p,\text{max}}} \quad (3.11)$$

where \bar{C} = effective saturation for the injected polymer solution within the total aqueous phase in the cell

If the salt-sensitive option is active, the above expressions are still suitable for the effective polymer and water viscosity terms. The injected salt concentration needs to be specified in order to evaluate the maximum polymer solution viscosity, μ_p . The effective salt component viscosity to be used in Equation (3.6) is set equal to the effective water viscosity.

3.3.2 Polymer Absorption

Adsorption is treated as an instantaneous effect in the model. The effect of polymer adsorption is to create a stripped water bank at the leading edge of the slug. Desorption effects may occur as the slug passes.

The adsorption model can handle both stripping and desorption effects. The user specifies an adsorption isotherm, which tabulates the saturated rock adsorbed concentration versus the local polymer concentration in solution.

There are currently two adsorption models which can be selected. The first model ensures that each grid cell retraces the adsorption isotherm as the polymer concentration rises and falls in the cell. The second model assumes that the adsorbed polymer concentration on the rock may not decrease with time, and hence does not allow for any desorption. More complex models of the desorption process can be implemented if required.

3.3.3 Permeability Reduction and Dead Pore Volume

The adsorption process causes a reduction in the permeability of the rock to the passage of the aqueous phase and is directly correlated with the adsorbed polymer concentration. In order to compute the reduction in rock permeability, the user is required to specify the residual resistance factor (RRF) for each rock type. The actual resistance factor can then be calculated:

$$R_k = 1.0 + (RRF - 1.0) \frac{C_p^a}{C_p^{a_{max}}} \quad (3.12)$$

The value of the maximum adsorbed concentration, $C_{a,max}$, depends on the rock type and needs to be specified by the user. Alternative expressions for the resistance factor can also be implemented if required.

The dead pore space is specified by the user for each rock type. It represents the amount of total pore space in each grid cell which is inaccessible to the polymer solution. The effect of the dead pore space within each cell is to cause the polymer solution to travel at a greater velocity than inactive tracers embedded in the water. The ECLIPSE model assumes that the dead pore space for each rock type does not exceed the corresponding irreducible water saturation.

3.3.4 Non-Newtonian Rheology

The shear thinning of polymer has the effect of reducing the polymer viscosity at higher flow rates. ECLIPSE assumes that shear rate is proportional to the flow velocity. This assumption is not valid in general, for example, a given flow in a low permeability rock will have to pass through smaller pore throats than the same flow in a high permeability rock, and consequently the shear rate will be higher in the low permeability rock. For a single reservoir, however, this assumption is probably reasonable.

The water flow velocity is calculated as:

$$V_w = B_w \cdot \frac{F_w}{\phi A} \quad (3.13)$$

where

F_w	=	water flow rate in surface units
B_w	=	water formation volume factor
ϕ	=	average porosity of the two cells
A	=	flow area between two cells

The reduction in the polymer viscosity is assumed to be reversible and is given by:

$$\mu_{sh} = \mu_{w,eff} \left[\frac{1 + (P-1)M}{P} \right] \quad (3.14)$$

where

μ_{sh}	=	shear viscosity of the polymer solution (water+polymer)
$\mu_{w,eff}$	=	effective water viscosity
P	=	viscosity multiplier assuming no shear effect (entered using the PLYVISC or PLYVISCS keywords)
M	=	shear thinning multiplier supplied in the PLYSHEAR keyword

Note that for $M = 1$, or no shear thinning, we recover the effective water viscosity, and for $M = 0$, or maximum shear thinning, the shear viscosity is

$$\mu_{sh} = \frac{\mu_{w,eff}}{P} \quad (3.15)$$

which corresponds to the minimum viscosity that can be obtained. If the polymer concentration is zero ($P=1$), we recover the effective water viscosity which, in that particular case equals the water viscosity.

The well inflows are treated in a manner analogous to the treatment of block to block flows. The viscosity of the polymer solution flowing into the well is calculated assuming a velocity at a representative radius from the well. The representative radius is taken to be:

$$R_r = \sqrt{R_w R_a} \quad (3.16)$$

where R_w = well bore radius (taken from diameter input in COMPDAT)
 R_a = area equivalent radius of the grid block in which the well is completed

In the present version of ECLIPSE, the radial inflow equation is not integrated over distance from the well to account for the local viscosity reduction due the local velocity.

CHAPTER IV

MODELING APPROACH

4.1 Field Description

The oil field, Field PK, discussed in this study is an unconsolidated sand reservoir located in the lower Northern part of Thailand. Unfortunately, the reservoir has very low oil recovery factor due to early water breakthrough and sand production problem. The reservoir contains medium viscosity oil with low gas oil ratio (oil gravity of 17.2 °API, GOR of 111 Scf/STB). For this reason, various oil recovery techniques such as infill drilling, water flooding, or cyclic steam stimulation have been studied ^[19]. Field PK can be separated into two main structural areas, Main block and West flank, which have different oil water contacts and fluid properties.

Most of production wells are located in southern part of the main block which is an oil zone. So, this study will focus on this area. The distance between each producer is about 400-500 meters or 1312-1640 feet. This range will be used to construct reservoir simulation model in the next section.

4.2 Simulation Model Construction

In order to optimize oil recovery by polymer flooding technique, reservoir simulation was carried out by using ECLIPSE 100 reservoir simulator with special function for polymer flood model. A hypothetical reservoir model was constructed based on a quarter five-spot flooding pattern which represents behavior of five-spot pattern. The results from this study can be used in future pilot test for the area that has five-spot pattern.

4.2.1 Grid

The reservoir model dimension is 1000x1000x50 ft. It consists of 50x50x10 grid blocks. All grid block sizes are 20x20x5 ft. The injection and production wells are located on the opposite corners. The distance between the two wells is 1414 ft which is referred from the distance between each producer in Section 4.1. Figure 4.1 and Figure 4.2 depict the top view and 3D view of reservoir model. After reservoir model had been constructed, rock properties from PK field were assigned to the model. Reservoir dimensions and rock properties are shown in Table 4.1.

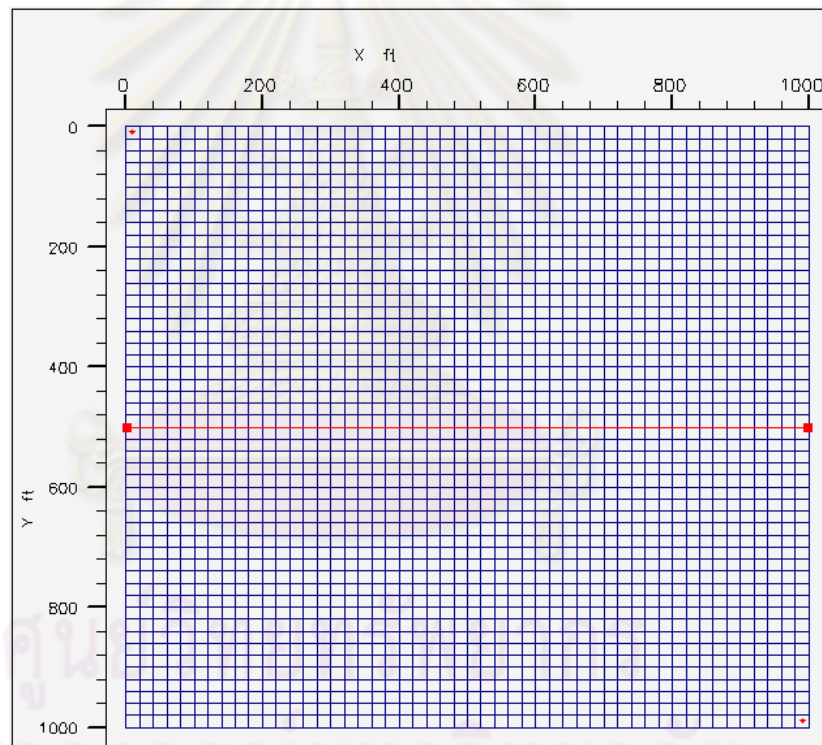


Figure 4.1: Top view of reservoir model.

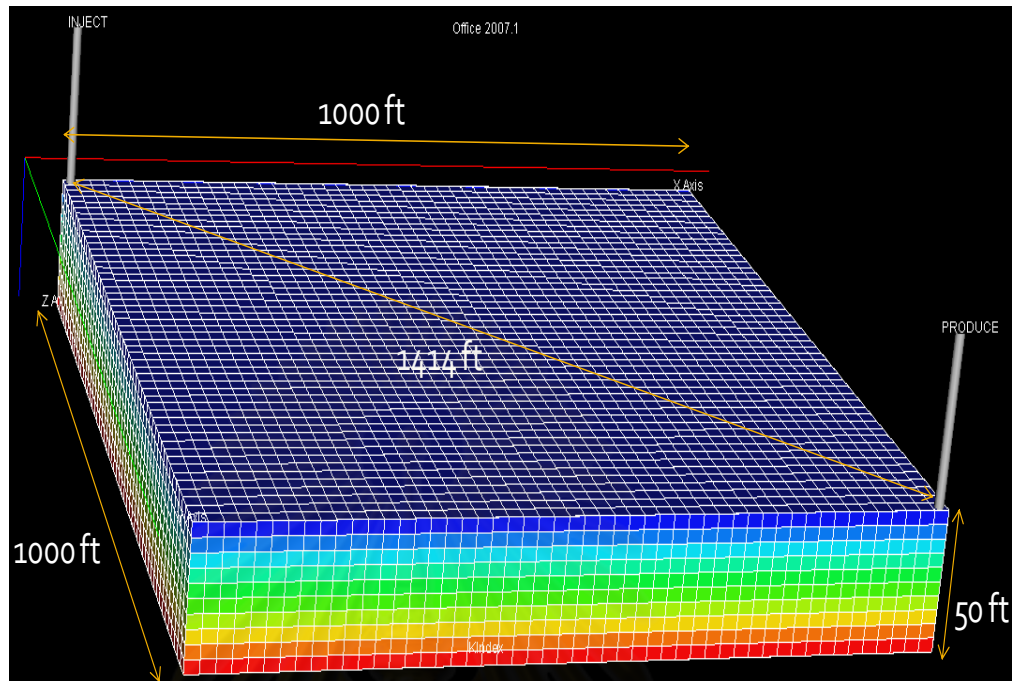


Figure 4.2: Reservoir model in 3D view.

Table 4.1: Reservoir dimensions and rock properties.

Parameters	Unit	Value
Grid dimension	block	50x50x10
Grid size	ft	20x20x5
Porosity	%	30
Horizontal permeability	md	500
Vertical permeability	md	5
Reservoir top face depth	ft	3200
Reservoir thickness	ft	50
OOIP	MMSTB	1.6216

4.2.2 PVT

Fluid properties at surface condition from PK field were used to estimate reservoir fluid properties by using default correlations in ECLIPSE. Table 4.2 summarizes the input data in PVT section. At initial reservoir condition, the reservoir fluids consist of oil and water. The oil has a calculated in-situ viscosity of 42.3 cp, and the in-situ viscosity of water is 0.47 cp. Figures 4.3 and 4.4 show a plot of dry gas and live oil PVT properties, respectively.

Table 4.2: Input data for PVT section.

Parameters	Unit	Value
Oil gravity (stock tank condition)	°API	17.2
Gas gravity (separator condition)	-	0.798
Solution gas/oil ration, R_s	scf/STB	111
Surface temperature	°F	60
Surface pressure	psia	14.7
Reservoir temperature	°F	140
Reservoir pressure	psia	1430
Rock type	-	Unconsolidated sandstone

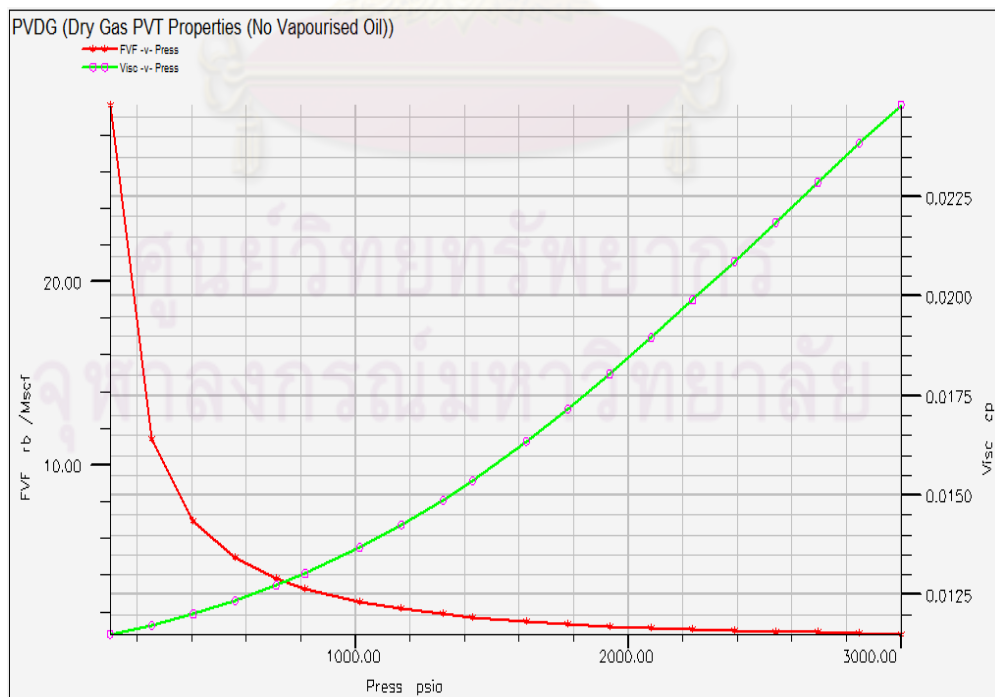


Figure 4.3: Dry gas PVT properties used in the simulations.

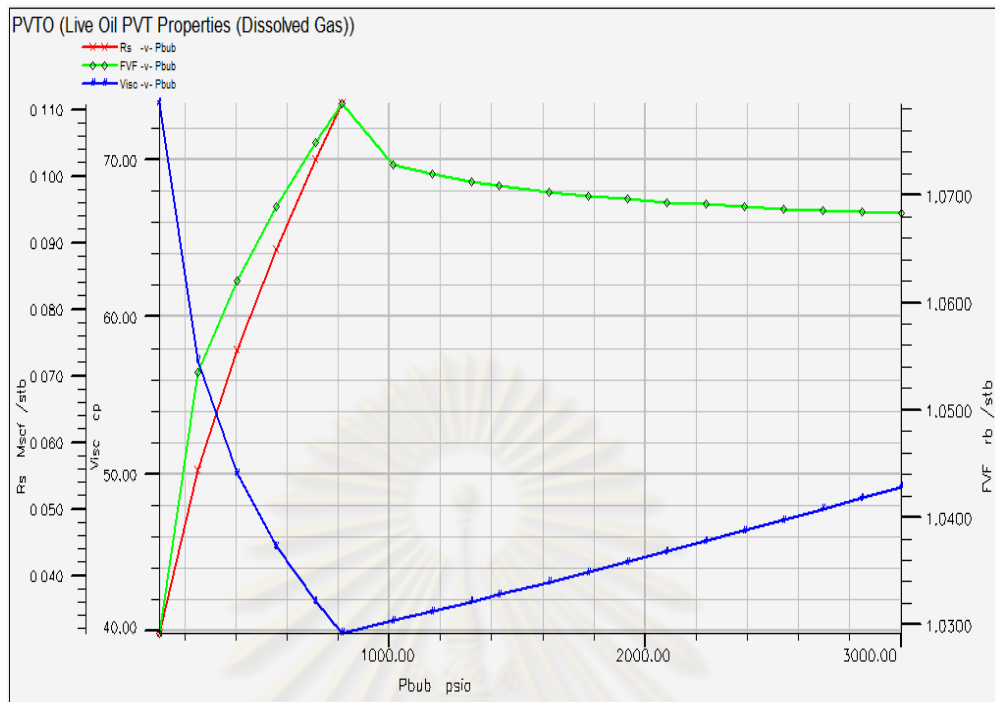


Figure 4.4: Live oil PVT properties used in the simulations.

4.2.3 Relative Permeability

Due to lack of SCAL data from PK field, Corey correlation was used to derive relative permeability curves. The input data, as shown in Table 4.3, were referred from a neighboring field which has the same rock formation. The plots of fluids relative permeability calculated by Corey correlation are shown in Figures 4.5 and 4.6.

Table 4.3: Input data for SCAL section.

Parameters	Symbol	Value
Connate water saturation	S_{wc}	0.35
Residual oil saturation to water	S_{orw}	0.25
Residual oil saturation to gas	S_{org}	0.06
Critical gas saturation	S_{gc}	0.07
End point oil relative permeability	k'_{ro}	0.90
End point water relative permeability	k'_{rw}	0.35
End point gas relative permeability	k'_{rg}	0.93
Oil Corey exponent	n_o	2.00
Water Corey exponent	n_w	2.80
Gas Corey exponent	n_g	2.80

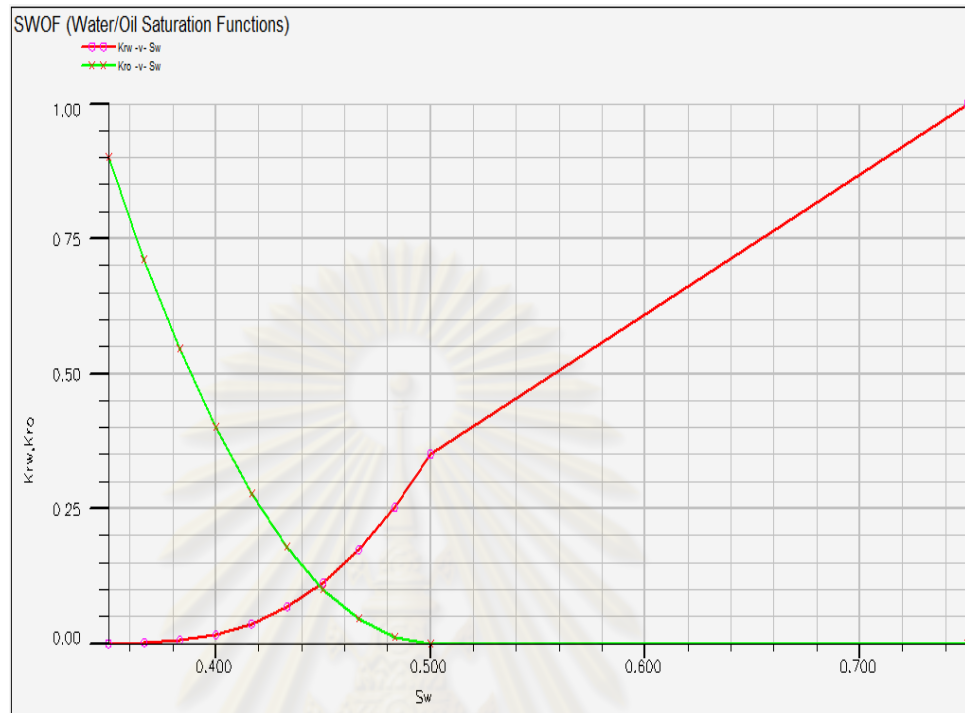


Figure 4.5: Water-oil relative permeability curve.

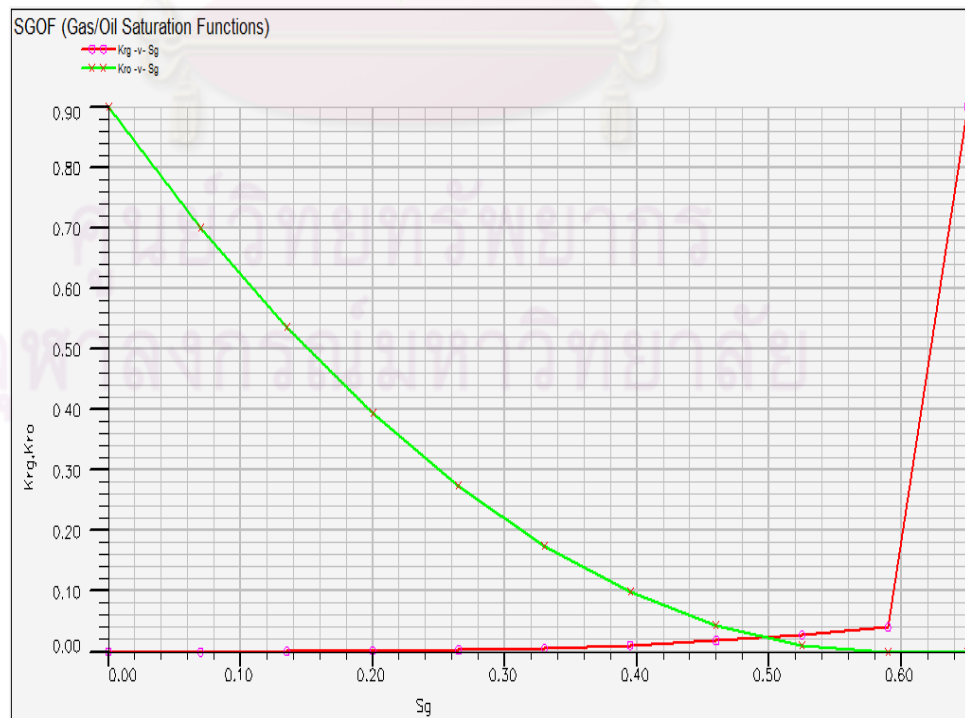


Figure 4.6: Gas-oil relative permeability curve.

4.2.4 Well Specification and Production Constraints

Both of injector and producer are vertical wells fully perforated the sand layer. For the injector, the maximum injection rate is constrained by the fracture pressure. This reservoir has a fracture pressure of 2,500 psia. For safety reason, the maximum injection bottom hole pressure (BHP) is limited at 90 % of the fracture pressure which is 2,250 psia. In this study, the maximum injection rate is set equal to the maximum production rate at 1,000 STB/D ($q_{inj} = q_{prod} = 1,000$ STB/D). For the time step, it is set generally at 1 month. Since the solution type is set as fully implicit, the simulation process is always stable. The economic limits and production constraints are summarized in Table 4.4.

Table 4.4: Production constraint and economic limits.

Parameters	Unit	Value
Maximum injection BHP	psia	2,250
Minimum production BHP	psia	500*
Maximum injection rate	STB/D	1,000
Maximum production rate	STB/D	1,000
Maximum water cut	fraction	0.98
Minimum oil rate	STB/D	20

*Note that we assume that electrical submersible pump is used.

As can be seen in Table 4.4, the economic limits of the producer are set at maximum water cut of 0.98 or minimum oil production rate of 20 STB/D. If the producer exceeds any economic limits, it will automatically shut in.

CHAPTER V

OPTIMIZATION AND SENSITIVITY STUDY

This chapter describes the optimization method and simulation results from polymer flooding. In order to find the optimum polymer concentration and slug size, the results of each scenario of polymer flooding are compared and analyzed with the base case of water flooding. There are three scenarios of polymer flooding as follows:

- **Single polymer slug:** various polymer concentrations (500 ppm, 1000 ppm, 2000 ppm, and 3000 ppm) are injected till breakthrough.
- **Two polymer slugs:** the 1st polymer slug size is adjusted till both slugs break through simultaneously.
- **Two polymer slugs with drive water:** the 2nd polymer slug size is adjusted till both polymer slugs and drive water break through simultaneously.

Furthermore, the optimum case of polymer flooding will be chosen for sensitivity study to observe the impact of uncertainty parameters related to polymer flooding on oil recovery factor.

5.1 Base Case of Water Flooding

After reservoir model construction had been completed (as described in Chapter 4), water flooding was simulated as a base case before each scenario of polymer flooding was evaluated. In this approach, water was injected since the beginning of the production till a production constraint of production well was reached.

Figures 5.1 to 5.6 show simulation results of the base case. Figure 5.1 shows the injection rate of water flooding. At an initial period before breakthrough, the injection rate decreases as a function of time due to the limitation in maximum injection BHP of 2250 psia as seen in Figure 5.2. After water breakthrough, the average reservoir pressure starts to decline (Figure 5.3) and abruptly drop again after the injection rate increases until reaching the maximum injection rate of 1000 STB/D.

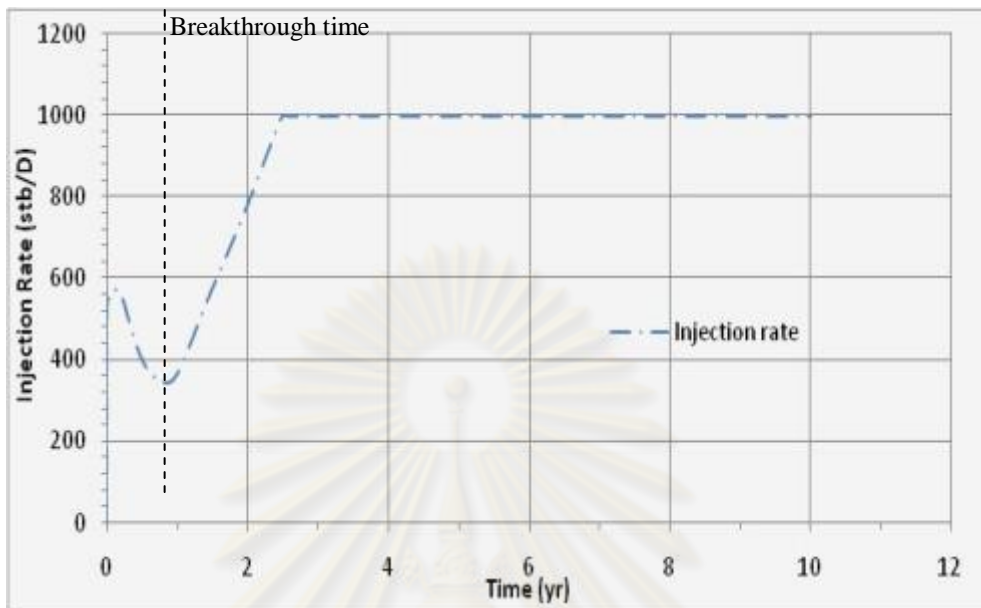


Figure 5.1: Injection rate for base case of water flooding.

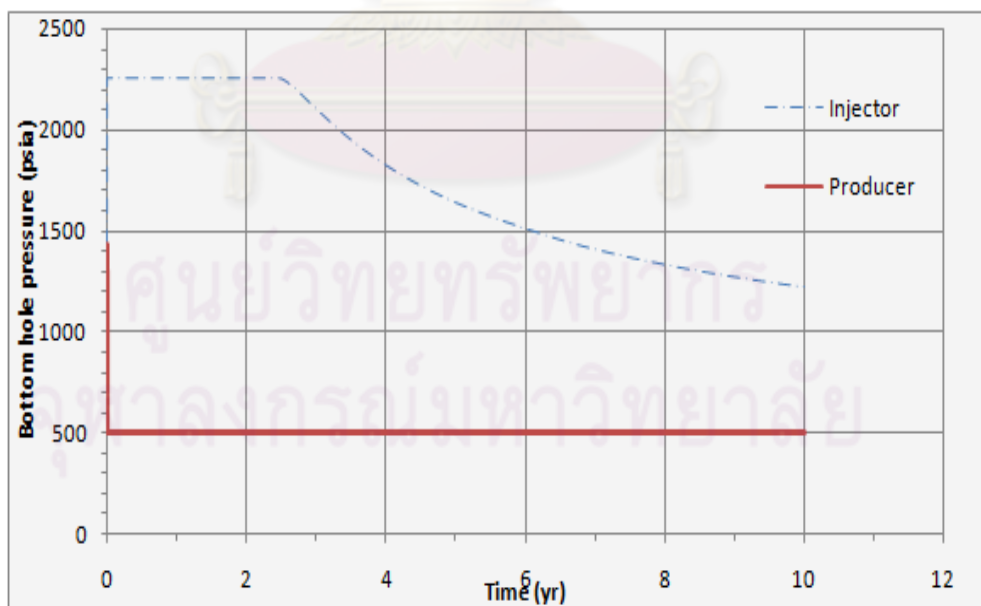


Figure 5.2: Bottom hole pressure for base case of water flooding.

The plot of water cut is shown in Figure 5.4. It can be seen that there is a water breakthrough at 304 days or 0.8 year. At early times, there is a small amount of produced water although the connate water saturation is equal to the critical water saturation ($S_{wc} = S_{wcr} = 0.35$). This is because the connate water expands as the pressure around the producer becomes lower. The expanded water gives rise to an increase in water saturation. As the water saturation becomes higher than the critical water saturation, water can flow near the producer. As the water saturation becomes higher than the critical water saturation, water can flow near the producer.

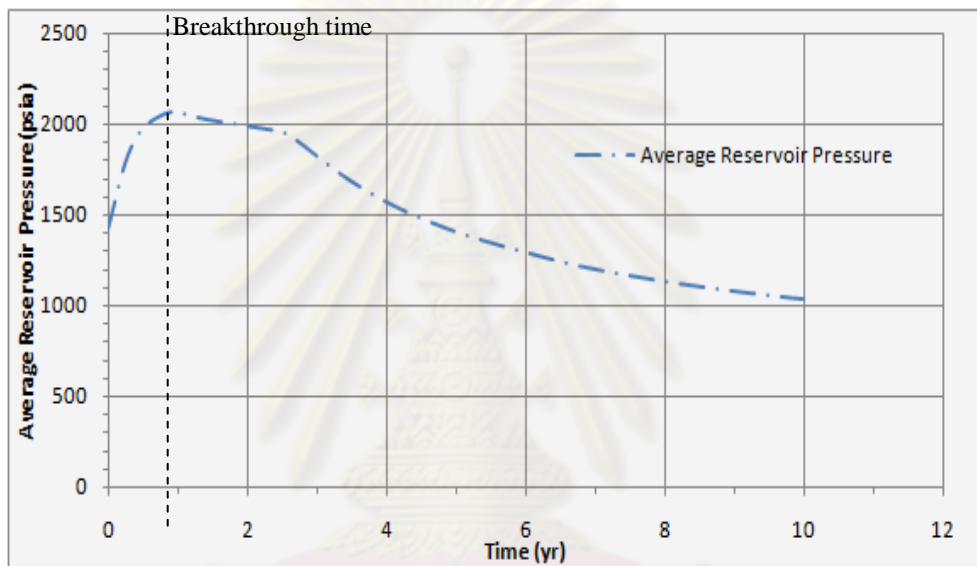


Figure 5.3: Average reservoir pressure for base case of water flooding.

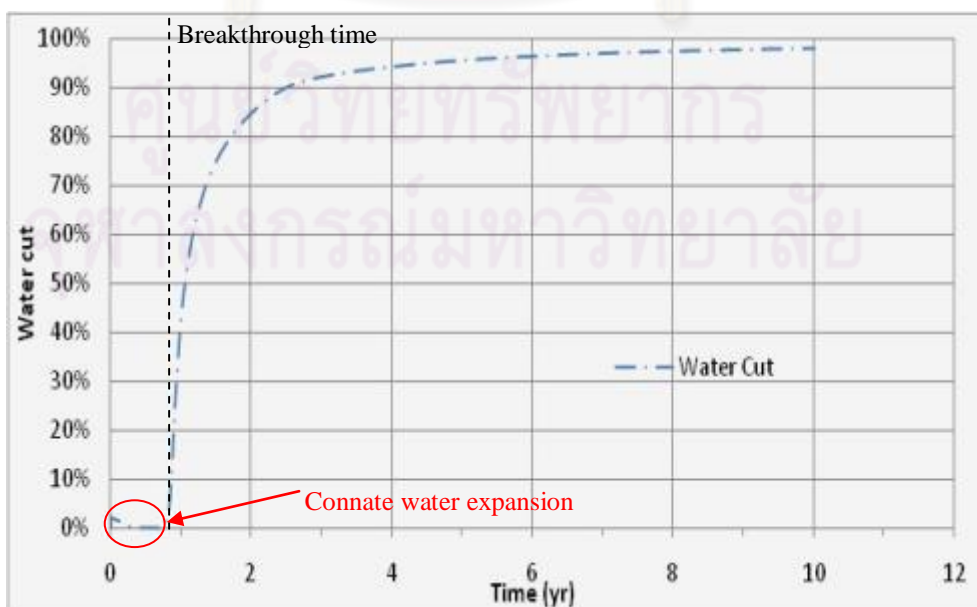


Figure 5.4: Water cut for base case of water flooding.

Figure 5.5 and 5.6 show the oil production rate and recovery factor, respectively. As seen in Figure 5.5, at initial period of production, the oil rate still decreases although water flooding is already started. This is because the oil is slightly compressible and viscous, so it takes a certain time to transfer pressure response to the producer. The producer is shut at 10 years because the oil rate reaches the minimum oil rate of 20 STB/D. The total oil production is 274.575 MSTB. From Figure 5.6, recovery factor obtained from water flooding is 16.93% with production time of 3652 days or 10 years.

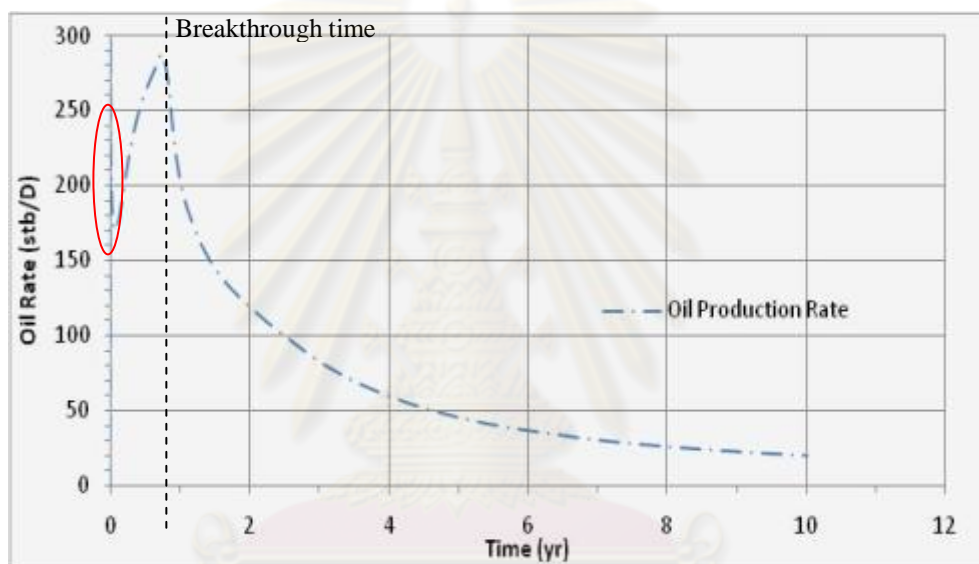


Figure 5.5: Oil production rate for base case of water flooding.

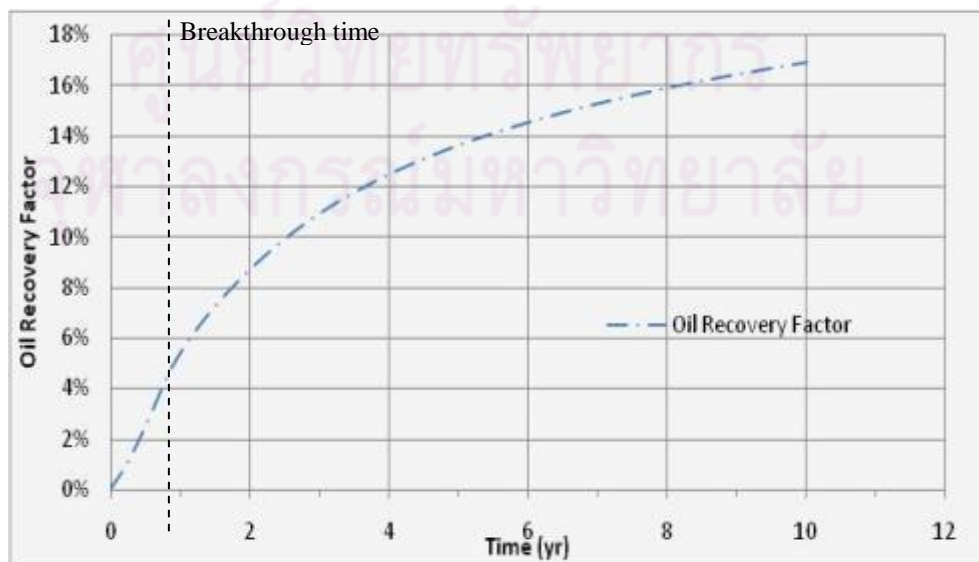


Figure 5.6: Oil recovery factor for base case of water flooding.

5.2 Single Polymer Slug

In this scenario, single slug polymer flooding was evaluated using the black oil mode with polymer flooding option in ECLIPSE. The simulator is capable of modeling polymer using a non-Newtonian rheology. This model targets the shear thinning of polymer that has the effect of reducing polymer viscosity at higher flow rates. The apparent viscosity of commercial HPAM polymer (Flopaam 3330S) as a function of shear rate, polymer concentration, polymer molecular weight and temperature^[8] as shown in Figure 5.7 and 5.8 were used in the model. Note that the measurement condition of Figure 5.7 is at 25 °C. As seen in Figure 5.8, the apparent viscosity at polymer concentration of 2000 ppm at reservoir conditions can be obtained by interpolating to reservoir temperature which is 60 °C. The apparent viscosity of Flopaam 3330S at reservoir conditions is between 2.06 to 60.98 cp as summarized in Table 5.1. Note that the in-situ oil viscosity is 42.3 cp.

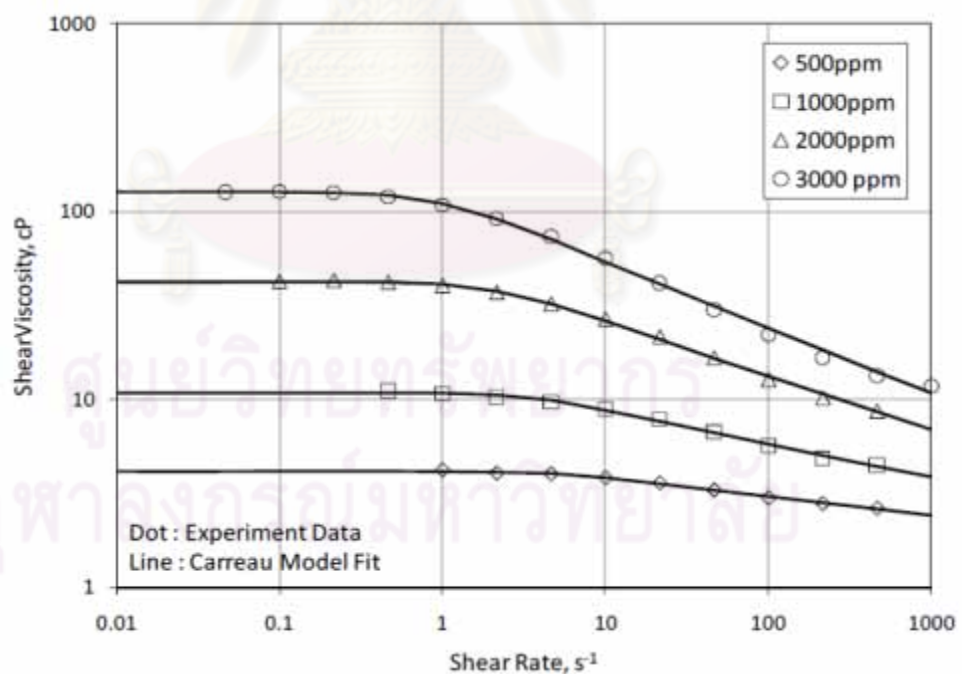


Figure 5.7: Effect of polymer concentration on shear viscosity^[8].

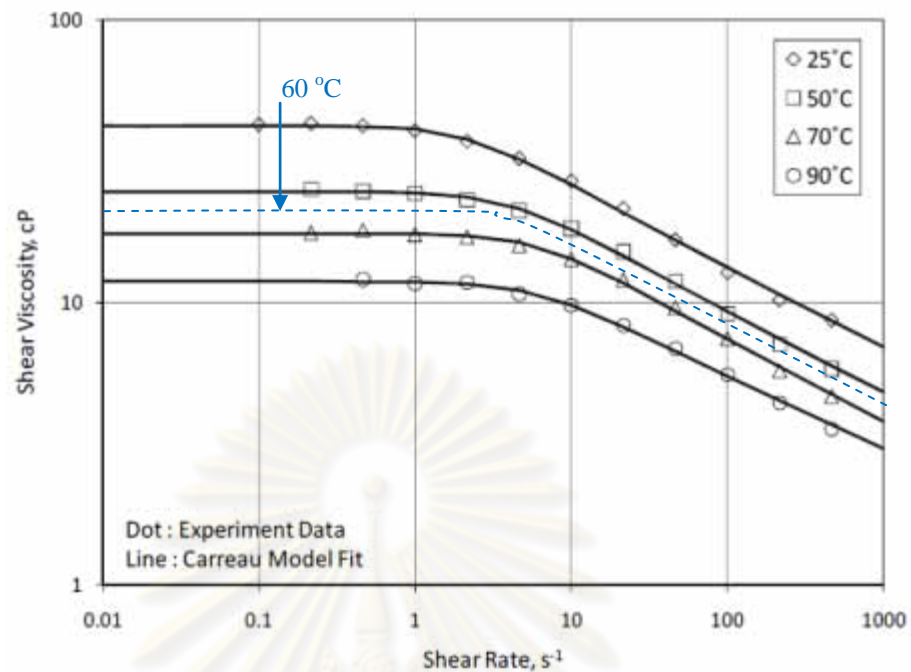


Figure 5.8: Effect of temperature on apparent viscosity^[8].

Table 5.1: Apparent viscosity of Flopaam 3330S.

Polymer concentration		Apparent viscosity (cp)		F_m
ppm	lb/STB	@25 °C	@60 °C	
500	0.1751	4	2.06	4.4
1000	0.3502	10	5.63	12
2000	0.7004	40	20.64	44
3000	1.0506	120	60.98	130

Remark: C_p = polymer concentration
 F_m = multiplier to water viscosity
 In-situ water viscosity = 0.469 cp

As required by ECLIPSE simulator, the PLYVISC keyword, polymer solution viscosity function is expressed as a set of multipliers to water viscosity as shown in Figure 5.9. For example, when polymer concentration is 0.7004 lb/STB, the multiplier to water viscosity is 44, the corresponding viscosity is 20.64 cp which is the in-situ polymer solution viscosity.

Similar to PLYSHEAR keyword, polymer shear thinning data are expressed as a set of shear thinning factor which is multiplied by in-situ polymer solution viscosity. The factor decreases as water phase flow velocity increases. Figure 5.10 shows shear thinning function used in the simulations. In addition, the shear thinning data of Flopaam 3330S used in the simulations are presented in Appendix A.

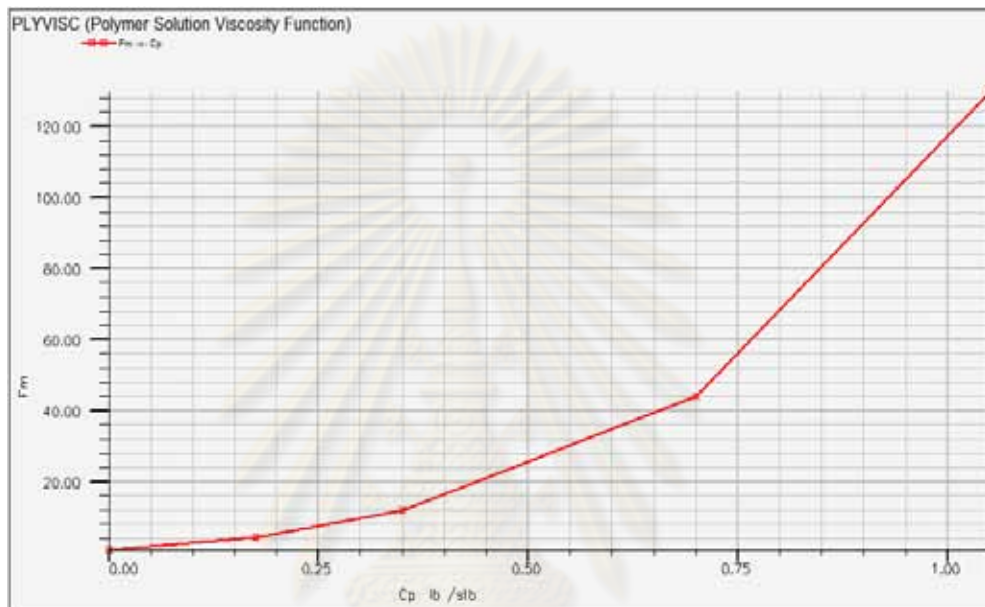


Figure 5.9: Polymer solution viscosity function used in the simulations.

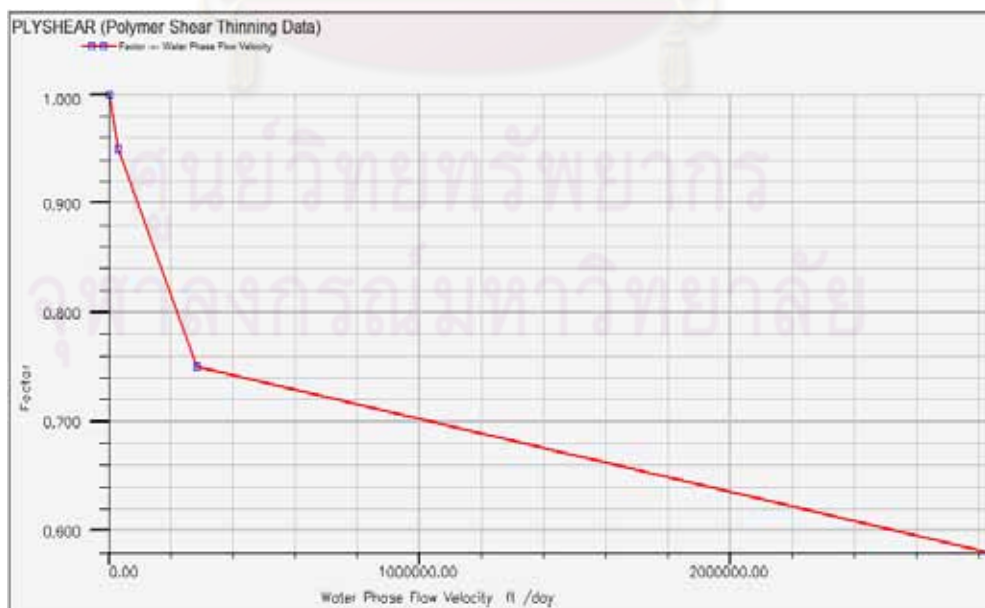


Figure 5.10: Polymer shear thinning data used in the simulations.

Due to lack of information, some input parameters related to polymer flooding such as polymer adsorption, inaccessible pore volume, mixing parameter and residual resistance factor were assumed. Polymer adsorption function is assumed to be 1% of polymer concentration as shown in Figure 5.11. Note that P_{lc} is polymer concentration in the solution (lb/STB) and P_{sc} is concentration of polymer adsorbed by the rock formation (lb/lb).

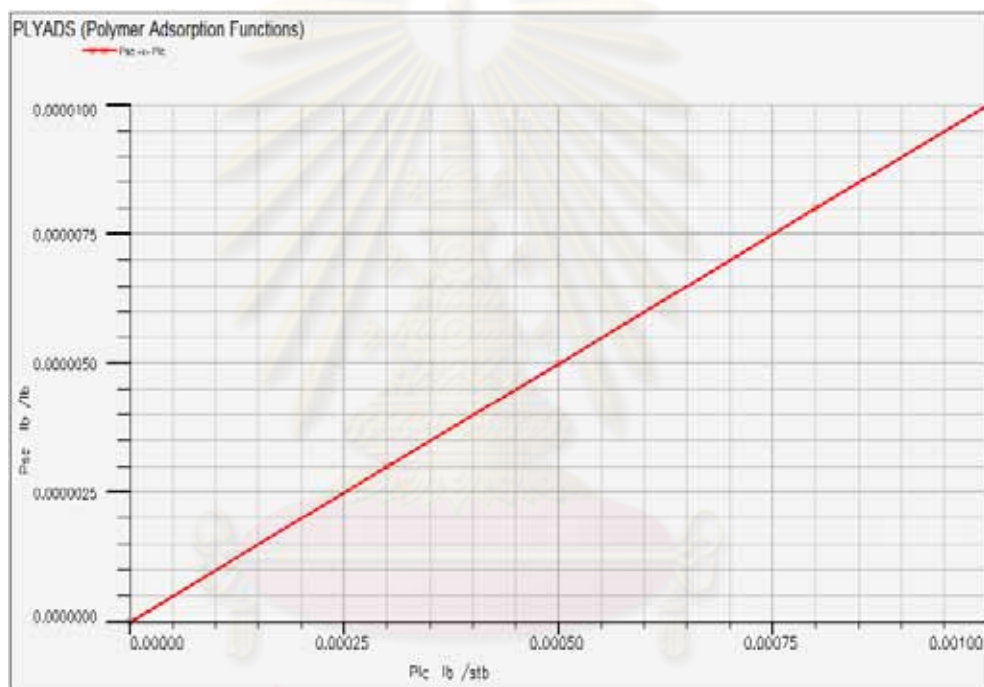


Figure 5.11: Polymer adsorption function used in the simulations.

The vertical injector and producer in the quarter five-spot pattern of in this scenario are still the same as the ones for water flooding. In order to determine the most suitable polymer concentration, four different polymer concentrations were used in the flooding as follows:

Case 1A: Single slug of 500 ppm polymer concentration

Case 1B: Single slug of 1000 ppm polymer concentration

Case 1C: Single slug of 2000 ppm polymer concentration

Case 1D: Single slug of 3000 ppm polymer concentration

Simulation results for all cases of this scenario are compared with water flooding as a base line. Figure 5.12 shows water injection rate for all cases of single slug injection. It is clear that injection with higher polymer concentration results in lower injection rate because the BHP at the injector reaches the well constraint due to high viscosity of the injected fluid. The decrease in injection rate results in lower oil production rate as shown in Figure 5.13. However, the case with low injection and production rate lasts a lot longer than other cases. The average oil production rate obtained from cases 1A, 1B, 1C and 1D is 87, 83, 56 and 38 STB/D, respectively.

Water cut profile for all cases of single slug injection are shown in Figure 5.14. It is observed that higher concentration of injected polymer leads to lower water cut and slower water breakthrough time since the injection rate is lower. There is another interesting phenomenon that should be discussed here. The abrupt increase in water cut profile can be divided into two periods. The first rise in water cut is caused by water bank breakthrough while the second one is caused by polymer front breakthrough. Note that the water bank occurs at the leading edge of injected fluid at which there is no polymer since the polymer is lost to the formation. The polymer front is the leading edge of the part of the injected fluid that still contains polymer as shown in Figure 5.15.

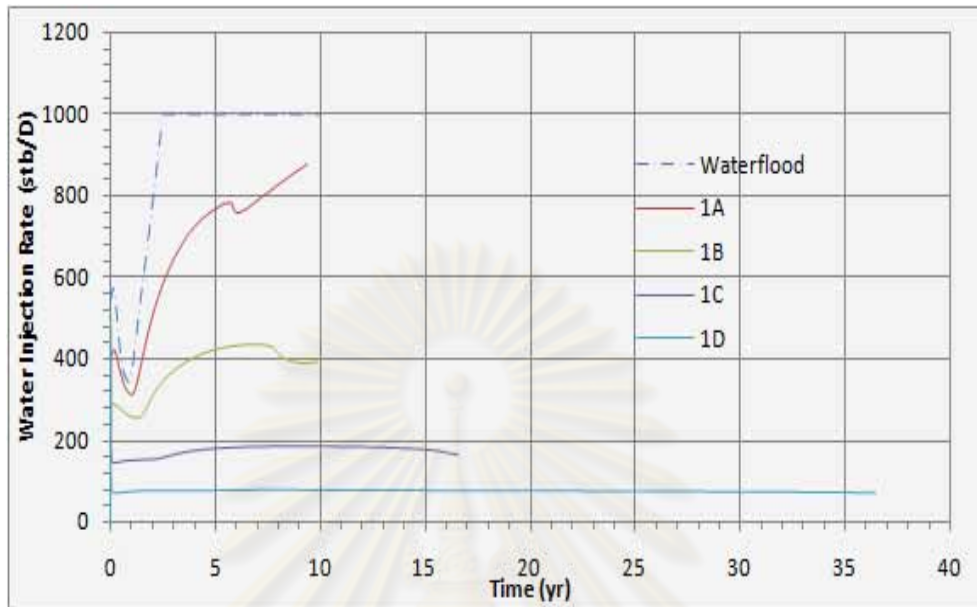


Figure 5.12: Water injection rates for Cases 1A, 1B, 1C, and 1D.

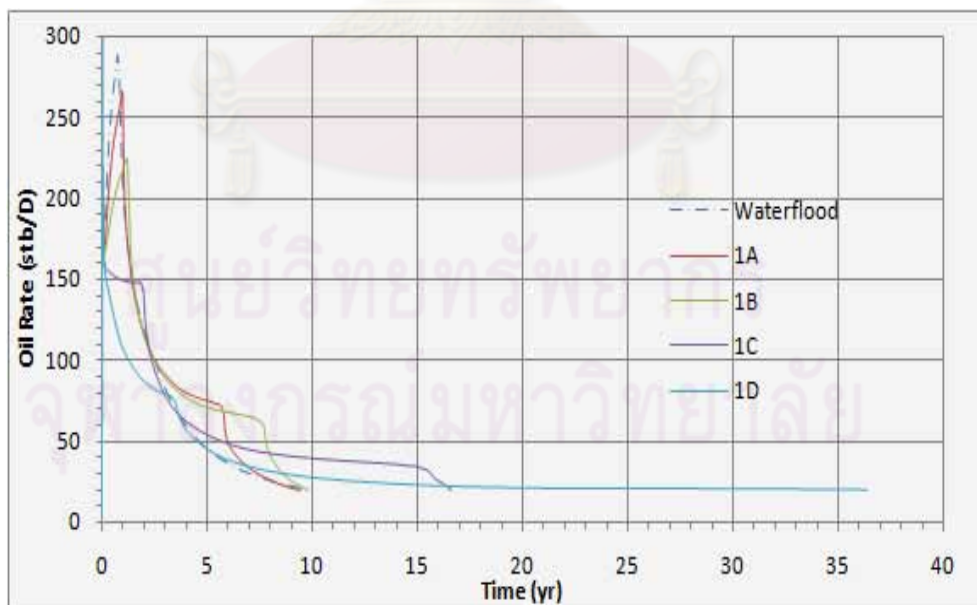


Figure 5.13: Oil production rate for Cases 1A, 1B, 1C, and 1D.

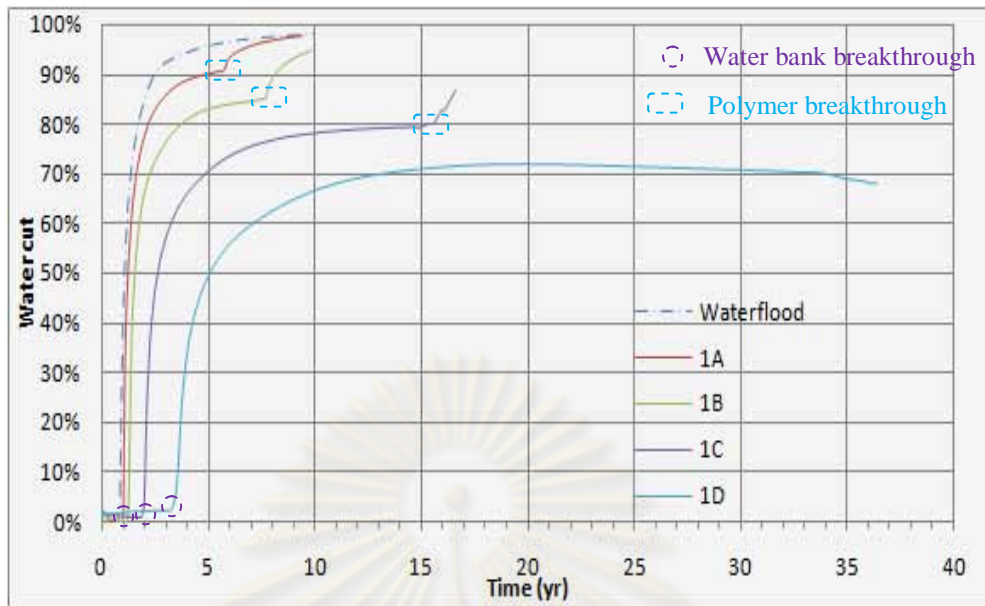


Figure 5.14: Water cuts for Cases 1A, 1B, 1C, and 1D.

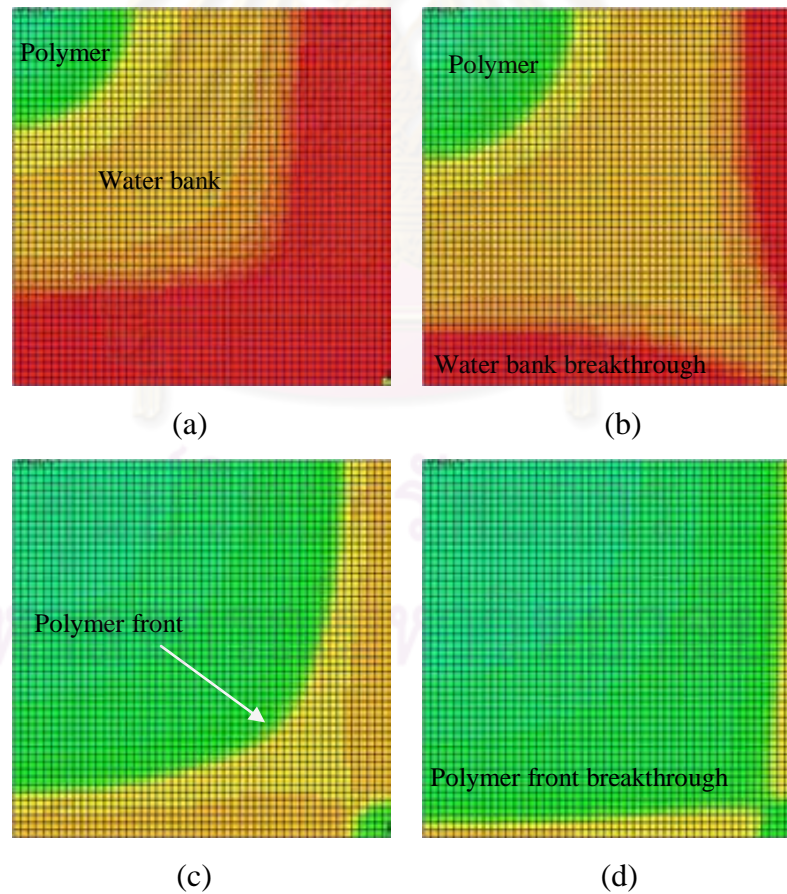


Figure 5.15: Water bank occurring when polymer is lost to the formation.

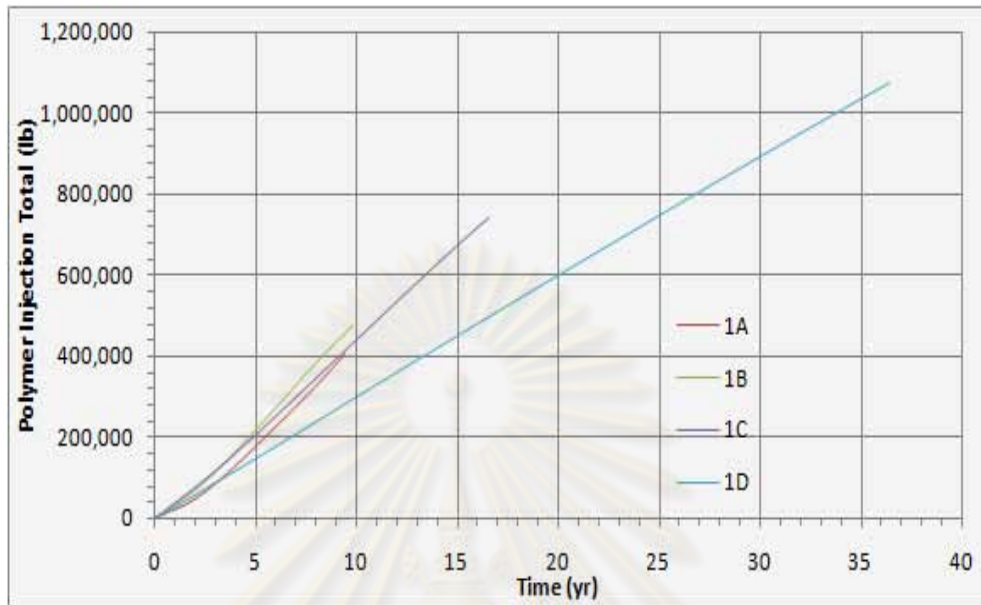


Figure 5.16: Polymer injection totals for Cases 1A, 1B, 1C, and 1D.

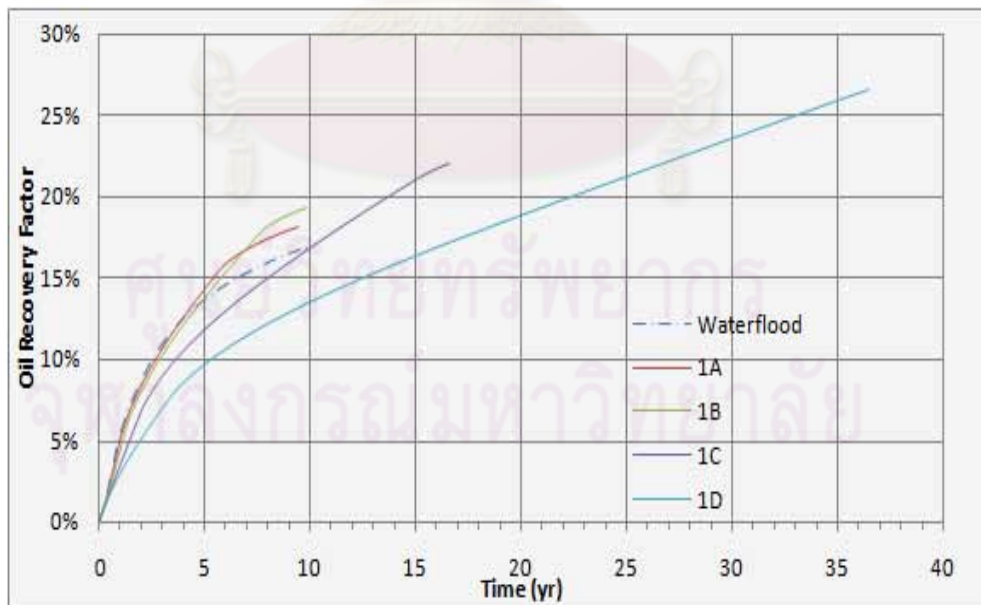


Figure 5.17: Oil recovery factors for Cases 1A, 1B, 1C, and 1D.

Plot of cumulative polymer injection and oil recovery factor for all cases is shown in Figure 5.16 and Figure 5.17, respectively. From Figures 5.16 and 5.17, higher concentration of injected polymer leads to larger total amount of polymer injection and better RF. When compared among all cases, Case 1D not only takes a much longer time but also has the highest total amount of polymer used (1,072,808 lb). Therefore, Case 1D is not attractive for single slug injection.

Table 5.2: Summary of results for single polymer slug.

Case	Production time (Years)	RF (%)	Total polymer used (lb)	Incremental oil/ Total polymer used (STB/lb polymer)
Water flood	10.0	16.93	-	-
1A	9.4	18.17	404,226	0.0495
1B	9.8	19.26	474,220	0.0795
1C	16.6	21.99	743,213	0.1104
1D	36.4	26.53	1,072,808	0.1450

Simulation results of single polymer slug are summarized in Table 5.2. It can be seen that the maximum RF of 26.53% and the highest incremental oil per total polymer used of 0.1450 STB/lb polymer are obtained in Case 1D. However, the longest production time of 36.4 years are also obtained in this case.

ศูนย์วิทยทรัพยากร
จุฬาลงกรณ์มหาวิทยาลัย

5.3 Two Polymer Slugs

The objectives of injecting two slugs of polymer with progressive decrease in polymer concentration are to reduce the total amount of polymer used and to reduce viscous fingering of lower concentration fluid into regions of higher concentration fluid. The optimum size of the first polymer slug can be found by allowing the first and second slugs to break through simultaneously because it is the case that utilizes the least amount of polymer. This can be done by trial and error. ECLIPSE simulator is able to calculate the effective polymer solution viscosity at fixed location. In order to determine the movement of the second slug of polymer, we choose to observe polymer concentration at locations [10,10], [40,40], [45,45], [48,48], [50,50]. These locations are shown in Figure 5.18. Note that injector and producer location is [1,1] and [50,50], respectively.

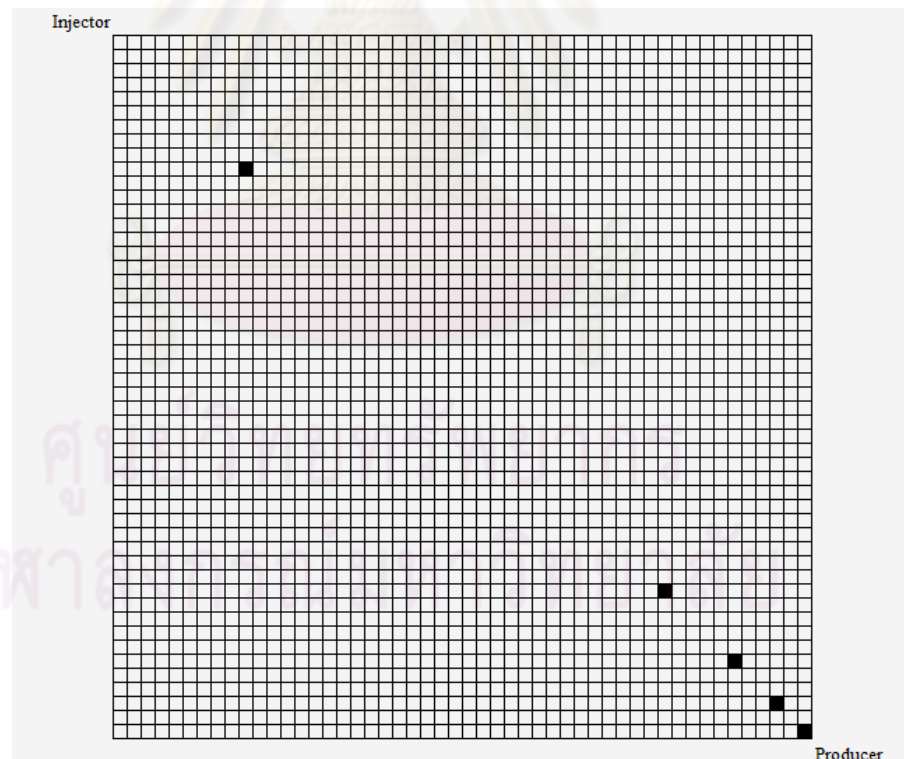
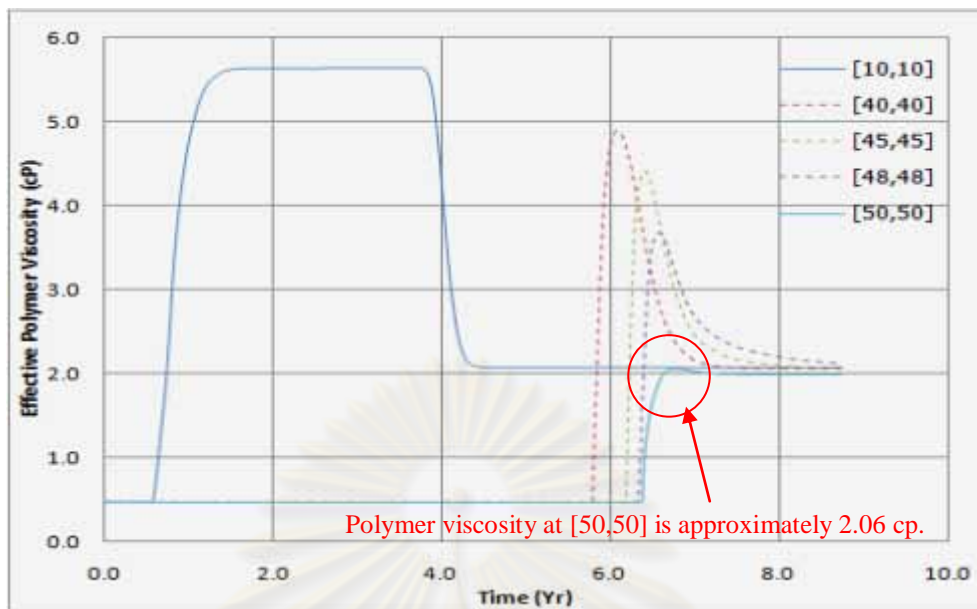


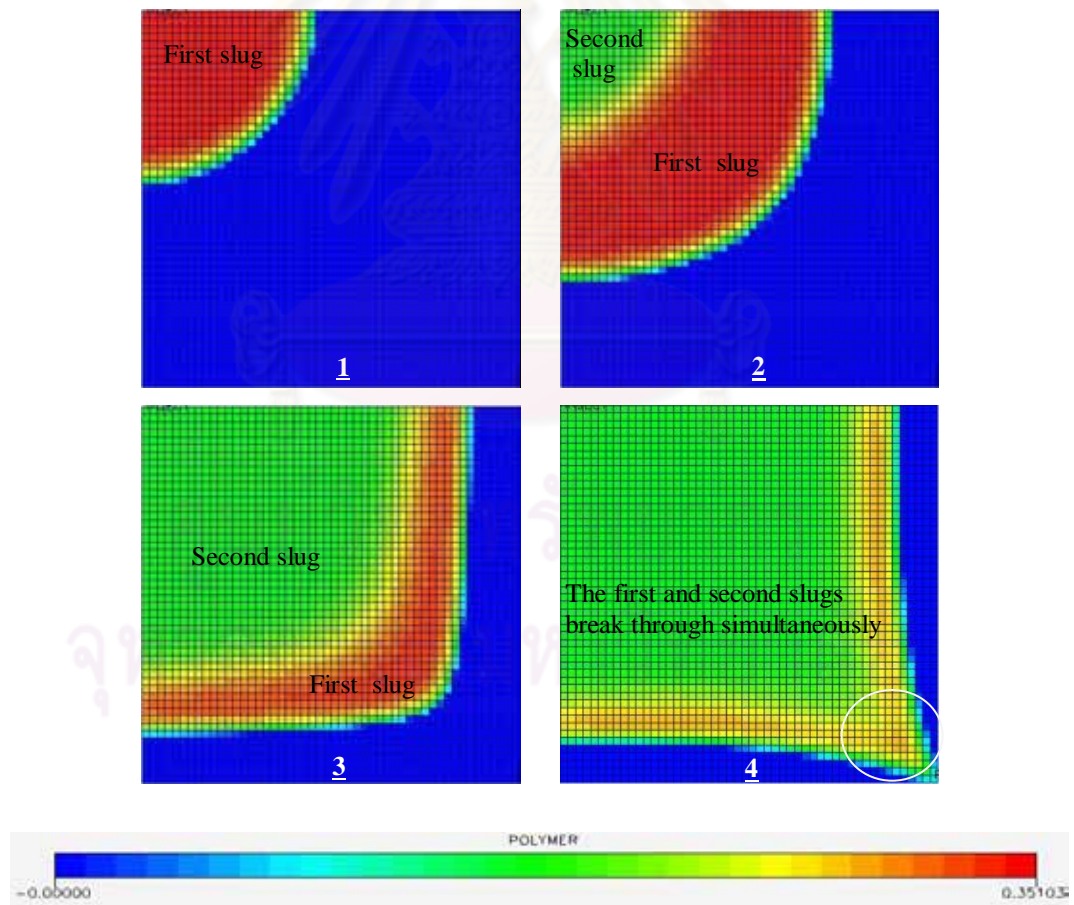
Figure 5.18: Location at which the effective polymer solution viscosity is calculated (black box).

As shown in Figure 5.19, when the second slug of polymer reaches or passes through a certain location, the effective viscosity becomes 2.06 cp. Therefore, we used this value as a reference value for the arrival of the second slug. If the first and second slugs arrive at the producer at the same time, the effective polymer viscosity at the producer will jump from 0.47 (original water viscosity) to 2.06 cp (effective polymer viscosity). This is the case for optimal injection. An example of this optimal case is shown in Figure 5.19.

If the first slug of the polymer arrives before the second slug, the effective viscosity at the producer will jump to a value higher than 2.06 cp. In this case, we over inject the first slug. An example of this behavior is depicted in Figure 5.20. On the other hand, if the first slug of the polymer arrives after the second slug, the effective viscosity at the producer will jump to a value lower than 2.06. In this case, we under inject the polymer as shown in Figure 5.21.

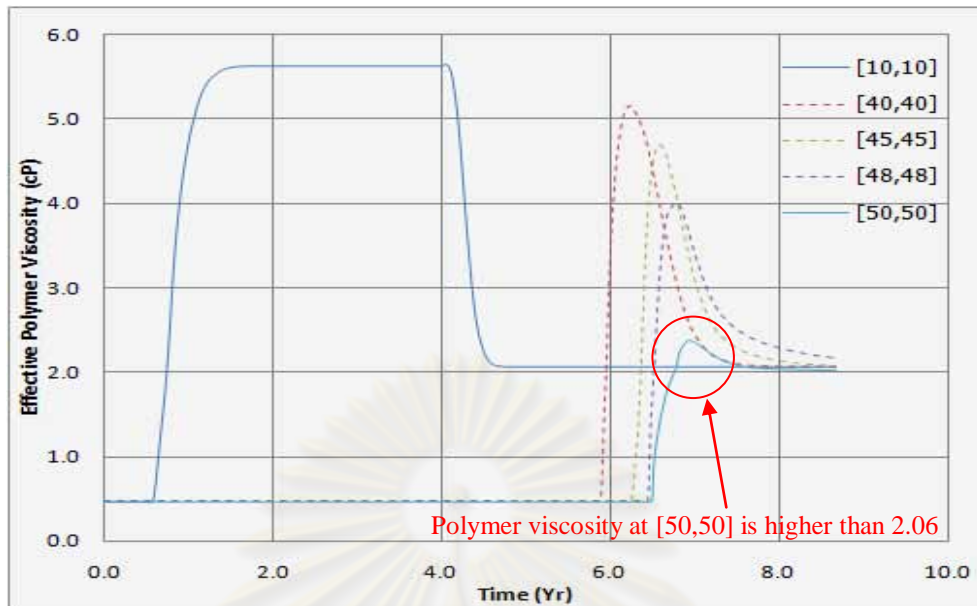


(a) Effective polymer viscosity at fixed locations.

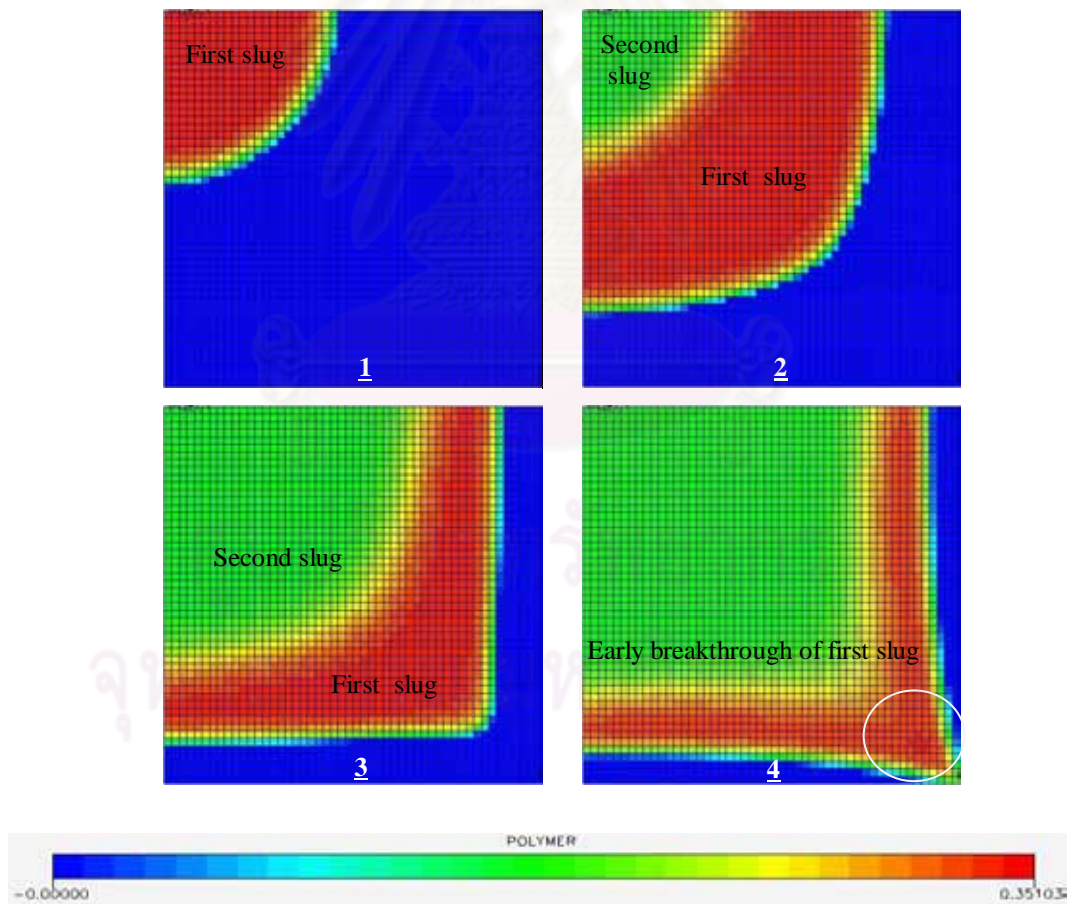


(b) Top view of polymer front location.

Figure 5.19: Determination of the optimal size of the first polymer slug for two-slug injection.

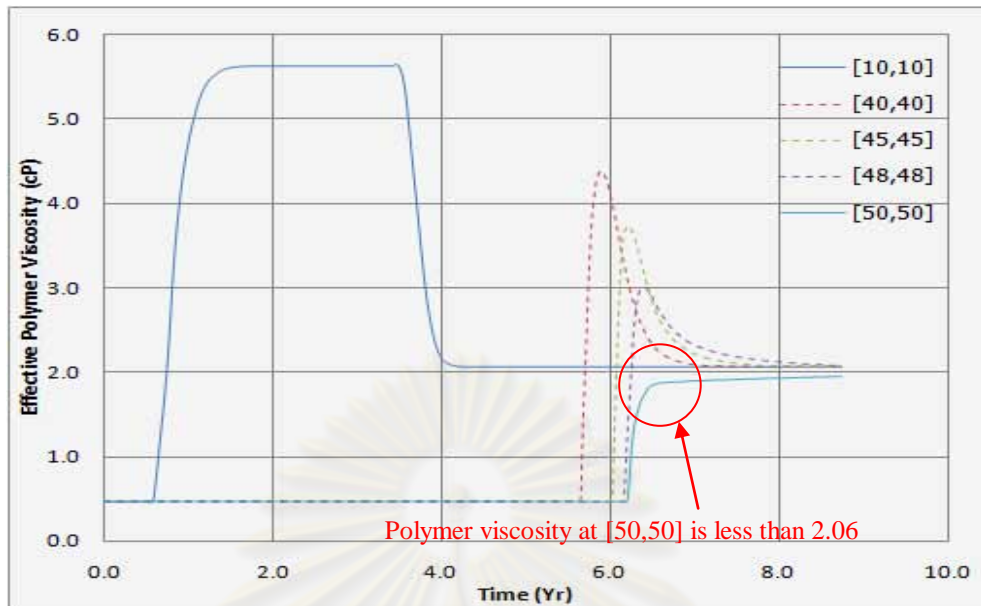


(a) Effective polymer viscosity at fixed locations.

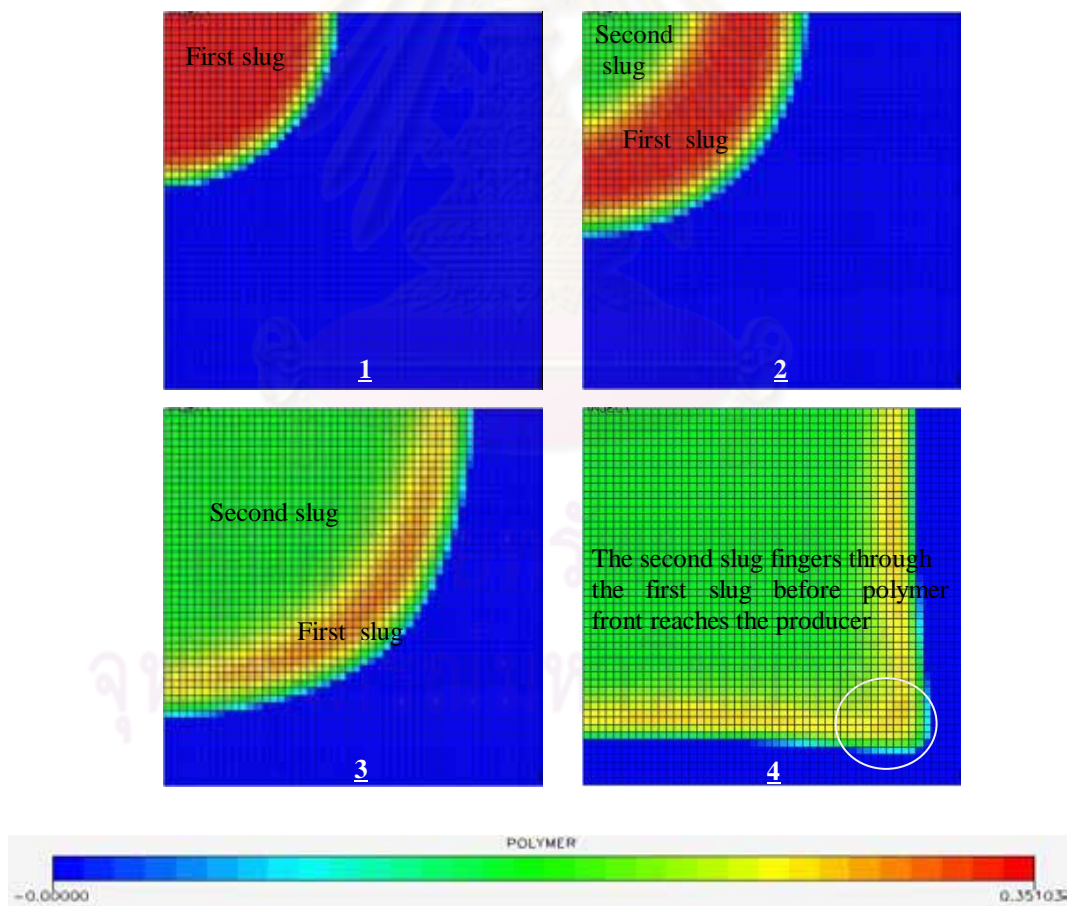


(b) Top view of polymer front location.

Figure 5.20: Overinjection of the first polymer slug for two-slug injection.



(a) Effective polymer viscosity at fixed locations.



(b) Top view of polymer front location.

Figure 5.21: Underinjection of the first polymer slug for two polymer-slug injection.

In order to determine the best polymer injection strategy, four cases of two-slug injection with different slug concentrations were studied:

Case 2A: Two-slug injection with the first slug concentration of 500 ppm followed by water

Case 2B: Two-slug injection with the first slug concentration of 1000 ppm and the second slug concentration of 500 ppm

Case 2C: Two-slug injection with the first slug concentration of 2000 ppm and the second slug concentration of 1000 ppm

Case 2D: Two-slug injection with the first slug concentration of 3000 ppm and the second slug concentration of 2000 ppm

Table 5.3: Summary of apparent viscosity for Cases 2A, 2B, 2C, and 2D.

Case	Apparent viscosity (cp)	
	1 st slug	2 nd slug
2A	2.06	0.47
2B	5.63	2.06
2C	20.64	5.63
2D	60.98	20.64

Table 5.3 summarizes the apparent viscosity of first and second slug for each case. After several trials & errors were performed, the optimum first slug size can be found for all cases. Figures 5.22 to 5.26 show simulation results for all cases of this scenario by comparing with water flooding as a base line.

Figure 5.22 shows water injection rate for all cases of two-slug injection. It can be seen that injection with higher polymer concentration causes lower injection rate. Note that the injection rate increases when the second slug which has lower viscosity is injected. The time that we start injecting the second slug in cases 2A, 2B, 2C and 2D is 3.8, 5.0, 5.0 and 8.1 years, respectively.

Figure 5.23 shows a comparison of oil production rate for all cases. From the plot, average oil production rate obtained from cases 2A, 2B, 2C and 2D is 102, 94, 82 and 47 STB/D, respectively.

Water cut profiles for all cases of two-slug injection are shown in Figure 5.24. It can be seen that higher concentration of injected polymer leads to lower water cut

and slower polymer breakthrough time since the injection rate is lower. The other point that should be noted is that drastic increase in water cut profile is divided into three periods. The first one is caused by water bank breakthrough, the second one is caused by injection of second slug, and the third one is caused by polymer front breakthrough.

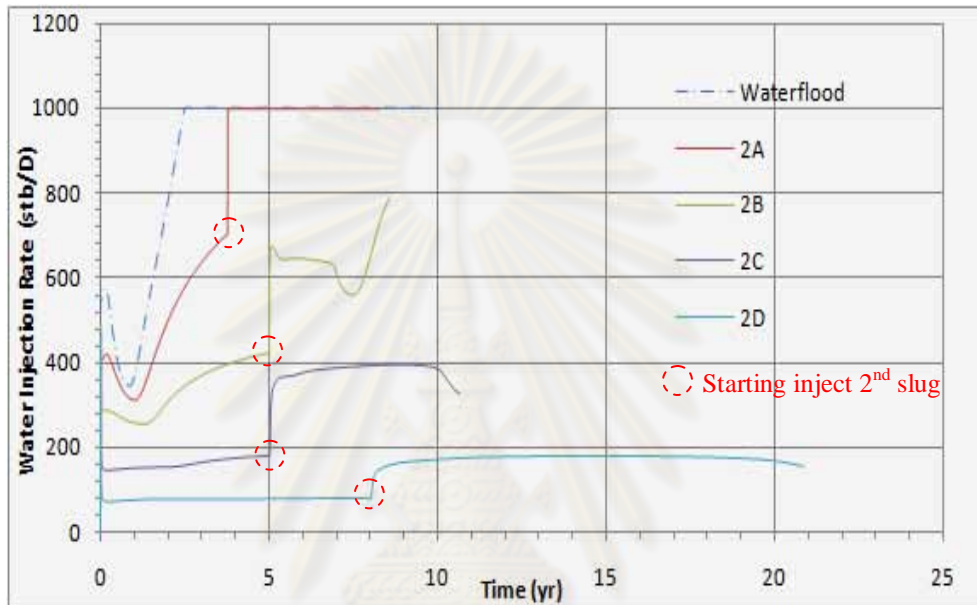


Figure 5.22: Water injection rates for Cases 2A, 2B, 2C, and 2D.

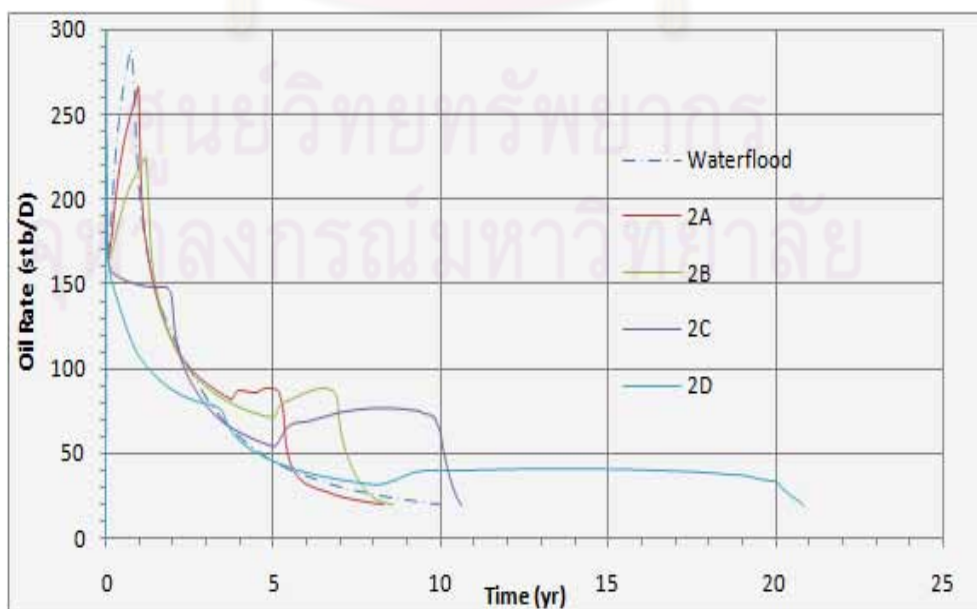


Figure 5.23: Oil production rate for Cases 2A, 2B, 2C, and 2D.

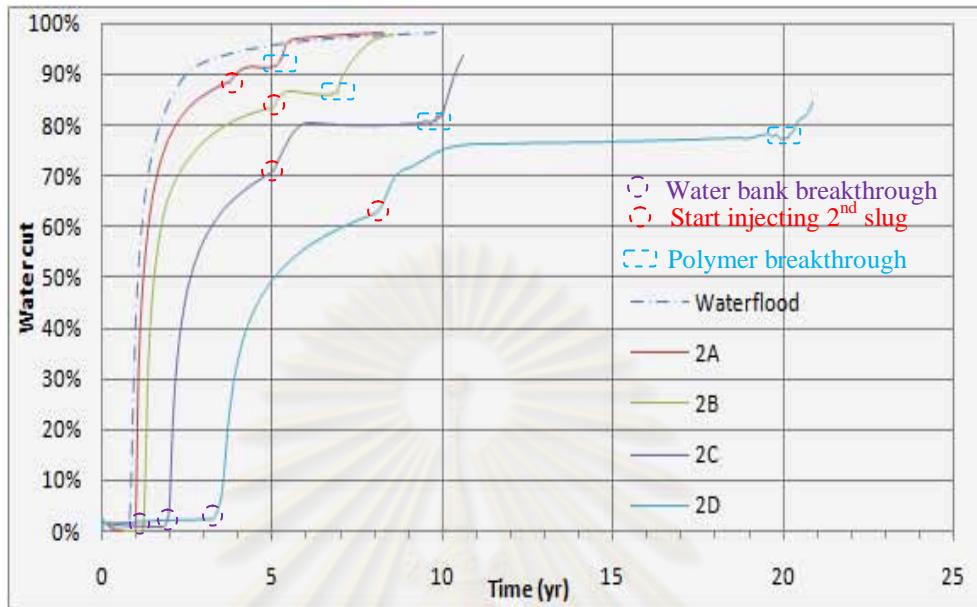


Figure 5.24: Water cuts for Cases 2A, 2B, 2C, and 2D.

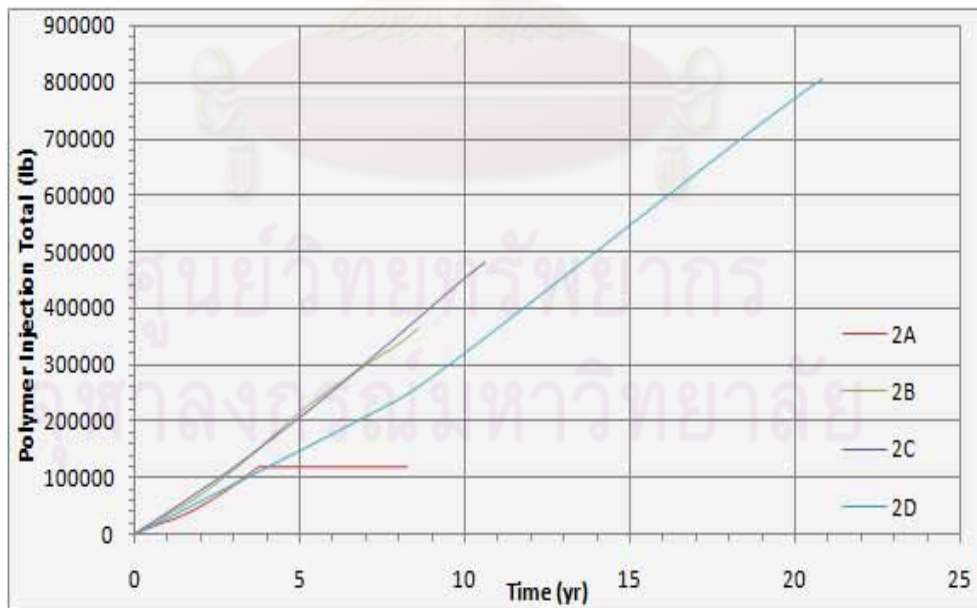


Figure 5.25: Polymer injection totals for Cases 2A, 2B, 2C, and 2D.

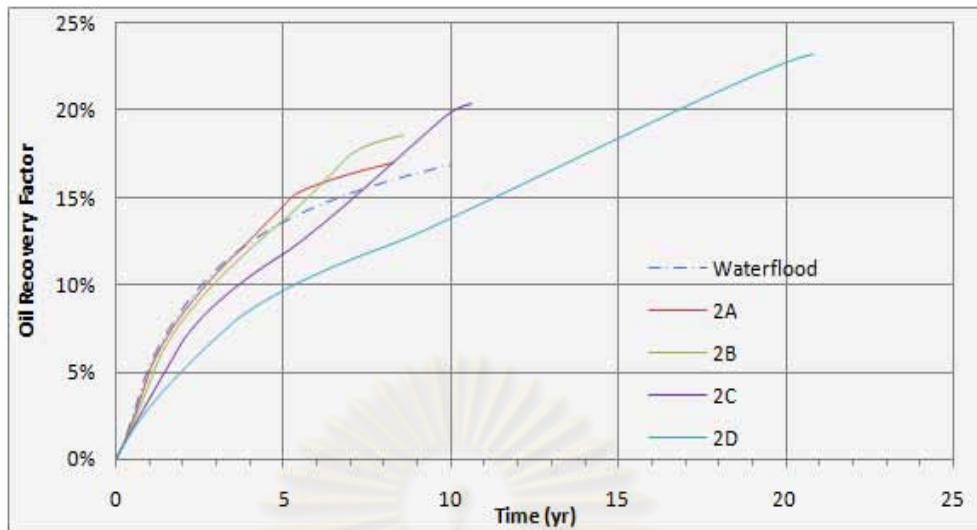


Figure 5.26: Oil recovery factors for Cases 2A, 2B, 2C, and 2D.

Plot of cumulative polymer injection and oil recovery factor for all cases is shown in Figure 5.25 and Figure 5.26, respectively. From Figures 5.25 and 5.26, higher concentration of injected polymer leads to higher total amount of polymer injection and better RF. When comparing among all cases in this scenario, Case 2D takes a much longer time to reach the ultimate recovery and has very high polymer injection total of 806,270 lb.

Table 5.4: Summary of results for two-slug injection.

Case	Production time (Years)	RF (%)	Polymer used (lb)			Incremental oil/ Total polymer used (STB/lb polymer)
			1 st slug	2 nd slug	Total	
Water flood	10.0	16.93	-	-	-	-
2A	8.3	17.02	118189	0	118189	0.0122
2B	8.6	18.63	216819	147381	364200	0.0754
2C	10.6	20.43	206214	273125	479339	0.1182
2D	20.8	23.22	238690	567580	806270	0.1265

The results of optimum first slug size for all cases are summarized in Table 5.4. When comparing among all cases of two-slug injection, Case 2D has the highest RF of 23.22% and the highest incremental oil per total polymer used of 0.1265 STB/lb polymer but the longest production time of 20.8 years.

5.4 Two Polymer Slugs with Drive Water

After obtaining the optimum first slug size from Section 5.3, drive water was injected to chase two slugs of polymer toward the producer in this scenario. The objective is to reduce the total amount of polymer used by decreasing the second slug size. The optimum size of the second polymer slug can be found by allowing the two polymer slugs and drive water to break through simultaneously. This can be done by trial and error in the same manner as in the case of two-slug injection. The method of finding the optimum size of second slug is shown in Figures 5.27 to 5.29.

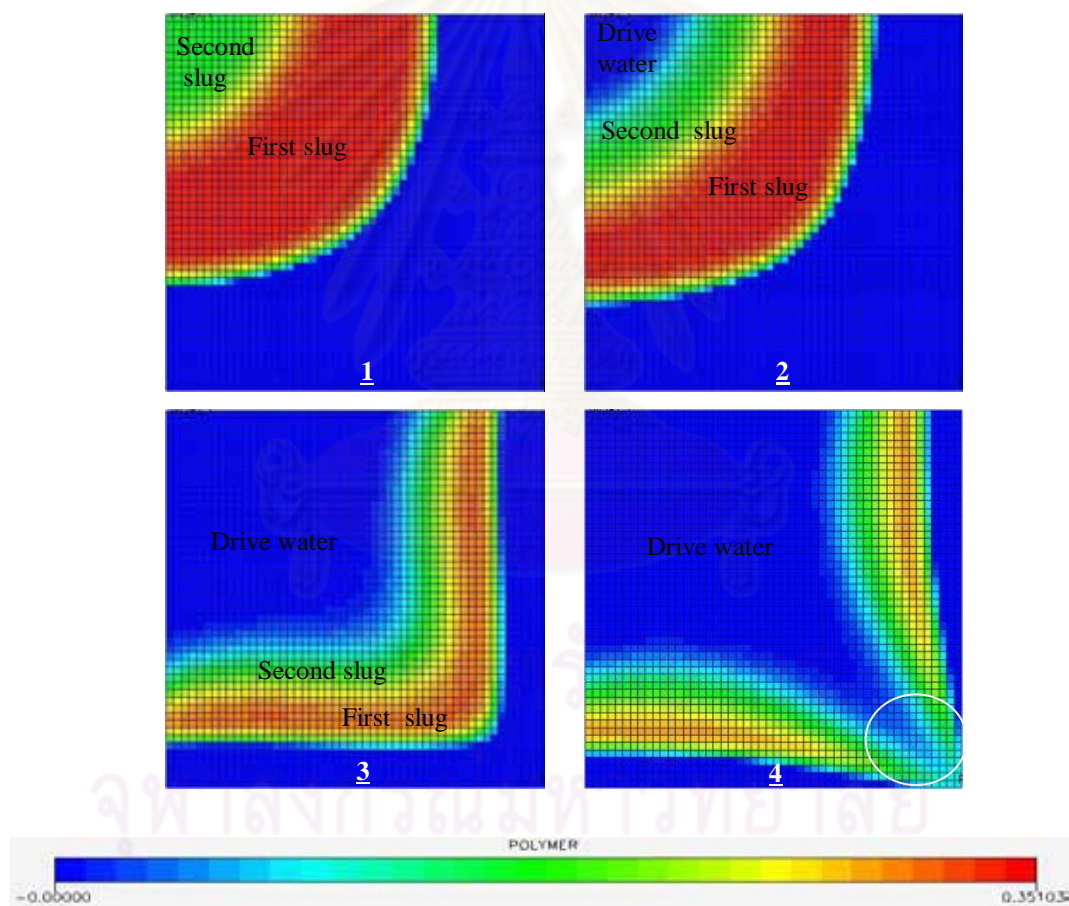


Figure 5.27: Two polymer slugs and drive water break through simultaneously (optimal case).

Figure 5.27 depicts the optimum size of the second polymer slug. It can be seen that two polymer slugs and drive water break through at the same time. Figure 5.28 and Figure 5.29 show an overinjection and underinjection of the second slug,

respectively. In Figure 5.28, two slugs of polymer break through before drive water. This means that the size of the second slug is too large. As seen in Figure 5.29, if the size of the second slug is too small, drive water will finger through the two slugs of polymer. This is the case of polymer underinjection.

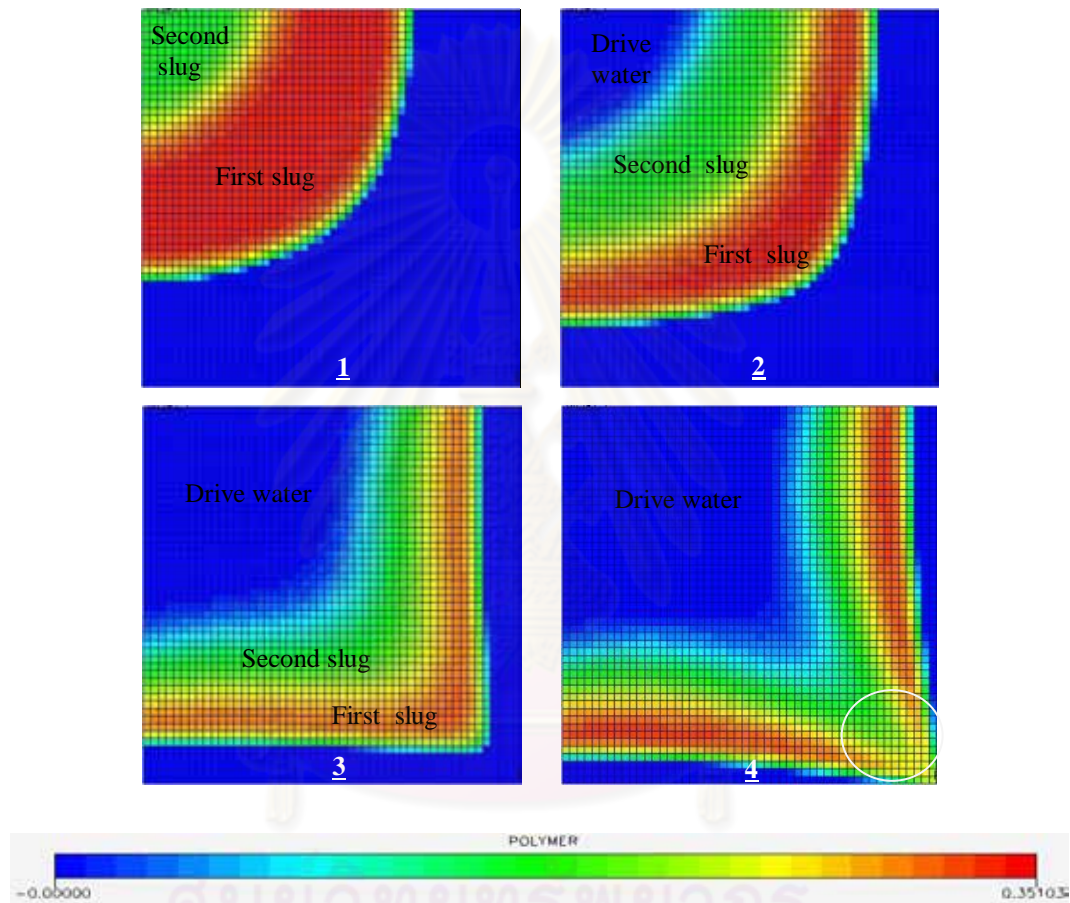


Figure 5.28: Two polymer slugs break through before drive water (overinjection).

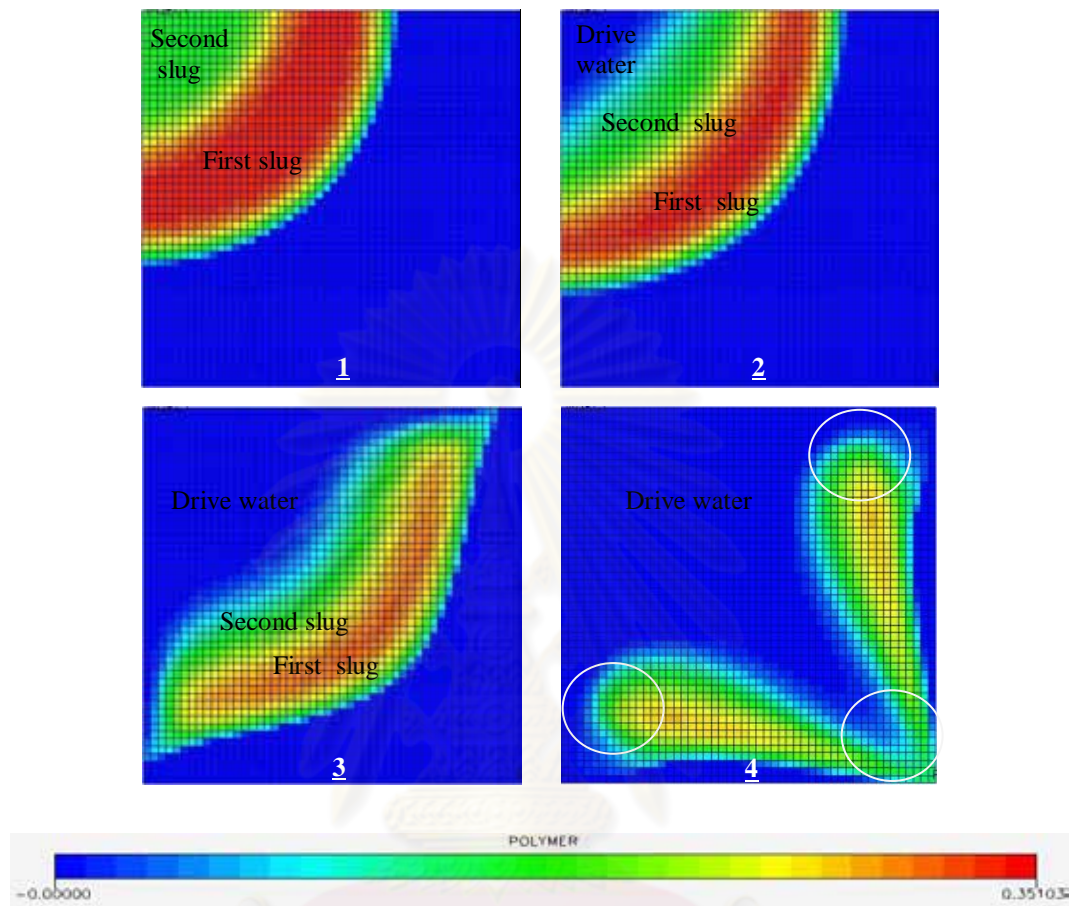


Figure 5.29: Drive water is fingering through two-slug of polymer (underinjection).

ศูนย์วิทยทรัพยากร
จุฬาลงกรณ์มหาวิทยาลัย

In order to determine the best polymer injection strategy of two polymer slugs with drive water, three cases with different slug concentrations were studied:

Case 3B: Two polymer slugs chased by drive water with the first slug concentration of 1000 ppm and the second slug concentration of 500 ppm

Case 3C: Two polymer slugs chased by drive water with the first slug concentration of 2000 ppm and the second slug concentration of 1000 ppm

Case 3D: Two polymer slugs chased by drive water with the first slug concentration of 3000 ppm and the second slug concentration of 2000 ppm

Table 5.5: Summary of apparent viscosity for Cases 3B, 3C, and 3D.

Case	Apparent viscosity (cp)		
	1 st slug	2 nd slug	Driver water
3B	5.63	2.06	0.47
3C	20.64	5.63	0.47
3D	60.98	20.64	0.47

Table 5.5 summarizes the apparent viscosity of first slug, second slug and driver water for each case. After several trials & errors were performed, the optimum second slug size can be found for all cases. Figures 5.30 to 5.34 show simulation results for all cases of this scenario by comparing with water flooding as a base line.

Figure 5.30 shows water injection rate for all cases of two polymer slugs with drive water. It can be seen that the injection rate drastically increases at two different periods. The first jump happens when the second slug of polymer is injected and the second one is when drive water is injected. The time that we start injecting drive water in cases 3B, 3C and 3D is 6.0, 6.4 and 14.0 years, respectively.

Figure 5.31 shows a comparison of oil production rate for all cases. From the plot, average oil production rate obtained from cases 3B, 3C and 3D is 93, 100 and 65 STB/D, respectively.

Water cut profiles for all cases of two-slug and drive water injection are shown in Figure 5.32. It can be seen that drastic increase in water cut profile occurs four times. The first one is caused by water bank breakthrough, the second by second slug injection, the third by drive water injection and the fourth by polymer front breakthrough.

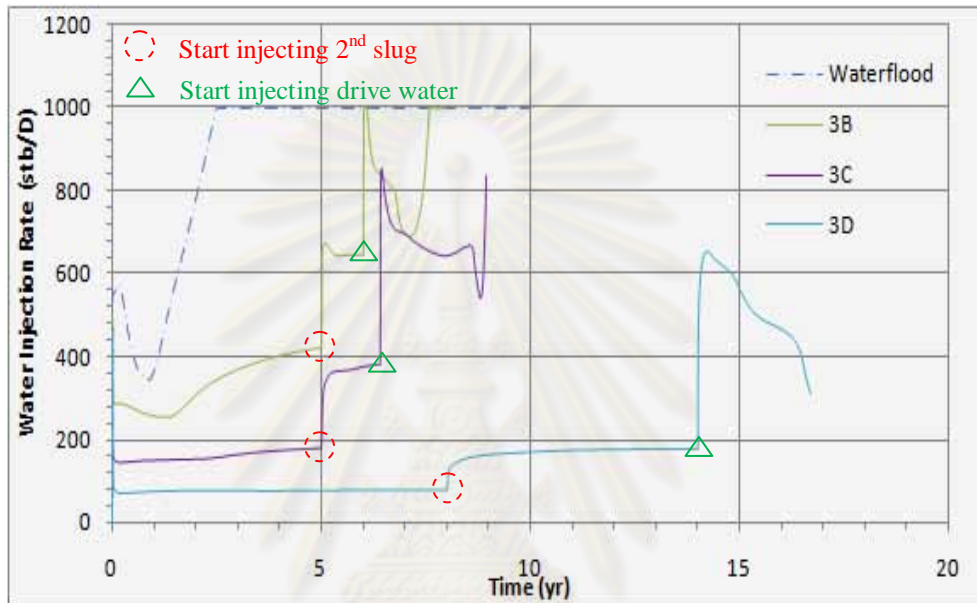


Figure 5.30: Water injection rates for Cases 3B, 3C, and 3D.

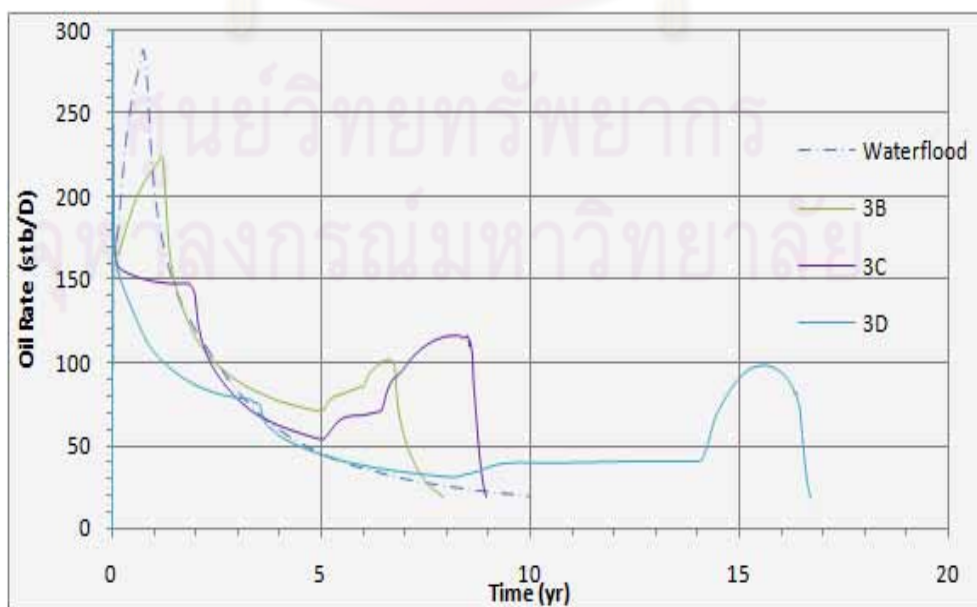


Figure 5.31: Oil production rate for Cases 3B, 3C, and 3D.

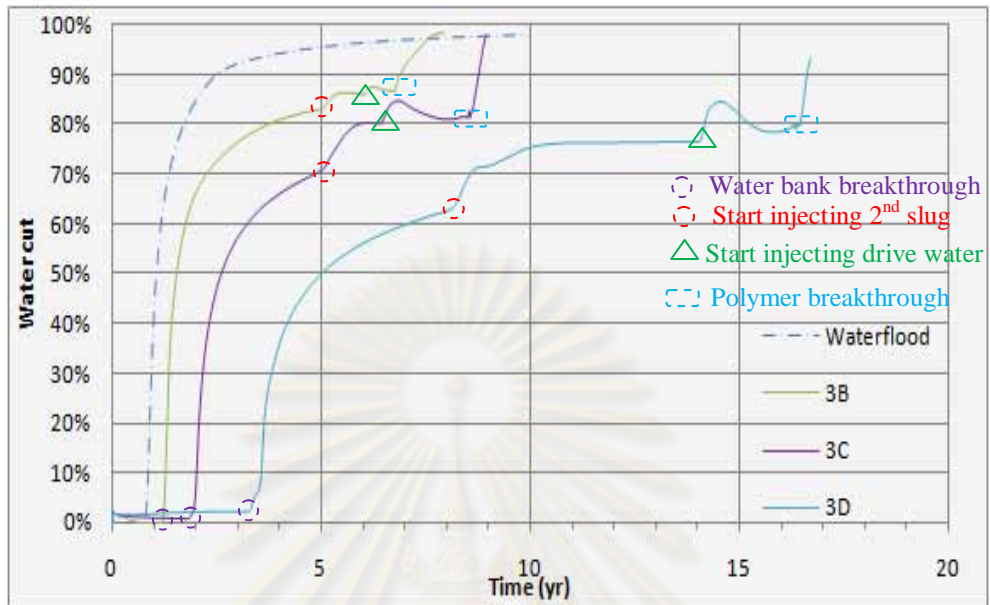


Figure 5.32: Water cuts for Cases 3B, 3C, and 3D.

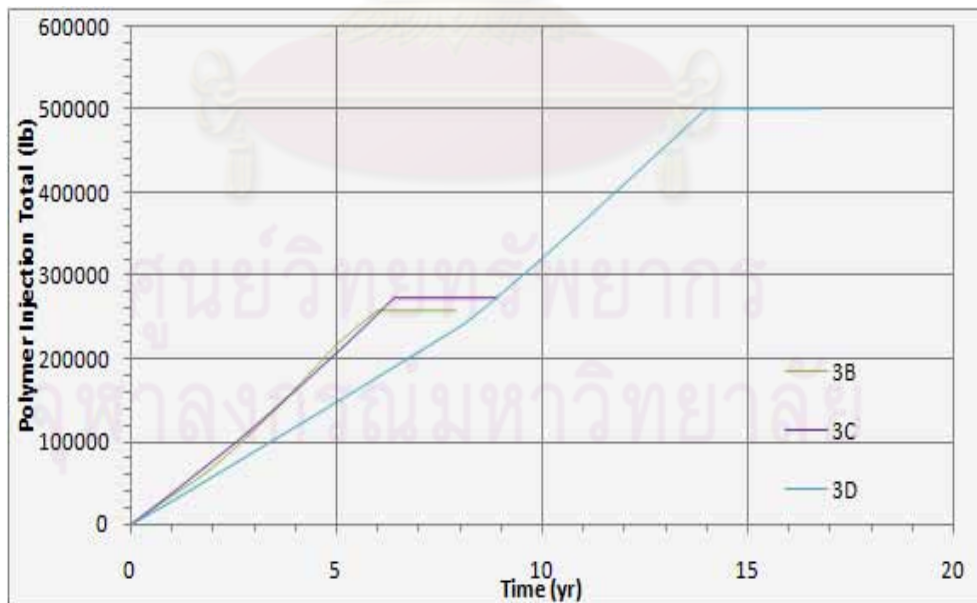


Figure 5.33: Polymer injection totals for Cases 3B, 3C, and 3D.

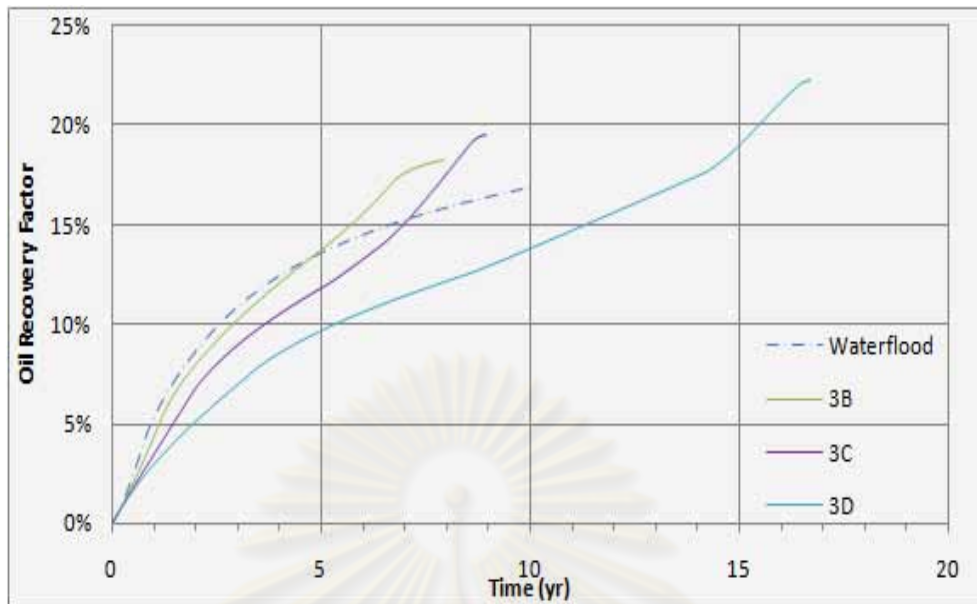


Figure 5.34: Oil recovery factors for Cases 3B, 3C, and 3D.

Plot of cumulative polymer injection and oil recovery factor for all cases is shown in Figure 5.33 and Figure 5.34, respectively. From Figures 5.33 and 5.34, higher concentration of injected polymer leads to higher total amount of polymer injection and better RF. When comparing among all cases in this scenario, Case 3D not only takes a much longer time to reach the ultimate recovery but also has the highest polymer injection total of 501,898 lb. This result implies that too high polymer concentration is not recommended.

Table 5.6: Summary of results for two polymer slugs with drive water.

Case	Production time (Years)	RF (%)	Polymer used (lb)			Incremental oil/ Total polymer used (STB/lb polymer)
			1 st slug	2 nd slug	Total	
Water flood	10.0	16.93	-	-	-	-
3B	7.9	18.25	216819	41567	258386	0.0828
3C	9.0	19.51	206214	66401	272615	0.1533
3D	16.7	22.30	238690	263208	501898	0.1735

The results of optimum second slug size for all cases are summarized in Table 5.6. In this section, the amount of polymer used in the second slug is less than previous section (Section 5.3) quite a lot because drive water is used to chase polymer

in the second slug. When comparing among all cases of two-slug and drive water injection, Case 3D has the highest RF of 22.30 and the highest incremental oil per total polymer used of 0.1735 STB/lb polymer but the longest production time of 16.7 years.

For comparison, the results were divided into groups based on concentration of the first slug. The number 1, 2 and 3 represents the number of slug injection and the alphabet A, B, C, and D represents the first slug concentration of 500 ppm, 1000 ppm, 2000 ppm and 3000 ppm, respectively. Table 5.7 summarizes the results of all scenarios (single-slug, two-slug, two-slug with water), and comparative plots of oil recovery factor are presented in Figures 5.35 to 5.38.

Table 5.7: Summary of results for all scenarios.

Case	Description	Production time (years)	RF (%)	Incremental oil/ Total polymer used (STB/lb polymer)
Base	Water flood	10.0	16.93	-
1A	500 ppm	9.4	18.17	0.0495
2A	500 ppm + water	8.3	17.02	0.0122
1B	1000ppm	9.8	19.26	0.0795
2B	1000ppm+500ppm	8.6	18.63	0.0754
3B	1000ppm+500ppm+water	7.9	18.25	0.0828
1C	2000ppm	16.6	21.99	0.1104
2C	2000ppm+1000ppm	10.6	20.43	0.1182
3C	2000ppm+1000ppm+water	9.0	19.51	0.1533
1D	3000ppm	36.4	26.53	0.1450
2D	3000ppm+2000ppm	20.8	23.22	0.1265
3D	3000ppm+2000ppm+water	16.7	22.30	0.1735

As can be seen from Table 5.7 and Figures 5.35 to 5.38, increase number of slug injection leads to shorten production time and better polymer utilization. Nevertheless, the oil recovery factor slightly decreases due to decrease in displacement efficiency. The top ranks when considered incremental oil per total polymer used are Case 3D and 3C, respectively. But when considering production time, Case 3C is shorter than Case 3D for 8 years, approximately. Hence, Case 3C is

used as the optimum strategy for polymer flooding. This case is chosen for sensitivity study in Section 5.5.

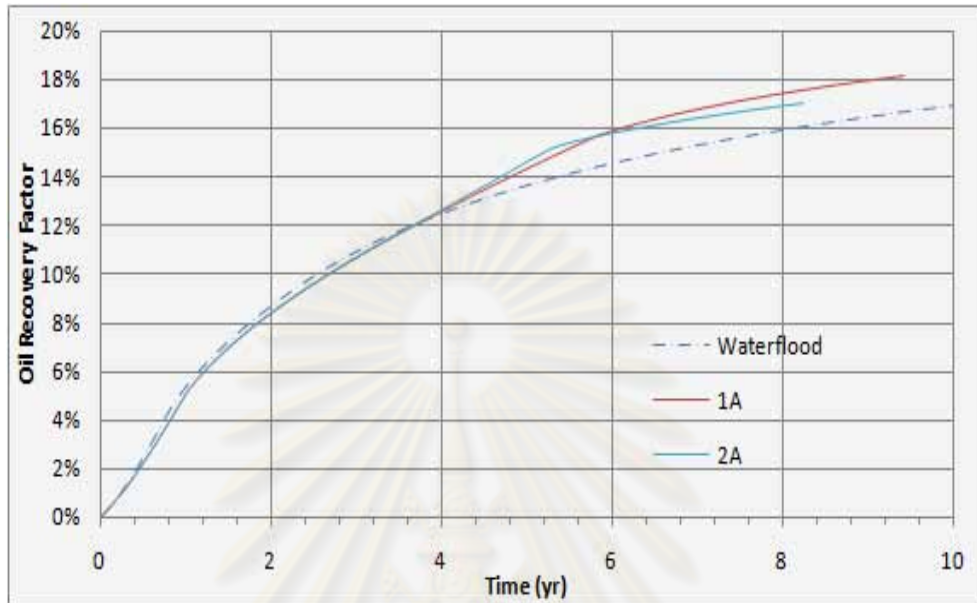


Figure 5.35: Comparative results when the first slug concentration is 500 ppm (A).

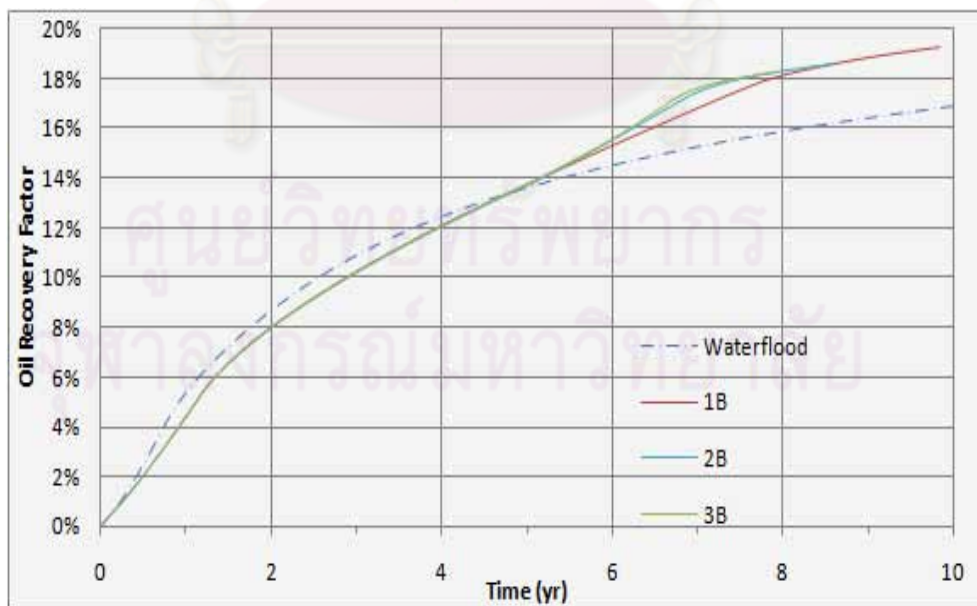


Figure 5.36: Comparative results when the first slug concentration is 1000 ppm (B).

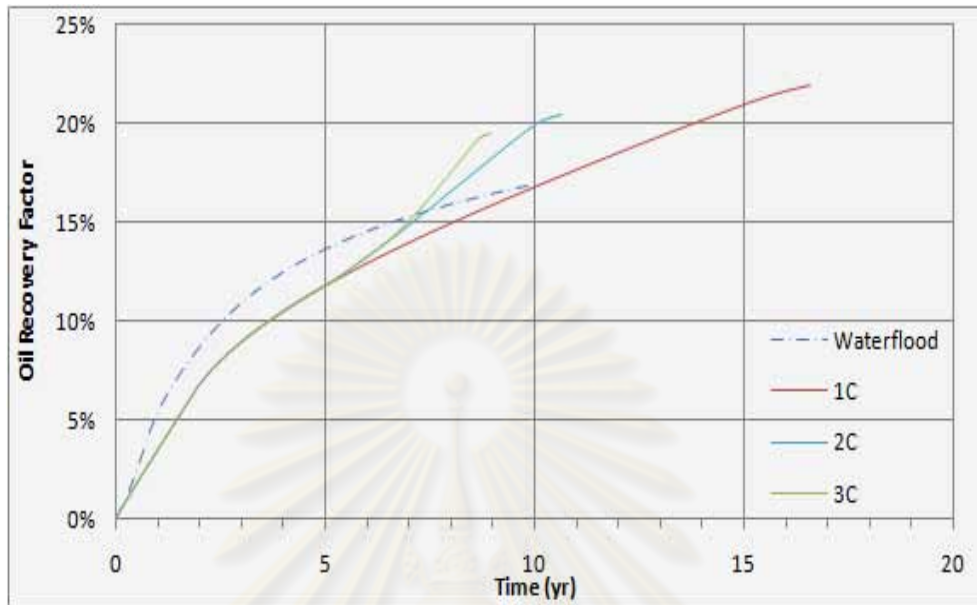


Figure 5.37: Comparative results when the first slug concentration is 2000 ppm (C).

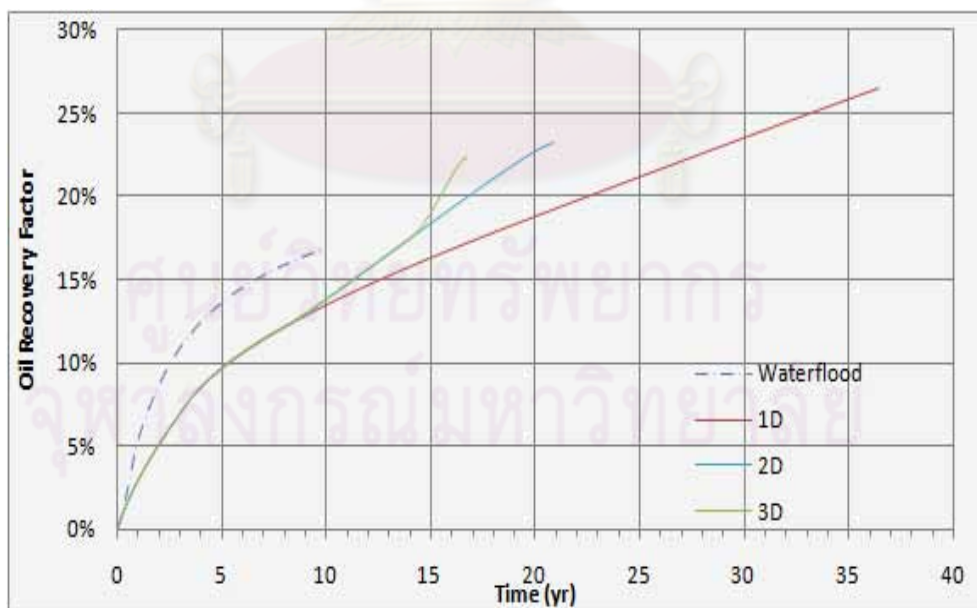


Figure 5.38: Comparative results when the first slug is concentration 3000 ppm (D).

5.5 Sensitivity Study

After we obtained the optimum polymer concentration and slug size of two polymer slugs with drive water injection, the influence of variations in input parameters related to polymer flooding is studied in this section. As mentioned in Section 5.2, some input parameters related to polymer flooding were assumed. Four uncertain parameters of concern are inaccessible pore volume (IPV), polymer adsorption, residual resistance factor (RRF) and mixing parameter. Each parameter is varied with the change of ± 0.5 times from the base case in order to rank sensitivities of each parameter as shown in Table 5.8. In addition, ECLIPSE script for the base case of sensitivity study is presented in Appendix B.

Table 5.8: Summary of input data for each parameter.

Parameters	Unit	Base case	Scenario1	Scenario2
IPV	fraction	0.13	0.07	0.20
Polymer adsorption	% of polymer conc.	1.0%	0.5%	1.5%
RRF*	fraction	1.2	1.0	1.8
Mixing parameter*	-	1.00	0.75	0.50

*Note that minimum value of RRF is 1.0 and value of mixing parameter is 0 to 1.

5.5.1 Effect of Inaccessible Pore Volume

The inaccessible pore volume is the fraction of pore space that polymer solution cannot enter. In order to observe the influence of inaccessible pore volume (IPV) on polymer flooding performance, simulations based on two different IPV's were performed by using the optimum polymer concentration and slug size of two polymer slugs with drive water injection, Case 3C, as a base case.

Plot of water cut and oil recovery factor at different inaccessible pore volumes is shown in Figure 5.39 and 5.40, respectively. It is observed that higher inaccessible pore volume leads to lower water cut, early polymer breakthrough and shorter production time. This is because polymer solution flows through less pore space, then polymer front moves faster.

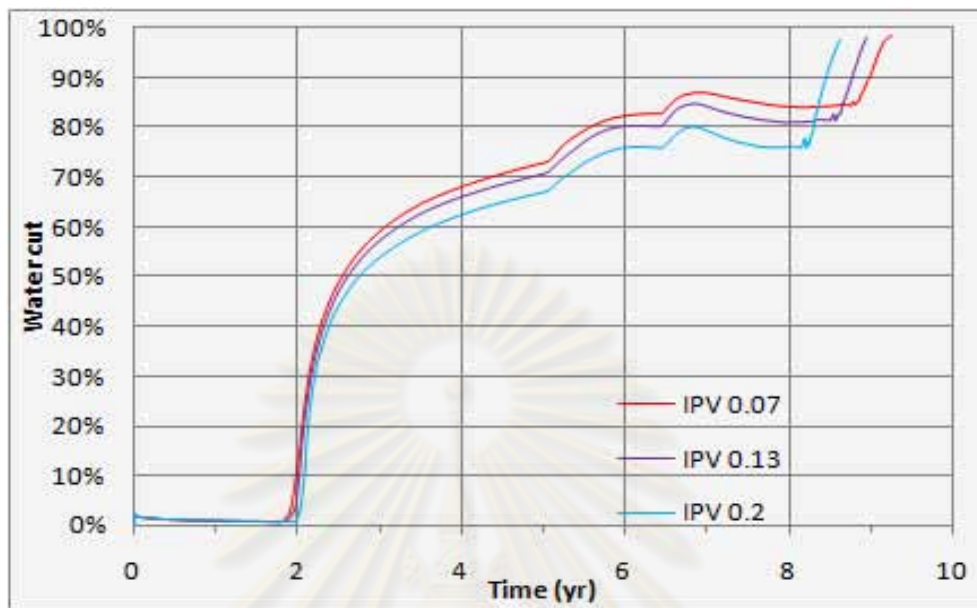


Figure 5.39: Water cut for different inaccessible pore volume cases.

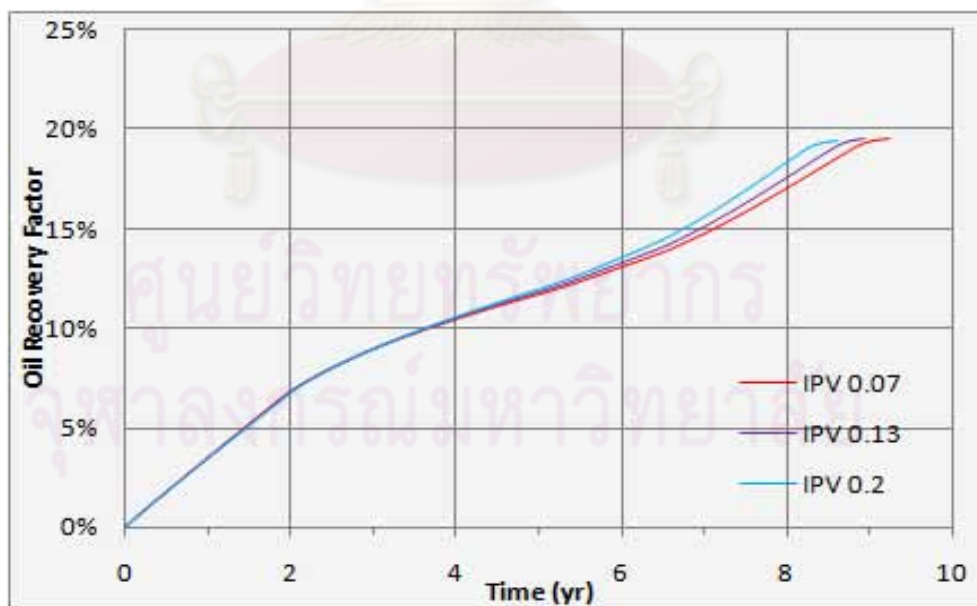


Figure 5.40: Oil recovery factor for different inaccessible pore volume cases.

Table 5.9: Summary of results for different inaccessible pore volumes.

Parameters	Unit	Base case	Scenario1	Scenario2
IPV	fraction	0.13	0.07	0.2
Production time	year	9.0	9.3	8.6
RF	%	19.51	19.53	19.45
Change in RF from base case	%	-	0.11	-0.30

Table 5.9 summarizes the results for the two inaccessible pore volumes in comparison with the base case. As can be seen in Table 5.9, higher IPV leads to shorter production time and lower oil recovery factor due to higher remaining trapped oil in pore space. However, there is almost no difference in recovery factor.

5.5.2 Effect of Polymer Adsorption

In order to observe the influence of polymer adsorption on polymer flooding performance, simulations for two different adsorption functions were performed by using the optimum polymer concentration and slug size of two polymer slugs with drive water injection, Case 3C, as a base case.

Figures 5.41 to 5.43 show simulation results for different polymer adsorption. From Figure 5.41, when percentage polymer adsorption is higher, the total adsorption also gets higher as well. This means that polymer loss will also be higher. As a result, the polymer flooding become less effective and higher water cut is obtained (Figure 5.42). This leads to lower oil recovery factor as seen in Figure 5.43.

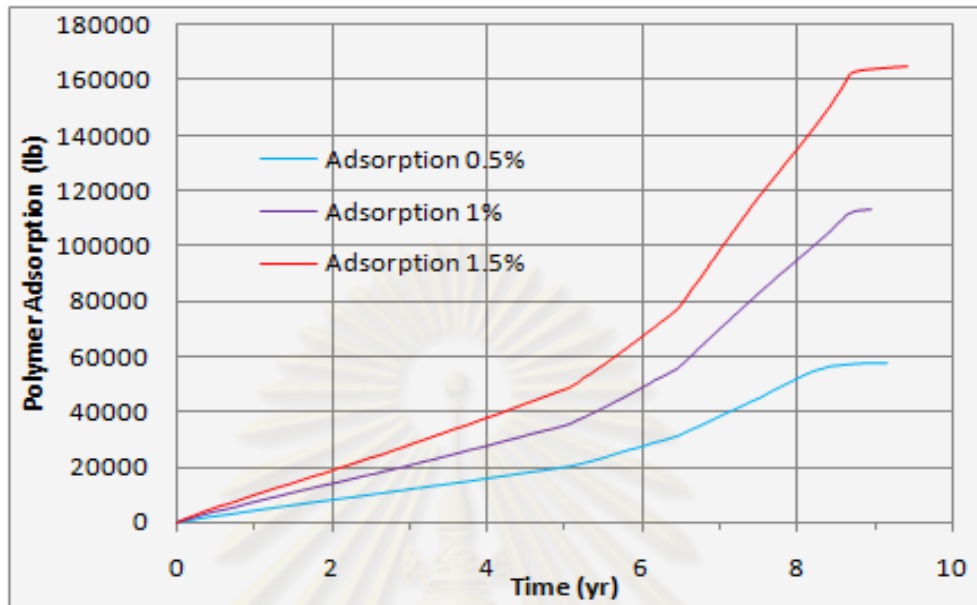


Figure 5.41: Cumulative polymer adsorption for different polymer adsorption cases.

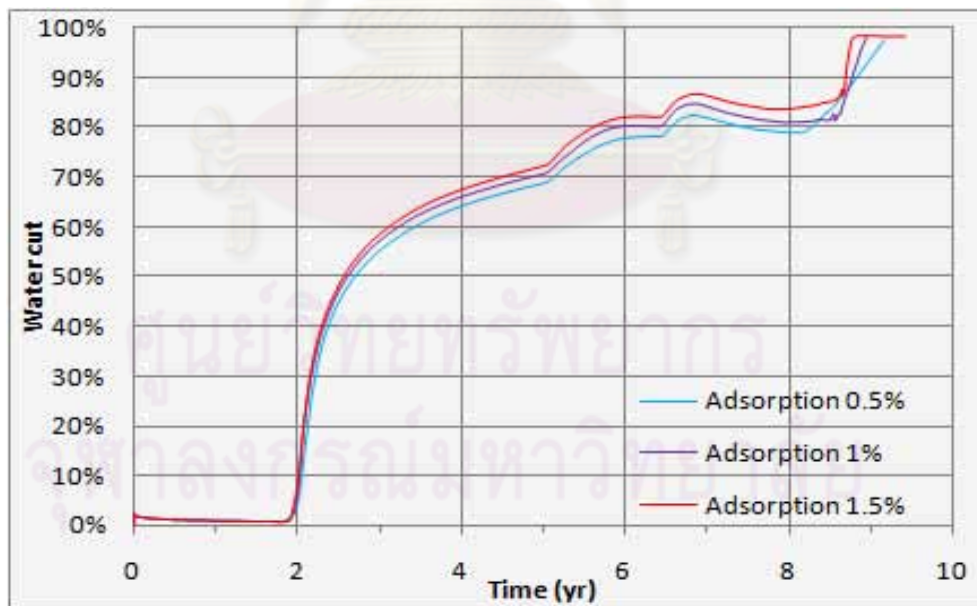


Figure 5.42: Water cut for different polymer adsorption cases.

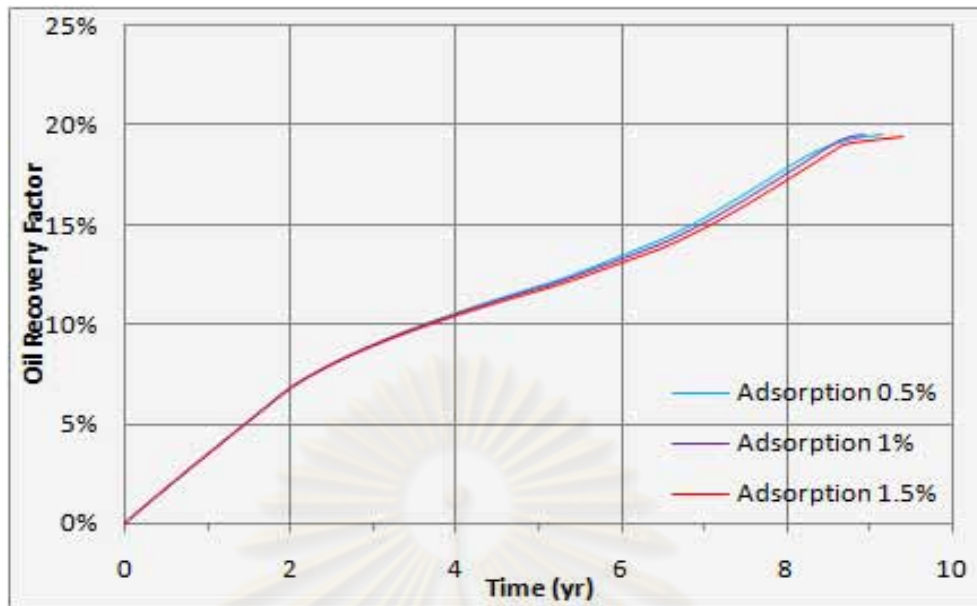


Figure 5.43: Oil recovery factor for different polymer adsorption cases.

Table 5.10: Summary of results for different polymer adsorptions.

Parameters	Unit	Base case	Scenario1	Scenario2
Polymer adsorption	% of polymer conc.	1%	0.5%	1.5%
Production time	year	9.0	9.2	9.4
RF	%	19.51	19.53	19.47
Change in RF from base case	%	-	0.11	-0.20

Table 5.10 summarizes the results for different polymer adsorptions in comparison with the base case. It can be seen that higher polymer adsorption results in a longer production time and a decrease in oil recovery.

5.5.3 Effect of Residual Resistant Factor

The residual resistant factor is the ratio of permeability to brine between before and after contact with polymer solution (k_w/k_{wp}). In order to observe the influence of residual resistant factor (RRF) on polymer flooding performance, simulations for two different RRFs were performed by using the optimum polymer concentration and slug size of two polymer slugs with drive water injection, Case 3C, as a base case.

Figures 5.44 to 5.46 show simulation results for different polymer adsorptions. With higher RRF, permeability to brine after contact with polymer solution, k_{wp} , will decrease. This results in lower injection rate and water cut as seen in Figure 5.44 and Figure 5.45. The production time and oil recovery factor will increase as RRF increases (Figure 5.46).

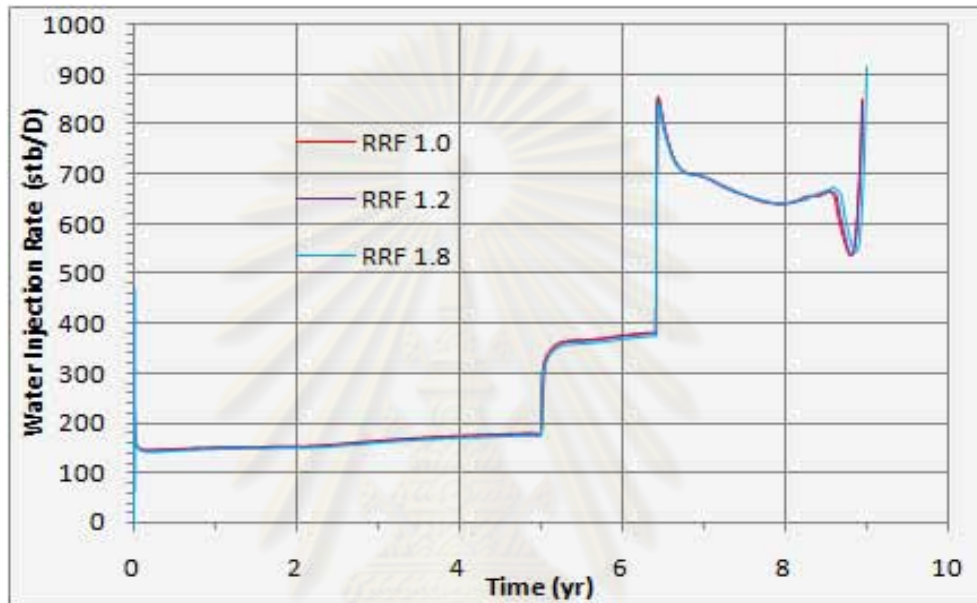


Figure 5.44: Injection rate for different residual resistant factor cases.

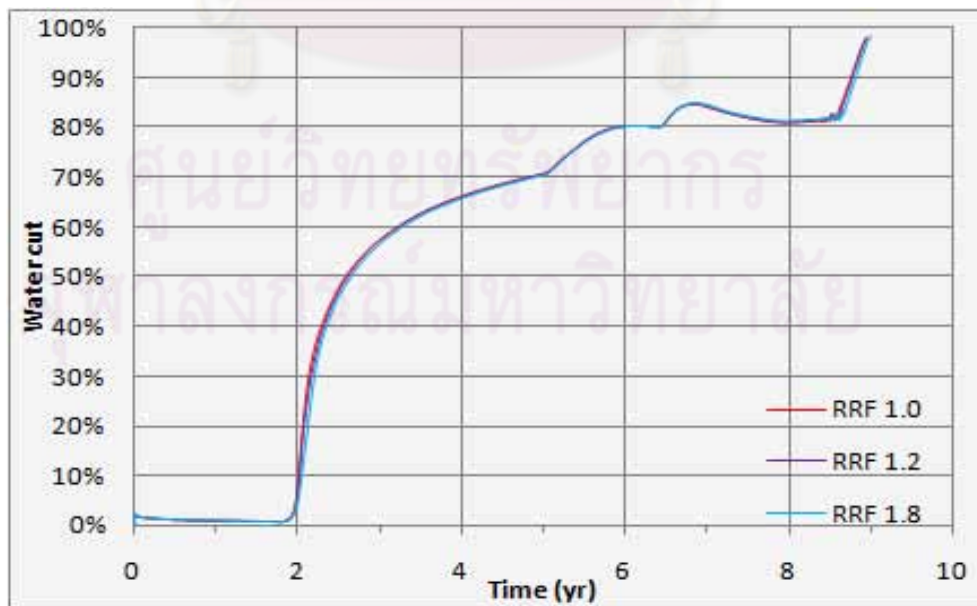


Figure 5.45: Water cut for different residual resistant factor cases.

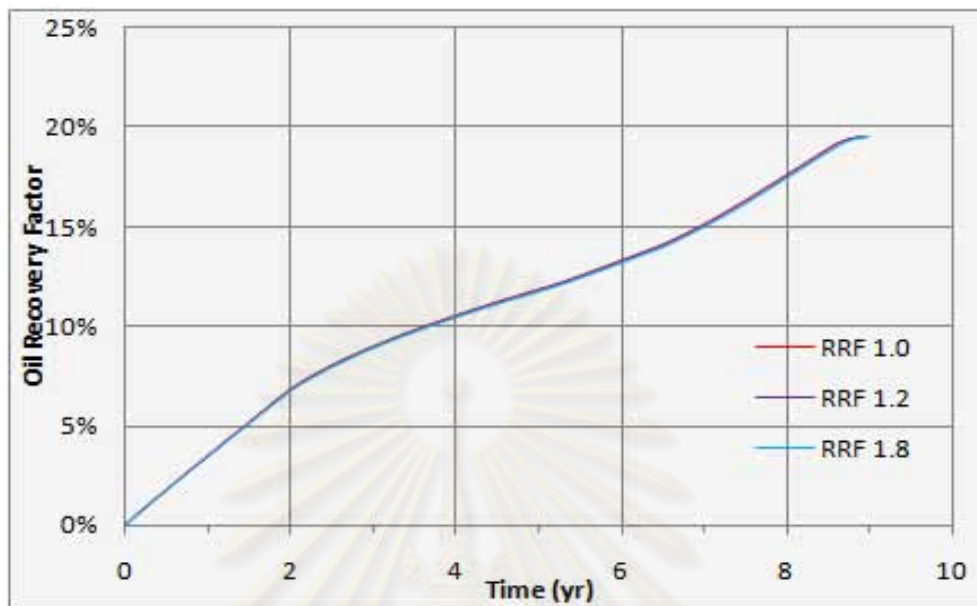


Figure 5.46: Oil recovery factor for different residual resistant factor cases.

Table 5.11: Summary of results in different residual resistant factor.

Parameters	Unit	Base case	Scenario1	Scenario2
Residual resistance factor	fraction	1.2	1.0	1.8
Production time	year	9.0	9.0	9.0
RF	%	19.51	19.50	19.52
Change in RF from base case	%	-	-0.02	0.06

Table 5.11 summarizes the results for different RRFs in comparison with the base case. A change in RRF has almost no impact on production time and recovery factor.

5.5.4 Effect of Mixing Parameter

The mixing parameter represents segregation between the water and the injected polymer solution. It ranges from 0 to 1. If mixing parameter equals to 1, then drive water is fully mixed with polymer slug (high viscous fingering). If mixing parameter equal to 0, then drive water is completely segregated from polymer slug (no viscous fingering). Lower mixing parameter means less fingering effect at the rare edge of polymer slug.

In order to observe the influence of mixing parameter on polymer flooding performance, simulations for two different mixing parameters were performed by using the optimum polymer concentration and slug size of two polymer slugs with drive water injection, Case 3C, as a base case.

Plot of water cut and oil recovery factor for different mixing parameters is shown in Figure 5.47 and 5.48, respectively. Low mixing parameter slows down breakthrough time of polymer front which increases production time and improves oil recovery factor as can be seen in Figures 5.47 and 5.48.

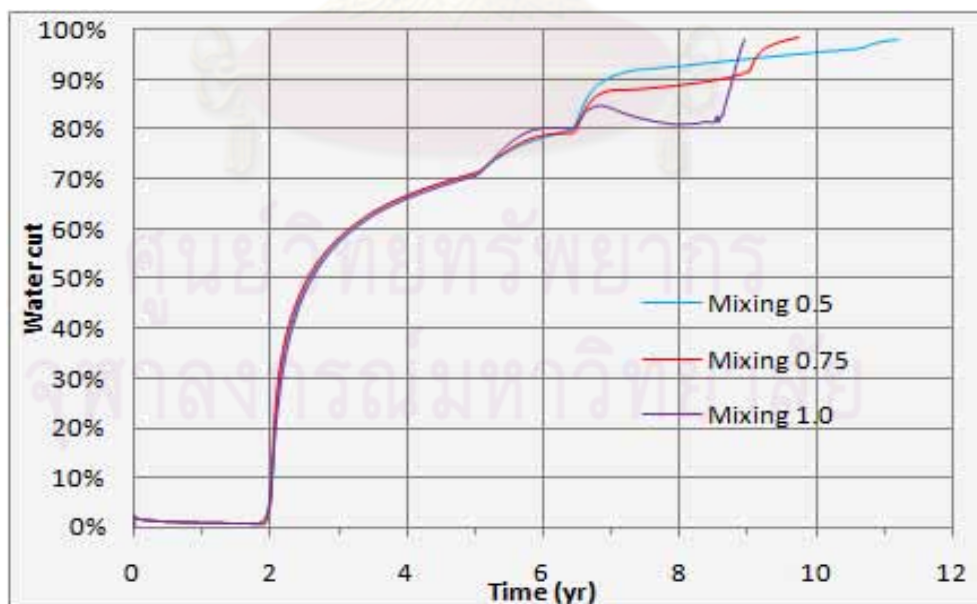


Figure 5.47: Water cut for different mixing parameter cases.

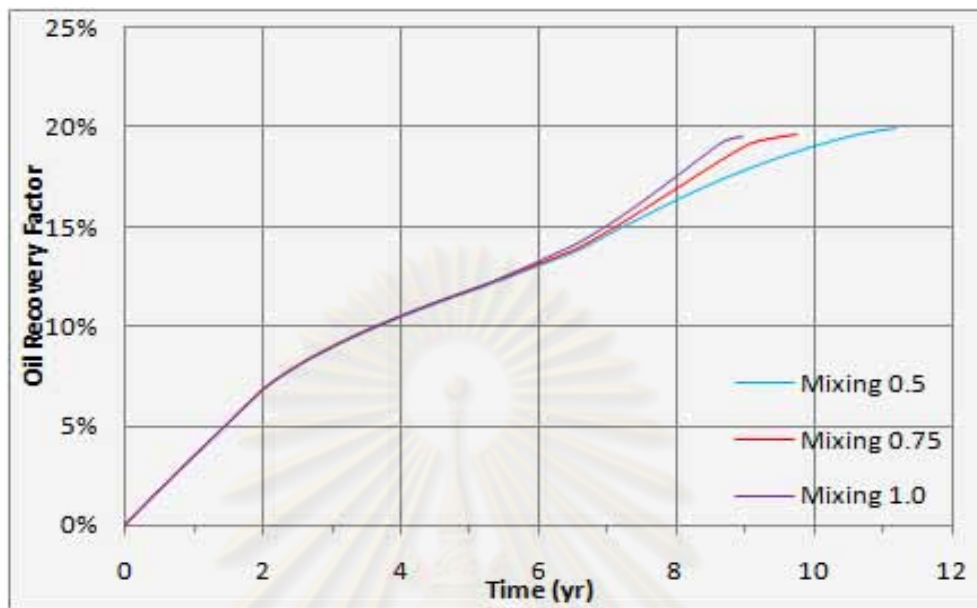


Figure 5.48: Oil recovery factor for different mixing parameter cases.

Table 5.12: Summary of results for different mixing parameters.

Parameters	Unit	Base case	Scenario1	Scenario2
Mixing parameter (0-1)	-	1.00	0.75	0.50
Production time	year	9.0	9.8	11.2
RF	%	19.51	19.61	19.97
Change in RF from base case	%	-	0.52	2.36

Table 5.12 summarizes the results for different mixing parameters in comparison with the base case. It is noticed that decrease in mixing parameter leads to slightly better oil recovery factor. However, this increase is quite small.

Table 5.13: Summary of percentage change in RF from base case.

Parameters	RF	Change in RF from base case
Base case	19.51%	-
Mixing parameter 0.50	19.97%	2.36%
Mixing parameter 0.75	19.61%	0.52%
IPV 0.20	19.45%	-0.30%
IPV 0.07	19.53%	0.11%
Polymer adsorption 1.5%	19.47%	-0.20%
Polymer adsorption 0.5%	19.53%	0.11%
Residual resistance factor (RRF) 1.8	19.52%	0.06%
Residual resistance factor (RRF) 1.0	19.50%	-0.02%

Table 5.13 summarizes the percentage change in RF from the base case, and tornado chart which ranks the sensitivities of input parameters related to polymer flooding is shown in Figure 5.49. When ranking the influence of variation in input parameters related to polymer flooding on percentage change in RF from the base case, mixing parameter is the most sensitive, followed by inaccessible pore volume (IPV), polymer adsorption and residual resistance factor (RRF), orderly.

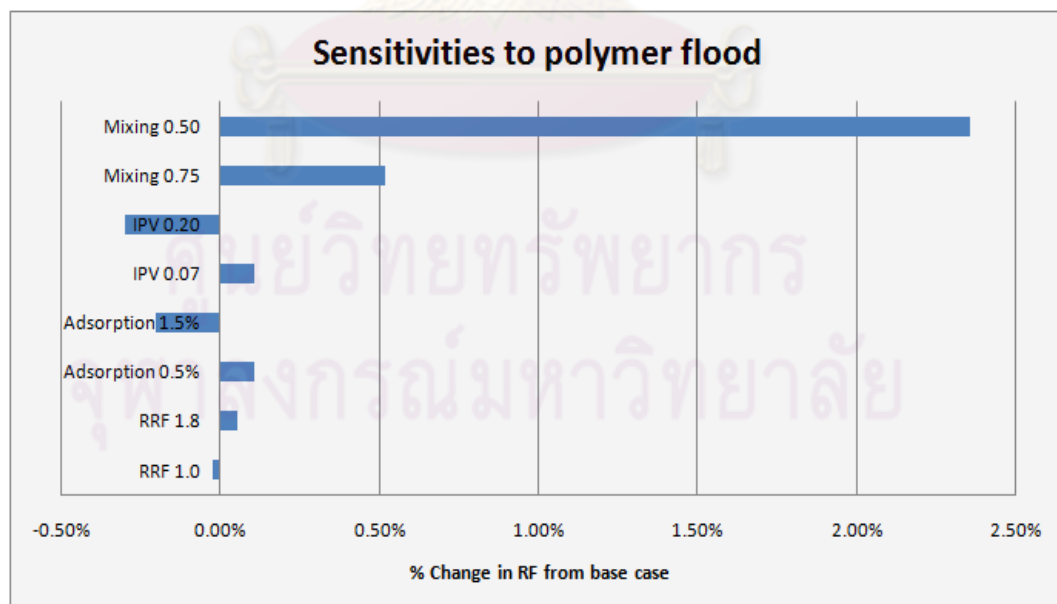


Figure 5.49: Tornado chart of input parameters related to polymer flooding.

CHAPTER VI

CONCLUSIONS AND RECOMMENDATIONS

This study demonstrates polymer flooding mechanism for three different methods which are single-slug, two-slug and two slugs of polymer with drive water. For the purpose of the study, commercial hydrolyzed polyacrylamide (Flopaam 3330S) has been selected for simulation. A hypothetical reservoir model was simulated by using ECLIPSE 100 reservoir simulator with special function for polymer flood model. The reservoir rock and fluid properties were taken from an onshore oilfield in Thailand which has medium oil viscosity.

The following conclusions can be drawn:

1. For single-slug injection, higher concentration of injected polymer leads to lower water cut and slower polymer breakthrough time. Water bank is created at the leading edge of polymer slug as a result of polymer loss due to adsorption onto rock surface.
2. Injecting two polymer slugs based on the criteria that the two slugs break through at the same time has better polymer utilization. However, the oil recovery factor is slightly lower due to decrease in displacement efficiency. In any case, the decrease in recovery factor can be compensated with a small amount of injected polymer and a shorter production time.
3. Injecting with two polymer slugs followed by drive water based on the criteria that two polymer slugs and drive water break through simultaneously leads to shorter production time and the highest incremental oil per total polymer used. Nevertheless, the oil recovery factor is slightly lower than injecting two-slug of polymer due to decrease in displacement efficiency. In any case, the decrease in recovery factor can be compensated with a small amount of injected polymer and a shorter production time.

4. The influences of variations in input parameters related to polymer flooding are summarized as follows:

a. Inaccessible pore volume (IPV)

Higher inaccessible pore volume leads to lower water cut, early polymer breakthrough, shorter production time and slightly lower oil recovery factor. This is because polymer solution flows through less pore space, then polymer front moves faster and higher amount of oil is trapped in pore space. However, there is almost no difference in recovery factor.

b. Polymer adsorption

Higher polymer adsorption has effects on higher polymer loss, and then polymer flooding becomes less effective. This leads to higher water cut, longer production time and decrease in oil recovery.

c. Residual resistance factor (RRF)

As the RRF is the ratio of permeability to brine between before and after contact with polymer solution (k_w/k_{wp}), higher RRF results in lower permeability to brine after contact with polymer solution, k_{wp} . However, a change in RRF has almost no impact on production time and recovery factor.

d. Mixing parameter

The mixing parameter represents segregation between the water and the injected polymer solution. Lower mixing parameter leads to slower breakthrough time of polymer front, increases production time and slightly increases oil recovery factor. However, this increase is quite small.

Sensitivity study shows that mixing parameter has the most impact on percentage change in RF from the base case. Inaccessible pore volume and polymer adsorption also show significant impact. The least important parameter is residual resistance factor.

Recommendations for future study are as follows:

1. In this study, polymer solution does not take into account the effect of salinity on polymer viscosity. In the case of using saline water mixed with polymer, generally for offshore oil fields, we have to account for effect of water salinity on effective polymer viscosity. This effect should be considered in future studies when the reservoir model is simulated from offshore fields.
2. In field scale implementation, reservoir is heterogeneous. Therefore, geological model should be investigated.
3. For more accuracy of the results, laboratory test of polymer core flood should be conducted to ensure input parameters related to polymer flooding.



References

- [1] Demin, W., Li, Q., Xiaohong, G., and Yan, W. The Engineering and Technical Aspects of Polymer Flooding in Daqing Oil Field. paper SPE 64722 presented at the SPE International Oil and Gas Conference and Exhibition, Beijing, China. 7-10 November, 2000.
- [2] Dass, C., Jain, M.A., Dhawan, A.K., and Misra, T.R. Monitoring of Polymer Flood project at Sanand field of India. paper SPE 113552 presented at the 2008 Indian Oil and Gas Technical Conference and Exhibition, Mumbai, India. 4-6 March, 2008.
- [3] Wassmuth, F.R., Green, K., Hodgins, L., and Turta, A.T. Polymer Flood Technology for Heavy Oil Reservoir. paper 2007-182 presented at the Petroleum Society's 8th Canadian International Petroleum Conference, Calgary, Alberta, Canada. 12-14 June, 2007.
- [4] Pu, H., and Xu, Q. An Update and Perspective on Field-Scale Chemical Floods in Daqing Oilfield. paper SPE 118746 presented at the 2009 SPE Middle East Oil & Gas Show and Conference, Bahrain. 15-18 March, 2009.
- [5] Azri, N., et al. Polymer injection in Heavy Oil Reservoir under Strong Bottom Water Drive. paper SPE 129177 presented at the SPE EOR Conference at Oil & Gas West Asia, Muscat, Oman. 11-13 April, 2010.
- [6] Liauh, W.W., and Liu, T.W. A Capillary Viscometer for the Study of EOR Polymers. paper SPE/DOE 12649 presented at the SPE/DOE Fourth Symposium on Enhanced Oil Recovery, Tulsa, USA. 15-18 April, 1984.

- [7] Demin, W., Youlin, J., Yan, W., Xiaohong, G. and Gang, W. Viscous-Elastic Polymer Fluids Rheology and Its Effect Upon Production Equipment. paper SPE 77496 first presented at the SPE Annual Technical Conference and Exhibition, San Antonio, Texas, USA. 29 September-2 October, 2002.
- [8] Lee, S., Kim, D.H., Huh, C. and Pope, G.A. Development of a Comprehensive Rheological Property Database for EOR Polymer. paper SPE 124798 presented at the SPE Annual Technical Conference and Exhibition, New Orleans, Louisiana, USA. 4-7 October, 2009.
- [9] Lindley, J. Chemical Flooding (polymer), [Online]. 2001. Available from: <http://www.netl.doe.gov>. [2010, March 1]
- [10] Sheng, J.J. Modern Chemical Enhanced Oil Recovery: Theory and practice. Elsevier, 2011.
- [11] Lake, L.W. Enhanced Oil Recovery. Prentice-Hall, 1989.
- [12] Patton, J.T., Coats, K.H., and Colegrove, G.T. Prediction of Polymer Flood Performance. paper SPE 2456 presented at The SPE 44th Annual Fall Meeting Denver, Colorado, USA. Sept. 28 - Oct. 1, 1969
- [13] Willhite, G.P., and Dominquez, J.G. Improved Oil Recovery by Surfactant and Polymer Flooding. New York City: Academic Press, 1977.
- [14] Littmann, W. Polymer Flooding. Amsterdam: Elsevier, 1988
- [15] Green, D.W., and Willhite, G.P. Enhanced Oil Recovery. U.S.A.: Society of Petroleum Engineers, 2003.

- [16] Stahl, G.A., and Schulz, D.N. Water-Soluble Polymer for Petroleum Recovery. New York City: Plenum Press, 1988.
- [17] Bragg, J. R., et al. Control Of Xanthan-Degrading Organisms In The Loudon Pilot: Approach, Methodology, Results. paper SPE 11989 presented at the SPE Annual Technical Conference and Exhibition, San Francisco, California, USA. 5-8 October, 1983.
- [18] ECLIPSE Technical Description Manual [Computer file]. Schlumberger, 2006.
- [19] Sirisawadwattana, J., and Ketmalee, T. Cyclic Steam Stimulation in PKM. presented at 14th PTTEP Technical Forum, Thailand. 19-20 August, 2010.



ศูนย์วิทยทรัพยากร
จุฬาลงกรณ์มหาวิทยาลัย



APPENDICES

ศูนย์วิทยทรัพยากร
จุฬาลงกรณ์มหาวิทยาลัย

APPENDIX A

Table A1: Shear thinning data of Flopaam 3330S used in the simulation.

Polymer Concentration	Water velocity (ft/day)	Shear thinning multiplier	In-situ viscosity (cp)
500 ppm	0	1.00	2.06
	283.5	1.00	2.06
	2834.6	1.00	2.06
	28346.5	0.95	1.96
	283464.6	0.75	1.55
	2834645.7	0.58	1.19
1000 ppm	0	1.00	5.63
	283.5	1.00	5.63
	2834.6	1.00	5.63
	28346.5	0.90	5.07
	283464.6	0.60	3.38
	2834645.7	0.40	2.25
2000 ppm	0	1.00	20.64
	283.5	1.00	20.64
	2834.6	1.00	20.64
	28346.5	0.70	14.45
	283464.6	0.33	6.71
	2834645.7	0.18	3.61
3000 ppm	0	1.00	60.98
	283.5	1.00	60.98
	2834.6	0.92	55.90
	28346.5	0.46	27.95
	283464.6	0.19	11.69
	2834645.7	0.09	5.59

APPENDIX B

ECLIPSE script for the optimum case.

RUNSPEC section

TITLE

Polymer Flooding

START

1 'JAN' 2010 /

FIELD

GAS

OIL

WATER

DISGAS

NSTACK

200 /

MONITOR

RSSPEC

NOINSPEC



ศูนย์วิทยทรัพยากร
จุฬาลงกรณ์มหาวิทยาลัย

MSGFILE

1 /

POLYMER

DISPDIMS

1 2 1 /

DIMENS

50 50 10 /

EQLDIMS

1 100 100 1 20 /

REGDIMS

1 1 0 0 /

TABDIMS

1 1 20 20 1 20 20 1 /

WELLDIMS

3 11 2 3 /

GRID section

ECHO

GRIDUNIT

--

-- Grid data units

--

ศูนย์วิทยทรัพยากร
จุฬาลงกรณ์มหาวิทยาลัย

'FEET' /

MAPAXES

--

-- Grid Axes wrt Map Coordinates

--

0 0 0 0 0 0 /

--*BOX panel edit: DX set equal to 20 ft for box (1:50, 1:50, 1:10)

--*BOX panel edit: DY set equal to 20 ft for box (1:50, 1:50, 1:10)

--*BOX panel edit: DZ set equal to 5 ft for box (1:50, 1:50, 1:10)

--*BOX panel edit: TOPS set equal to 3200 ft for box (1:50, 1:50, 1:1)

--*BOX panel edit: TOPS set equal to 3205 ft for box (1:50, 1:50, 2:2)

--*BOX panel edit: TOPS set equal to 3210 ft for box (1:50, 1:50, 3:3)

--*BOX panel edit: TOPS set equal to 3215 ft for box (1:50, 1:50, 4:4)

--*BOX panel edit: TOPS set equal to 3220 ft for box (1:50, 1:50, 5:5)

--*BOX panel edit: TOPS set equal to 3225 ft for box (1:50, 1:50, 6:6)

--*BOX panel edit: TOPS set equal to 3230 ft for box (1:50, 1:50, 7:7)

--*BOX panel edit: TOPS set equal to 3235 ft for box (1:50, 1:50, 8:8)

--*BOX panel edit: TOPS set equal to 3240 ft for box (1:50, 1:50, 9:9)

--*BOX panel edit: TOPS set equal to 3245 ft for box (1:50, 1:50, 10:10)

EQUALS

PORO 0.3 /

/

--*BOX panel edit: PERMR set equal to 200 mD for box (1:50, 1:50, 1:10)

EQUALS

PERMR 200 /

/

--*BOX panel edit: PERMTHT set equal to 200 mD for box (1:50, 1:50, 1:10)

EQUALS

PERMTHT 200 /

/

--*BOX panel edit: PERMZ set equal to 2 mD for box (1:50, 1:50, 1:10)

EQUALS

PERMZ 2 /

/

--*BOX panel edit: PERMR set equal to 500 mD for box (1:50, 1:50, 1:10)

EQUALS

PERMR 500 /

/

--*BOX panel edit: PERMTHT set equal to 500 mD for box (1:50, 1:50, 1:10)

EQUALS

PERMTHT 500 /

/

--*BOX panel edit: PERMZ set equal to 5 mD for box (1:50, 1:50, 1:10)

EQUALS

PERMZ 5 /

/

--*BOX panel edit: RS set equal to 0.111 Mscf /stb for box (1:50, 1:50, 1:10)

--*BOX panel edit: SGAS set equal to 0 for box (1:50, 1:50, 1:10)

--*BOX panel edit: SWAT set equal to 0.35 for box (1:50, 1:50, 1:10)

--*BOX panel edit: PRESSURE set equal to 1430 psia for box (1:50, 1:50, 1:10)

SCAL section

-- OFFICE-SCAL-HEADER-DATA

-- Off SCAL Saturation Tables: 1 1

-- Off SCAL "Saturation 1"

-- Off SCAL End Point Tables: 1 1

-- Off SCAL "End Points 1"

-- Off SCAL Petro Elastic Tables: 1 1

-- Off SCAL "Petro-elastic 1"

-- Correlation Data

-- -----

--

-- Off SCAL Corr Region : 1

--

--

-- Off SCAL Corr Off SCAL Corr Points : 11

-- Off SCAL Corr Off SCAL Corr OGExp : 2.0000000000000000e+000

-- Off SCAL Corr Off SCAL Corr OWExp : 2.0000000000000000e+000

-- Off SCAL Corr Off SCAL Corr Sorw : 2.5000000000000000e-001

-- Off SCAL Corr Off SCAL Corr Sgrw : 0.0000000000000000e+000

-- Off SCAL Corr Off SCAL Corr Sorg : 6.0000000000000000e-002

-- Off SCAL Corr Off SCAL Corr Sgr : 7.0000000000000000e-002

-- Off SCAL Corr Off SCAL Corr KroSwi : 9.0000000000000000e-001

-- Off SCAL Corr Off SCAL Corr KroSgi : 9.0000000000000000e-001

-- Off SCAL Corr Off SCAL Corr KrgSwi : 9.0000000000000000e-001

-- Off SCAL Corr Off SCAL Corr KrgSorg : 4.0000000000000e-002
 -- Off SCAL Corr Off SCAL Corr GExp : 2.8000000000000e+000
 -- Off SCAL Corr Off SCAL Corr WExp : 2.8000000000000e+000
 -- Off SCAL Corr Off SCAL Corr Sgirr : 0.0000000000000e+000
 -- Off SCAL Corr Off SCAL Corr Swirr : 3.5000000000000e-001
 -- Off SCAL Corr Off SCAL Corr Swmax : 7.5000000000000e-001
 -- Off SCAL Corr Off SCAL Corr Sgmax : 1.0000000000000e+000
 -- Off SCAL Corr Off SCAL Corr Swcr : 3.5000000000000e-001
 -- Off SCAL Corr Off SCAL Corr Swi : 3.5000000000000e-001
 -- Off SCAL Corr Off SCAL Corr Sgi : 0.0000000000000e+000
 -- Off SCAL Corr Off SCAL Corr KrwSorw : 3.5000000000000e-001
 -- Off SCAL Corr Off SCAL Corr KrwSgrw : 1.0000000000000e+000
 -- Off SCAL Corr Off SCAL Corr Kliquid : 1.0000000000000e+000
 -- Off SCAL Corr Off SCAL Corr KrwSwmax : 1.0000000000000e+000
 -- Off SCAL Corr Off SCAL Corr KrgSgmax : 9.3000000000000e-001

--

ECHO

PLYADS

--

-- Polymer Adsorption Functions

--

0	0
0.0003	3e-006
0.0005	5e-006
0.0008	8e-006
0.001	1e-005

/

PLYROCK

--

-- Polymer Rock Properties

--

0.13	1.2	1880	2	0.0002
------	-----	------	---	--------

/

SGOF

--

-- Gas/Oil Saturation Functions

--

0	0	0.9	0	
0.07	0	0.69910945	0	
0.135	0.00011841536	0.53525567	0	
0.2	0.00082469244	0.39324907	0	
0.265	0.0025665371	0.27308963	0	
0.33	0.0057434918	0.17477736	0	
0.395	0.01072813	0.098312267	0	
0.46	0.017874402	0.043694341	0	
0.525	0.027522162	0.010923585	0	
0.59	0.04	0	0	
0.65	0.9	0	0	

/

SWOF

--

-- Water/Oil Saturation Functions

--

0.35	0	0.9	0	
0.36666667	0.00074505617	0.71111111	0	
0.38333333	0.0051888726	0.54444444	0	
0.4	0.016148364	0.4	0	

0.41666667	0.036137408	0.27777778	0
0.43333333	0.067500195	0.17777778	0
0.45	0.11246374	0.1	0
0.46666667	0.17316636	0.04444444	0
0.48333333	0.25167552	0.01111111	0
0.5	0.35	0	0
0.75	1	0	0

/

PVT section

```
-- OFFICE-PVTN-HEADER-DATA
-- Off PVTN PVT Tables:      1      1
-- Off PVTN "PVT 1"
-- Off PVTN Rock Tables:    1      1
-- Off PVTN "Rock Compact 1"
-- Off PVTN Miscible Tables: 1      1
-- Off PVTN "Miscible 1"
-- Off PVTN Correlation Data: 37     1
-- Off PVTN "PVT 1"
-- Off PVTN "CUSTOMIZED"
-- Off PVTN "SET VALUE FOR STANDARD_TEMPERATURE TO
59.99999999999999 IN F;"
-- Off PVTN "SET VALUE FOR STANDARD_PRESSURE TO 14.7 IN psia;"
-- Off PVTN "SET VALUE FOR POROSITY TO 0.3 IN dimensionless;"
-- Off PVTN "SET VALUE FOR REF_PRESSURE TO 1430 IN psia;"
-- Off PVTN "SET VALUE FOR ROCK_TYPE TO
UNCONSOLIDATED_SANDSTONE;"
-- Off PVTN "SET VALUE FOR GAS_GRAVITY TO 0.798 IN sg_Air_1;"
-- Off PVTN "SET VALUE FOR OIL_GRAVITY TO 17.2 IN APIoil;"
-- Off PVTN "SET VALUE FOR GOR TO 111 IN scf /stb;"
-- Off PVTN "SET VALUE FOR SALINITY TO 0 IN fraction;"
```

```
-- Off PVTN "SET VALUE FOR SEP_TEMPERATURE TO 59.9999999999999 IN F;"
-- Off PVTN "SET VALUE FOR SEP_PRESSURE TO 14.7 IN psia;"
-- Off PVTN "SET VALUE FOR TEMPERATURE TO 140 IN F;"
-- Off PVTN "SET VALUE FOR N2 TO 0 IN fraction;"
-- Off PVTN "SET VALUE FOR H2S TO 0 IN fraction;"
-- Off PVTN "SET VALUE FOR CO2 TO 0 IN fraction;"
-- Off PVTN "SET CORRELATION FOR ROCK TO NEWMAN;"
-- Off PVTN "SET CORRELATION FOR GAS_CRIT_PROPS TO CorredorGrav;"
-- Off PVTN "SET CORRELATION FOR GAS_ZFACTOR TO HALL;"
-- Off PVTN "SET CORRELATION FOR GAS_FVF TO SPIVEY;"
-- Off PVTN "SET CORRELATION FOR GAS_VISCOSITY TO LEE;"
-- Off PVTN "SET CORRELATION FOR OIL_RS TO VELARDE;"
-- Off PVTN "SET CORRELATION FOR OIL_PB TO VALKO;"
-- Off PVTN "SET CORRELATION FOR OIL_VISCOSITY TO BEGGS;"
-- Off PVTN "SET CORRELATION FOR OIL_COMPRESSIBILITY TO Calhoun;"
-- Off PVTN "SET CORRELATION FOR OIL_SAT_COMPRESS TO Spivey;"
-- Off PVTN "SET CORRELATION FOR OIL_FVF TO CASEY;"
-- Off PVTN "SET CORRELATION FOR WATER_VISCOSITY TO KESTINKHALIFA;"
-- Off PVTN "SET CORRELATION FOR WATER_COMPRESSIBILITY TO MEEHAN;"
-- Off PVTN "SET CORRELATION FOR WATER_FVF TO McCain;"
-- Off PVTN "SET CORRELATION FOR WATER_DENSITY TO SPIVEYMCCAIN;"
-- Off PVTN "SET CORRELATION FOR OIL_VISCOSITY_SAT TO BEGGSROB;"
-- Off PVTN "SET CORRELATION FOR OIL_VISCOSITY_UNSAT TO VASQUEZBEGGS;"
-- Off PVTN "SET VALUE FOR MIN_PRESSURE TO 100 IN psia;"
-- Off PVTN "SET VALUE FOR MAX_PRESSURE TO 3000 IN psia;"
-- Off PVTN "SET VALUE FOR TABLE_LENGTH TO 20;"
```


ECHO

PMAX

--

-- Maximum Simulation Pressure

--

3000 1* 1* 1*

/

ECHO

PLYMAX

--

-- Polymer/Salt Concentrations

--

0.7004 0

/

PLYSHEAR

--

-- Polymer Shear Thinning Data

--

0 1

283.5 0.9999

2834.6 0.9998

28346.5 0.7

283464.6 0.33

2834645.7 0.18

/



ศูนย์วิทยทรัพยากร
จุฬาลงกรณ์มหาวิทยาลัย

PLYVISC

--

-- Polymer Solution Viscosity Function

--

0	1
0.1751	4.4
0.3502	12
0.7004	44
1.0506	130

/

PVTW

--

-- Water PVT Properties

--

1430	1.0065384923722	3.03064304274197e-006	0.469113762456873
3.20673362786454e-006			

/

PVDG

--

-- Dry Gas PVT Properties (No Vapourised Oil)

--

100	29.6391319306593	0.0115105516216512
252.631578947368	11.4515141626734	0.0117283097817309
405.263157894737	6.96718910977767	0.0120059524820981
557.894736842105	4.93993554053866	0.0123381511841895
710.526315789474	3.78706075013697	0.012725322695231
815.823232432773	3.24529473764516	0.0130256620159824
1015.78947368421	2.53034808338375	0.0136746609201838
1168.42105263158	2.15367424839862	0.0142426993720705
1321.05263157895	1.86802806653827	0.0148759282193061

1430 1.70398399027484 0.0153681132293377
 1626.31578947368 1.4691432161476 0.0163374971859684
 1778.94736842105 1.32701691642691 0.0171598034049622
 1931.57894736842 1.21129738915645 0.0180348298079781
 2084.21052631579 1.11623287814537 0.0189535530983361
 2236.84210526316 1.03753057753664 0.0199055708285227
 2389.47368421053 0.971902245320547 0.0208800660352467
 2542.10526315789 0.916783500157982 0.0218667230456687
 2694.73684210526 0.870152567504395 0.02285641204623
 2847.36842105263 0.830406232261656 0.0238415669146666
 3000 0.796269585427782 0.0248162813793367

/

PVTO

--

-- Live Oil PVT Properties (Dissolved Gas)

--

0.031396903 100 1.0292601 73.634395 /
 0.055785568 252.63158 1.0535404 57.244522 /
 0.073781378 405.26316 1.0620376 50.052813 /
 0.088953865 557.89474 1.0689198 45.383348 /
 0.10241919 710.52632 1.0748703 41.881585 /
 0.111 815.82323 1.0786001 39.874392
 1015.7895 1.0728461 40.647245
 1168.4211 1.0719536 41.247219
 1321.0526 1.0712678 41.856049
 1430 1.070868 42.296117
 1626.3158 1.0702831 43.100801
 1778.9474 1.0699177 43.736991
 1931.5789 1.0696102 44.382571
 2084.2105 1.0693477 45.037681
 2236.8421 1.0691212 45.70246

2389.4737 1.0689236 46.377051
 2542.1053 1.0687498 47.0616
 2694.7368 1.0685957 47.756253
 2847.3684 1.0684581 48.46116
 3000 1.0683345 49.176471 /

/

DENSITY

--

-- Fluid Densities at Surface Conditions

--

59.34666034745 62.4279737253144 0.0498175230328009

/

ECHO

ROCK

--

-- Rock Properties

--

1430 3.00000785502382e-005

/

ECHO

TLMIXPAR

--

-- Todd-Longstaff Mixing Parameters

--

1 1*

/

ศูนย์วิทยทรัพยากร
 จุฬาลงกรณ์มหาวิทยาลัย

SCHEDULE section

ECHO

WELSPECS

'INJECT' '1' 1 1 1* 'WATER' 1* 'STD' 'SHUT' 'NO' 1* 'SEG' 3* 'STD' /
/

COMPDAT

'INJECT' 2* 1 10 'OPEN' 2* 0.291666666666667 3* 'Z' 1* /
/

WCONINJE

'INJECT' 'WATER' 'OPEN' 'GRUP' 1000 1* 2250 3* /
/

WPOLYMER

'INJECT' 0.7004 0 2* /
/

WELSPECS

'PROD' '1' 50 50 1* 'OIL' 1* 'STD' 'SHUT' 'NO' 1* 'SEG' 3* 'STD' /
/

COMPDAT

'PROD' 2* 1 10 'OPEN' 2* 0.291666666666667 3* 'Z' 1* /
/

WCONPROD

'PROD' 'OPEN' 'GRUP' 1000 4* 500 3* /
/

WECON

'PROD' 20 1* 0.95 2* 'NONE' 'YES' 1* 'POTN' 1* 'NONE' 2* /
/

RPTSCHED

'RESTART=2' /

RPTRST

'BASIC=2' /

TUNING

10* /

11* /

2* 500 7* /

TSTEP

31.4166666666667 /

TSTEP

27.4166666666667 /

TSTEP

31.4166666666667 /

TSTEP

29.4166666666667 /

TSTEP

31.4166666666667 /

TSTEP

30.4166666666667 /



ศูนย์วิทยทรัพยากร
จุฬาลงกรณ์มหาวิทยาลัย

TSTEP

30.4166666666667 /

TSTEP

31.4166666666667 /

TSTEP

29.4166666666667 /

TSTEP

31.4166666666667 /

TSTEP

29.4166666666667 /

TSTEP

31.4166666666667 /

TSTEP

31.4166666666667 /

TSTEP

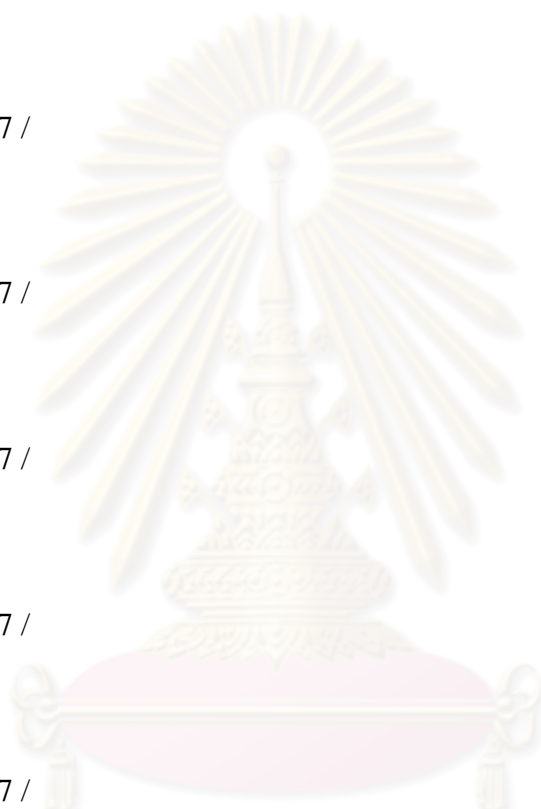
27.4166666666667 /

TSTEP

31.4166666666667 /

TSTEP

29.4166666666667 /



ศูนย์วิทยทรัพยากร
จุฬาลงกรณ์มหาวิทยาลัย

TSTEP

31.4166666666667 /

WPOLYMER

'INJECT' 0.3502 0 2* /

/

TSTEP

31.4166666666667 /

TSTEP

27.4166666666667 /

TSTEP

31.4166666666667 /

TSTEP

29.4166666666667 /

TSTEP

31.4166666666667 /

TSTEP

29.4166666666667 /

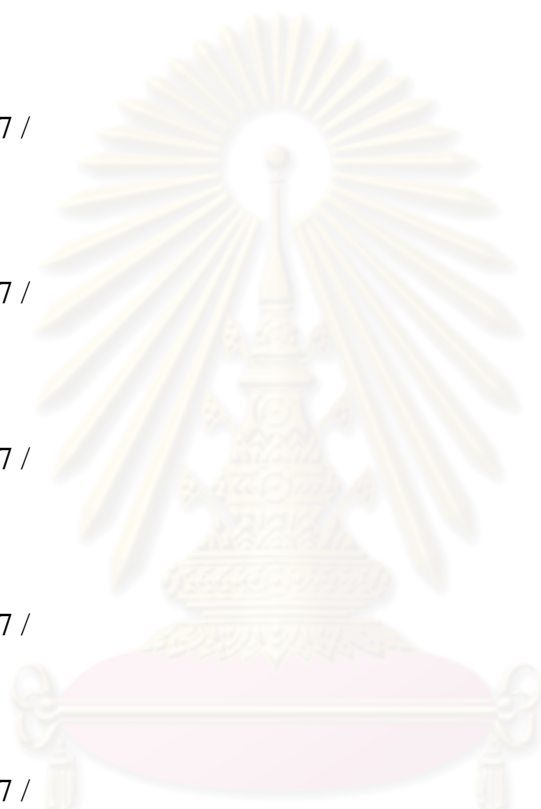
TSTEP

31.4166666666667 /

TSTEP

31.4166666666667 /

TSTEP



ศูนย์วิทยทรัพยากร
จุฬาลงกรณ์มหาวิทยาลัย

29.4166666666667 /

TSTEP

31.4166666666667 /

TSTEP

29.4166666666667 /

TSTEP

31.4166666666667 /

TSTEP

31.4166666666667 /

TSTEP

28.4166666666667 /

TSTEP

31.4166666666667 /

TSTEP

29.4166666666667 /

TSTEP

31.4166666666667 /

WPOLYMER

'INJECT' 0 0 2* /

/

TSTEP

29.4166666666667 /



ศูนย์วิทยทรัพยากร
จุฬาลงกรณ์มหาวิทยาลัย

TSTEP

31.4166666666667 /

SUMMARY section

ALL

BCAD

50 50 10 /

/

BCCN

50 50 10 /

/

BCIP

50 50 10 /

/

BVPOLY

10 10 5 /

/

BVPOLY

50 50 10 /

/

FCAD

FCIC

FCIP

FCIR

FCIT

FCPC

FCPR

FCPT

FOE

FSPR



ศูนย์วิทยทรัพยากร
จุฬาลงกรณ์มหาวิทยาลัย

WCIR

/

WCIT

/

WCPR

/

WCPT

/

WCPT

'PROD' /

BVPOLY

45 45 5 /

/

BVPOLY

48 48 5 /

/

BVPOLY

40 40 5 /

/

END



ศูนย์วิทยทรัพยากร
จุฬาลงกรณ์มหาวิทยาลัย

VITAE

Torpong Yaowapa was born on July 10, 1983 in Bangkok, Thailand. He received his B.Eng. in Petrochemicals and Polymeric Materials Engineering from the Faculty of Engineering, Silpakorn University in 2004. After graduating, he had worked in Petrochemical industry for two and half years and then started his career in Petroleum Industry by working with Nalco Industrial Services (Thailand) as a Technical Service Engineer for two years. He has been a graduate student in the Master of Petroleum Engineering program at the Department of Mining and Petroleum Engineering, Faculty of Engineering, Chulalongkorn University since 2009. Torpong is currently working for Weatherford KSP Company Limited based in Bangkok, Thailand.



ศูนย์วิทยทรัพยากร
จุฬาลงกรณ์มหาวิทยาลัย